Supplementary Material

A Reproducible Representation of Healthy Tibiofemoral Kinematics during Stair Descent using REFRAME – Part II: Exploring Optimisation Criteria and Inter-Subject Differences

Ariana Ortigas-Vásquez*[,1,2], William R. Taylor[3], Barbara Postolka[3,4], Pascal Schütz[3], Allan Maas[1,2], Thomas M. Grupp[1,2], Adrian Sauer[1,2]

[1] Research and Development, Aesculap AG, Tuttlingen, Germany;
[2] Department of Orthopaedic and Trauma Surgery, Musculoskeletal University Center Munich (MUM), Campus Grosshadern, Ludwig Maximilians University Munich, Munich, Germany;
[3] Laboratory for Movement Biomechanics, ETH Zurich, Switzerland;
[4] Human Movement Biomechanics Research Group, KU Leuven, Leuven, Belgium.

Corresponding author: ariana.ortigas_vasquez@aesculap.de

1 The relationship between REFRAME and FOOM

Importantly, the term REFRAME (REference FRame Alignment MEthod) is intended to encompass the overarching framework that leverages mathematical optimisation to target consistent local reference frame orientations and/or origin positions, and thus allow for more robust comparisons of joint rotation and/or translation signals. REFRAME users are free to choose between several different optimisation criteria (e.g. RMS, RMSE, variance, etc.), which can be flexibly weighted, to target a specific repeatable representation of joint movement in up to 6DOFs. FOOM, on the other hand, could be considered a specific sub-implementation of part of the REFRAME framework. FOOM, as its name describes (Frame **Orientation** Optimisation Method), targets only frame **orientations** (and can therefore only handle 3DOFs), through one of two possible formulations: 1) transformation of one dataset's frames to be aligned with those of another dataset acting as reference, or 2) transformation of both datasets' frames to minimise the RMS of out-of-sagittal-plane rotation signals during **gait** activities and thus find local axis orientations that reduce (this interpretation of) **cross-talk**. FOOM is therefore a limited and specific sub-method that could be implemented as part of the REFRAME framework.

2 Additional explanatory figures

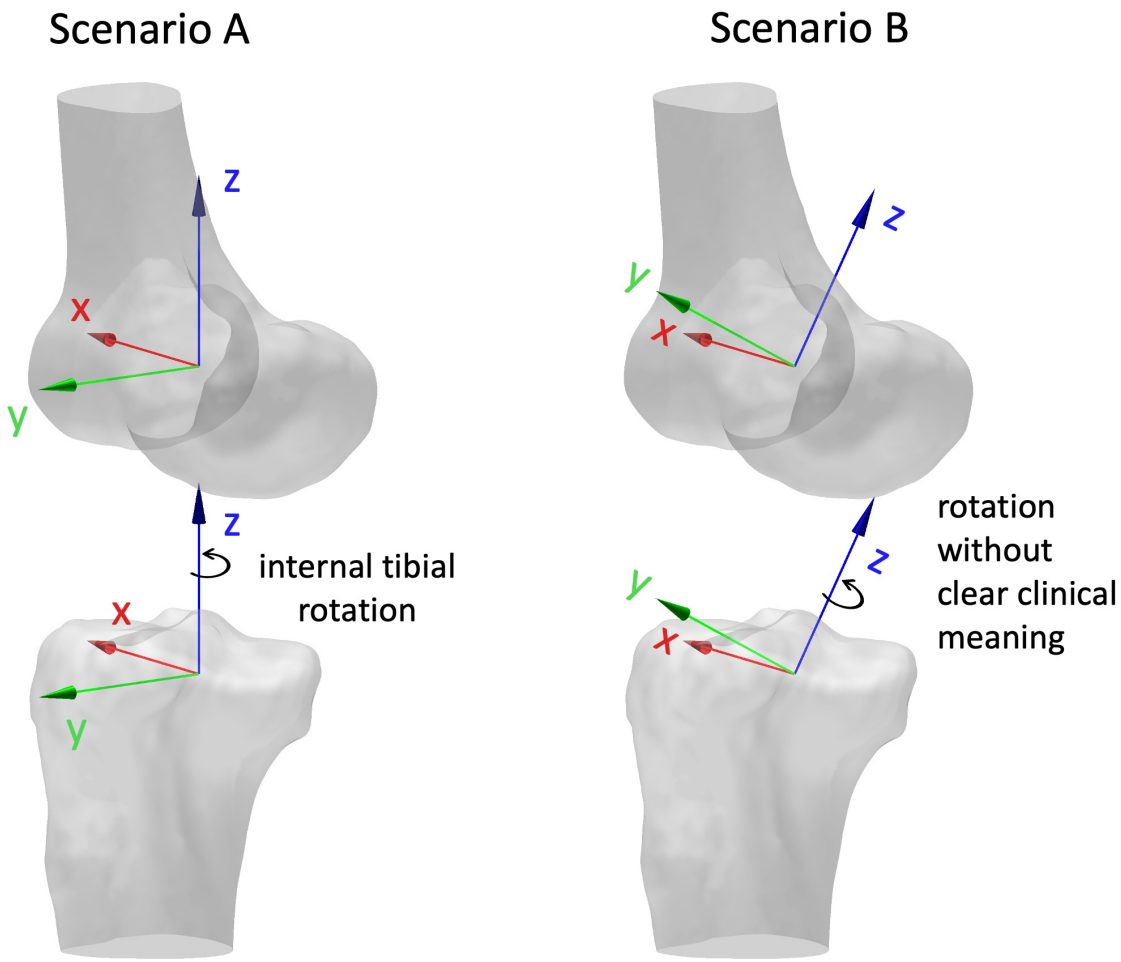

Supplementary Figure S1: Large changes in the orientation of the local frames' anteroposterior and longitudinal axes in the sagittal plane could lead to difficulties in clinical interpretation. E.g. A positive rotation around the z-axis illustrated in Scenario A is generally interpreted clinically as internal tibial rotation. In Scenario B, the clinical meaning of a rotation of the tibia around the z-axis is unclear.

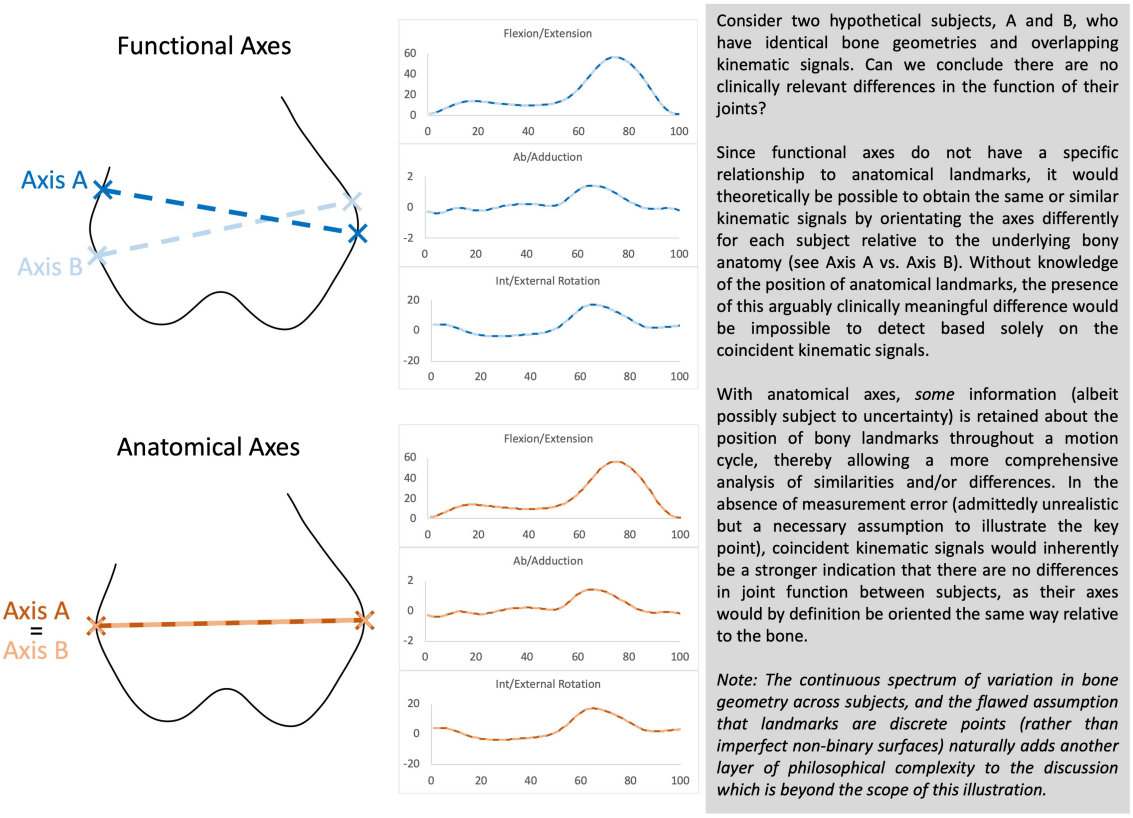

Supplementary Figure S2: Although the use of any functionally defined axes or reference frames is much less susceptible to experimental errors, functional methods may lack crucial information about the position of bony anatomy to assess whether kinematic signals represent similar motion in different subjects.

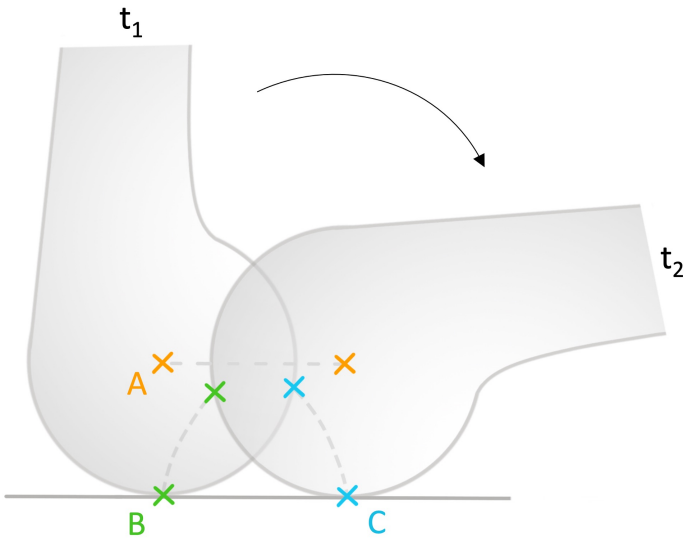

During rolling with slipping, the centre of rotation in the image plane would be at point A, at the centre of a circle fitted to the femoral condyle (for an idealised condyle of constant radius).

At timepoint = t_1
As soon as the motion changes to rolling without slipping, the centre of rotation becomes point B, at the contact point with the distal segment.

At timepoint = t_2
The instantaneous centre of rotation is always the point with zero velocity, so at t_2 it would be at contact point C.

Between t_1 and t_2
The centre of rotation describing the motion of the proximal segment from t_1 to t_2 is clearly not fixed relative to the bone geometry. A, B and C, as well as any other fixed points on the segment, evidently lead to a perceived translation relative to the distal segment.

Supplementary Figure S3: Illustration and explanatory description of cross-talk associated with anatomically fixed axes.

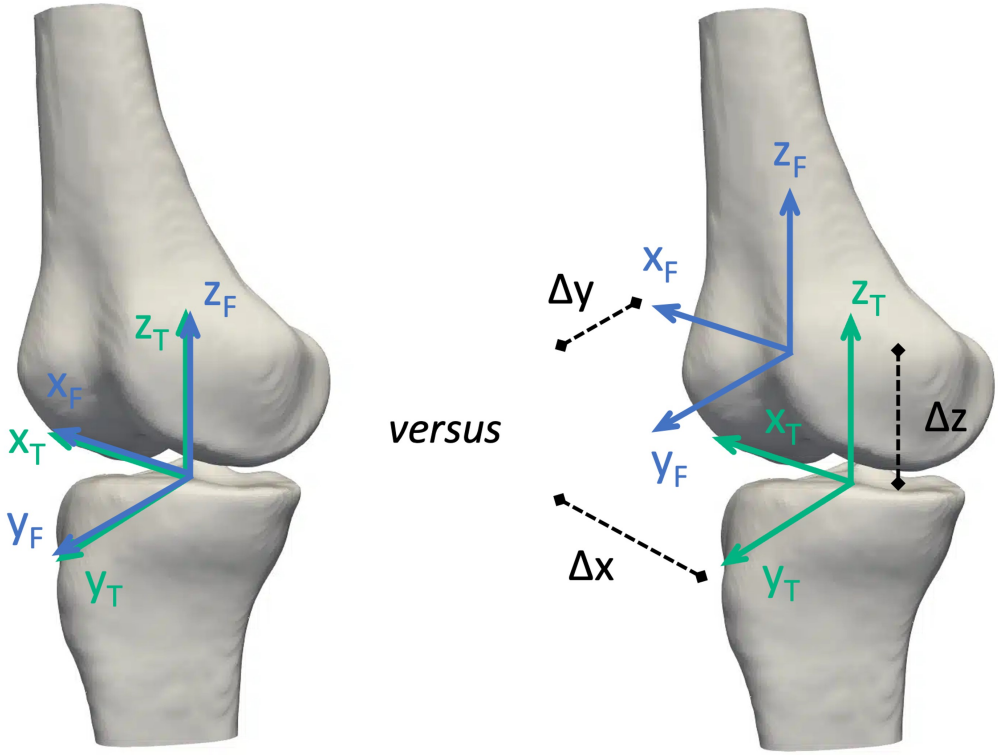

Supplementary Figure S4: Minimising the **root-mean-square** of all translational signals throughout a motion targets optimised frame origin positions that are coincident in neutral stance. In that scenario, the origin of the local femoral coordinate system ideally coincides with the origin of the local tibial coordinate system (left). Instead, minimising the **variance** of all translations still ensures local coordinate systems only minimally translate relative to their neutral positions, without assuming the reference frame origins coincide in neutral stance (right). For example, assuming a femoral frame origin positioned at approximately the centre of a circle fitted to the distal femoral condyle in the sagittal plane, and a tibial frame origin at the height of the tibial plateau, the relative displacement between femur and tibia origins along the proximodistal direction at neutral stance (i.e., Δz) could easily exceed 10 mm (as per Monk et al. 2014).

3 Individual subject results

3.1 Subject 1

3.1.1 Trial 1

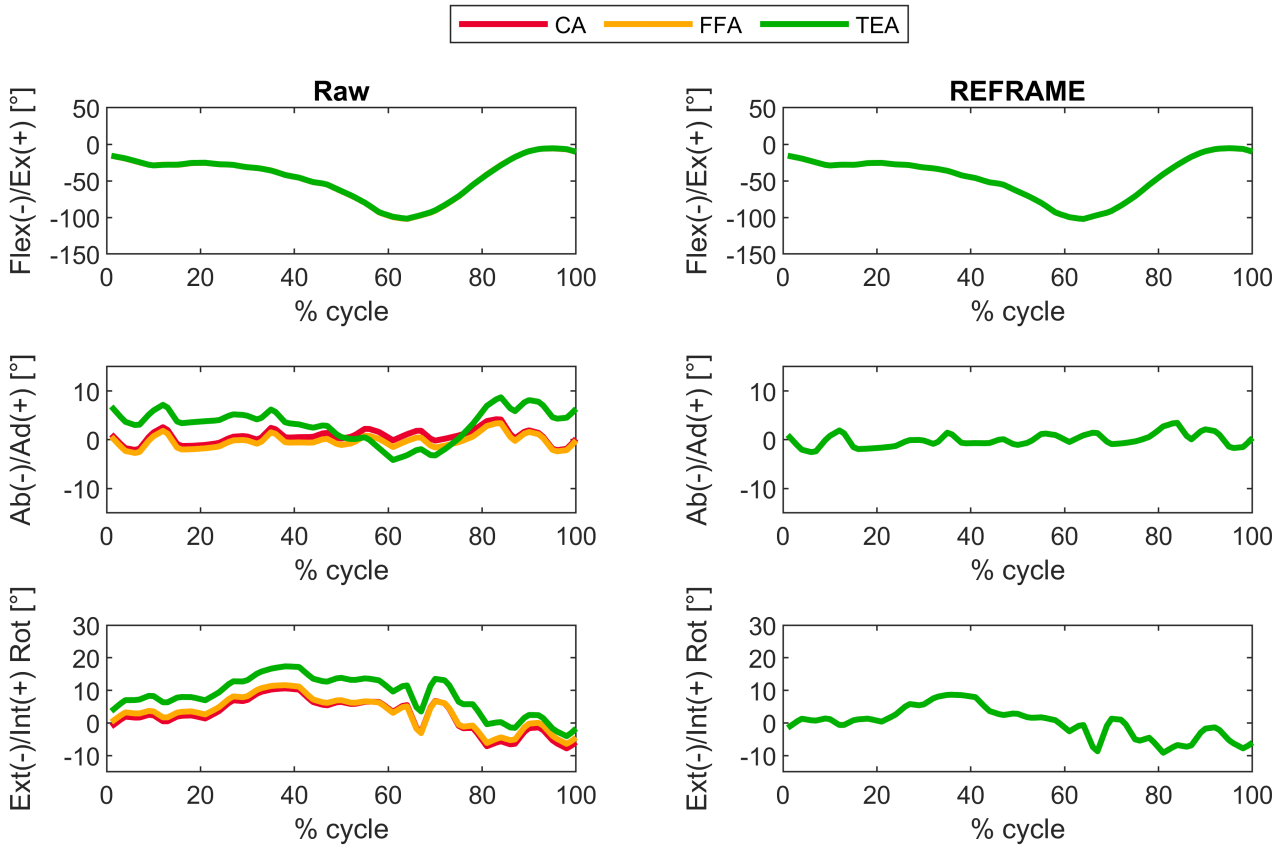

Supplementary Figure S5: Subject 1; Trial 1 – Rotational kinematics: Joint rotations (in degrees) of the tibial relative to the femoral segment frame for one cycle of stair descent, before (raw) and after REFRAME optimisation, for all three axis approaches (CA: cylindrical axis; FFA: functional flexion axis; TEA: transepicondylar axis). CA, FFA and TEA signals are shown in **all** subplots, but due to curve overlap in right-hand side plots, CA and FFA are covered by TEA. Note to readers from a clinical background: knee extension is illustrated here as **positive** because following the right-hand rule it corresponds with a positive rotation around the laterally pointing mediolateral axis for a right knee.

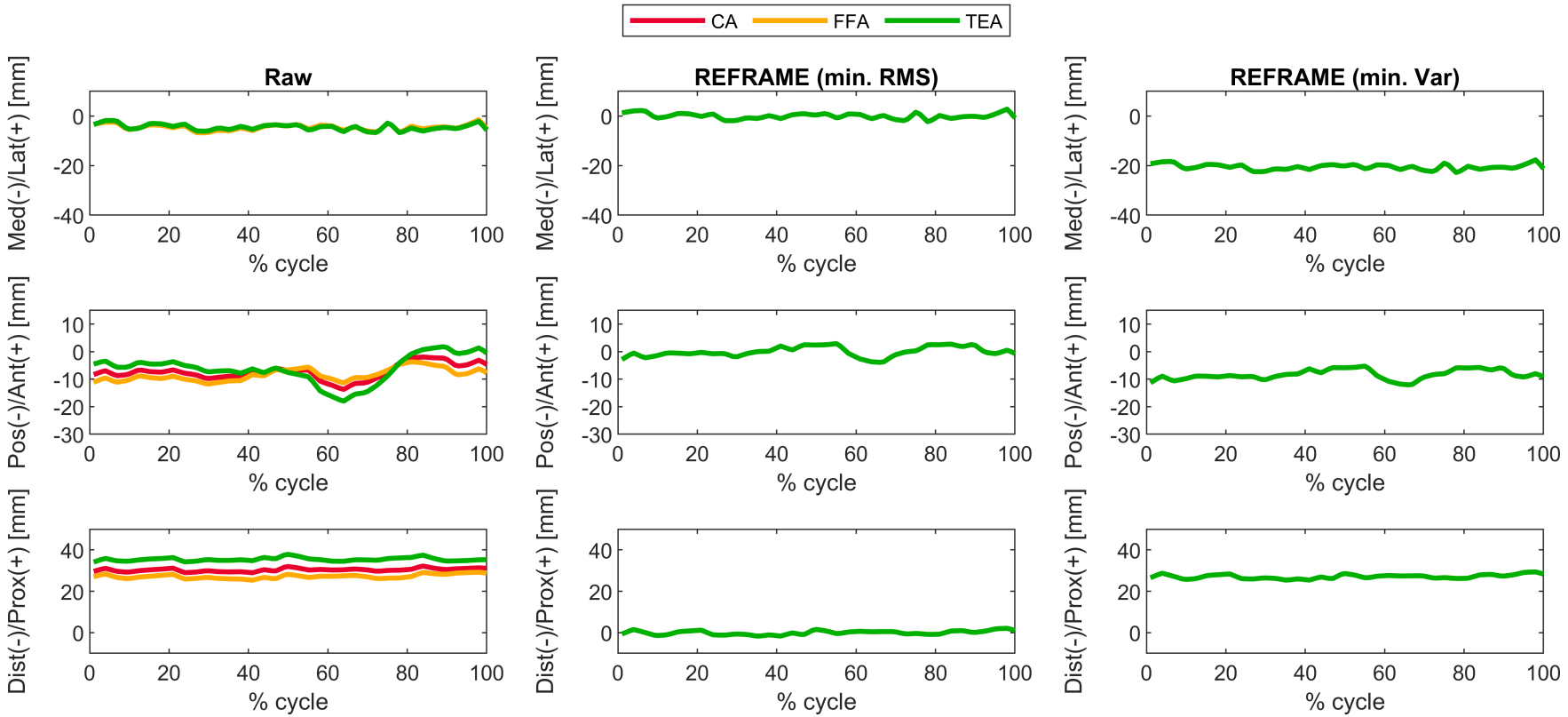

Supplementary Figure S6: Subject 1; Trial 1 – Translational kinematics: Joint translations (in mm) of the femoral relative to the tibial origin for one cycle of stair descent, before (raw, first column) and after application of the REFRAME optimisation (second column: based on the minimisation of translational root-mean-square; third column: based on the minimisation of translational variances), for all three axis approaches (CA: cylindrical axis; FFA: functional flexion axis; TEA: transepicondylar axis). CA, FFA and TEA signals are shown in **all** subplots, but due to curve overlap in the second and third columns, CA and FFA are covered by TEA.

3.1.2 Trial 2

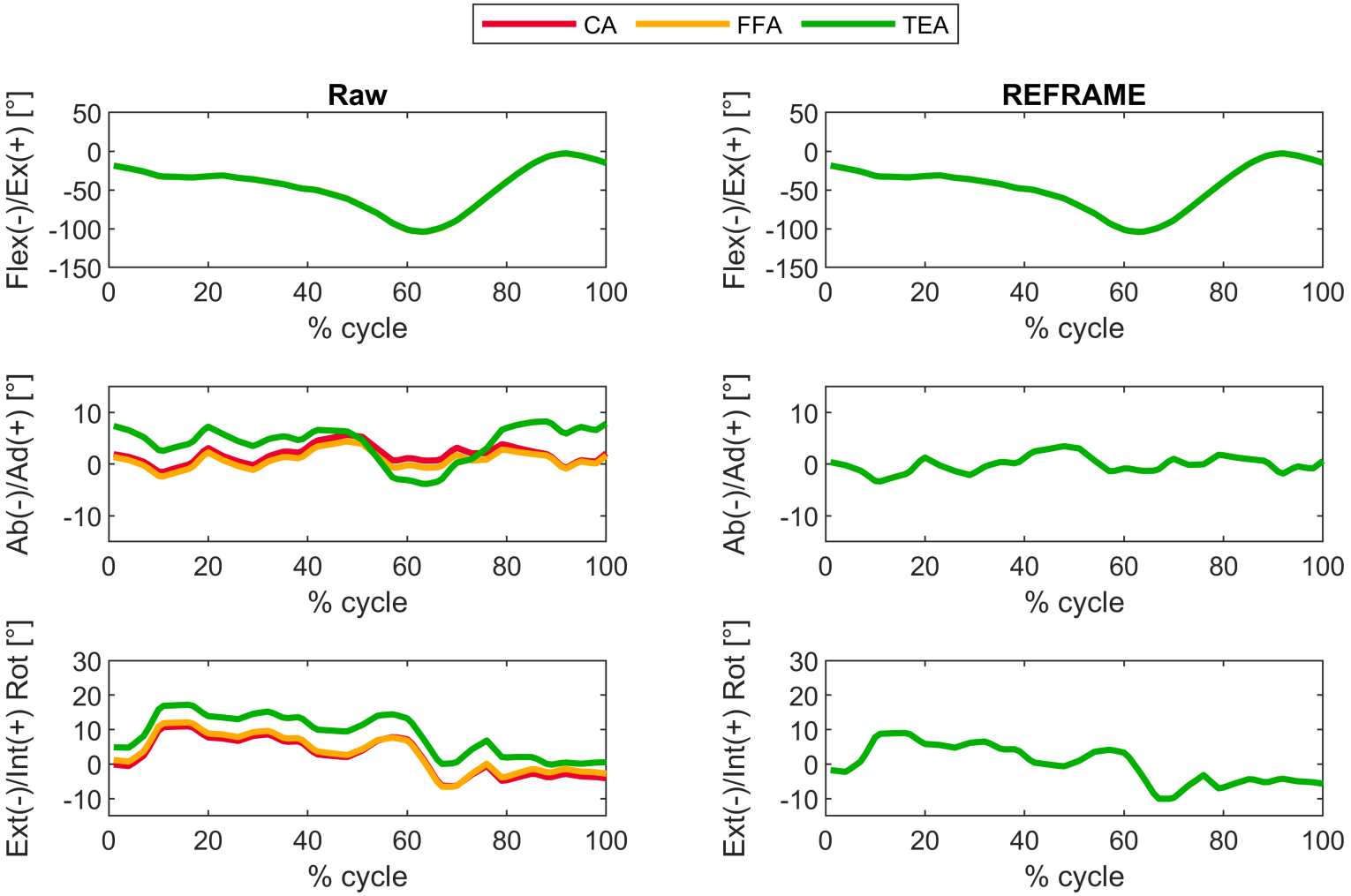

Supplementary Figure S7: Subject 1; Trial 2 – Rotational kinematics: Joint rotations (in degrees) of the tibial relative to the femoral segment frame for one cycle of stair descent, before (raw) and after REFRAME optimisation, for all three axis approaches (CA: cylindrical axis; FFA: functional flexion axis; TEA: transepicondylar axis). CA, FFA and TEA signals are shown in **all** subplots, but due to curve overlap in right-hand side plots, CA and FFA are covered by TEA. Note to readers from a clinical background: knee extension is illustrated here as **positive** because following the right-hand rule it corresponds with a positive rotation around the laterally pointing mediolateral axis for a right knee.

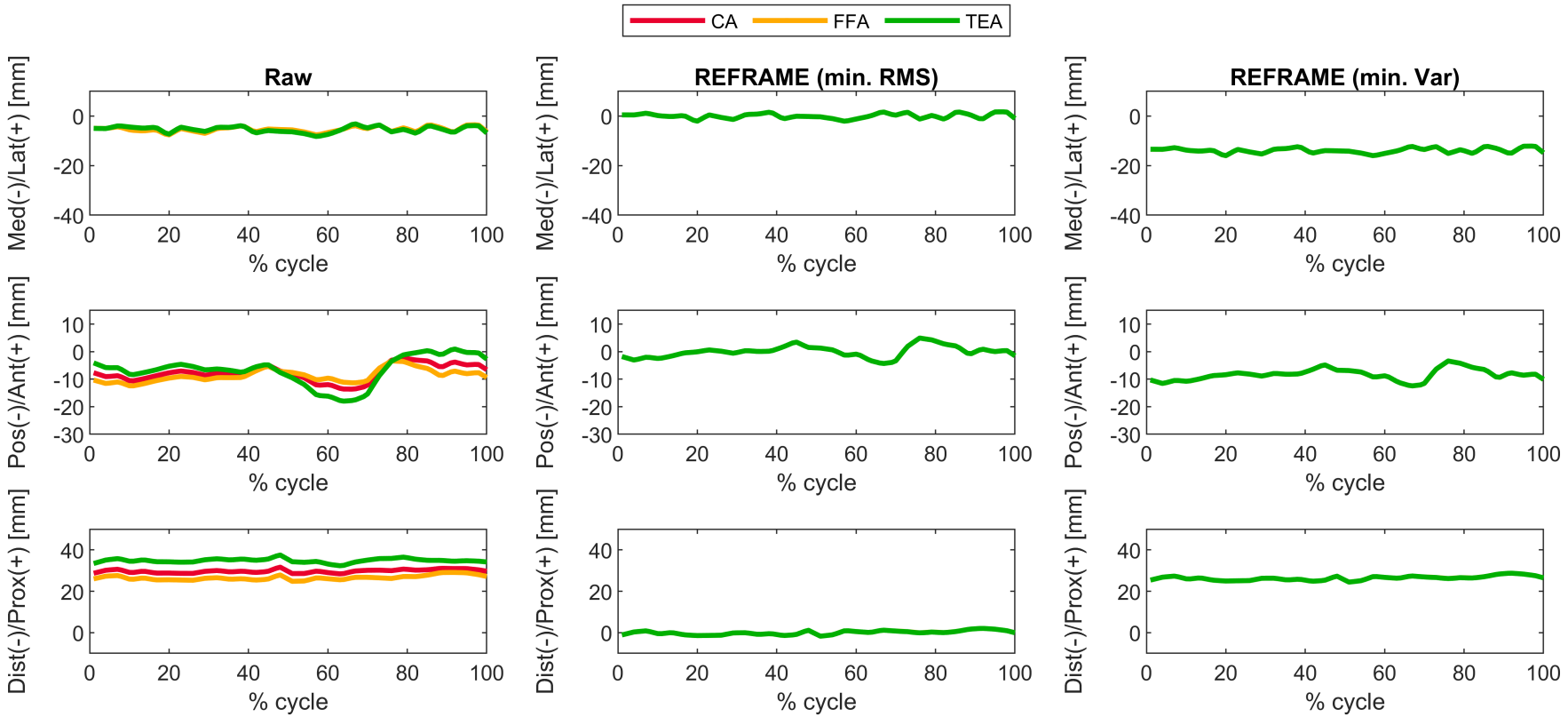

Supplementary Figure S8: Subject 1; Trial 2 – Translational kinematics: Joint translations (in mm) of the femoral relative to the tibial origin for one cycle of stair descent, before (raw, first column) and after application of the REFRAME optimisation (second column: based on the minimisation of translational root-mean-square; third column: based on the minimisation of translational variances), for all three axis approaches (CA: cylindrical axis; FFA: functional flexion axis; TEA: transepicondylar axis). CA, FFA and TEA signals are shown in **all** subplots, but due to curve overlap in the second and third columns, CA and FFA are covered by TEA.

3.1.3 Trial 3

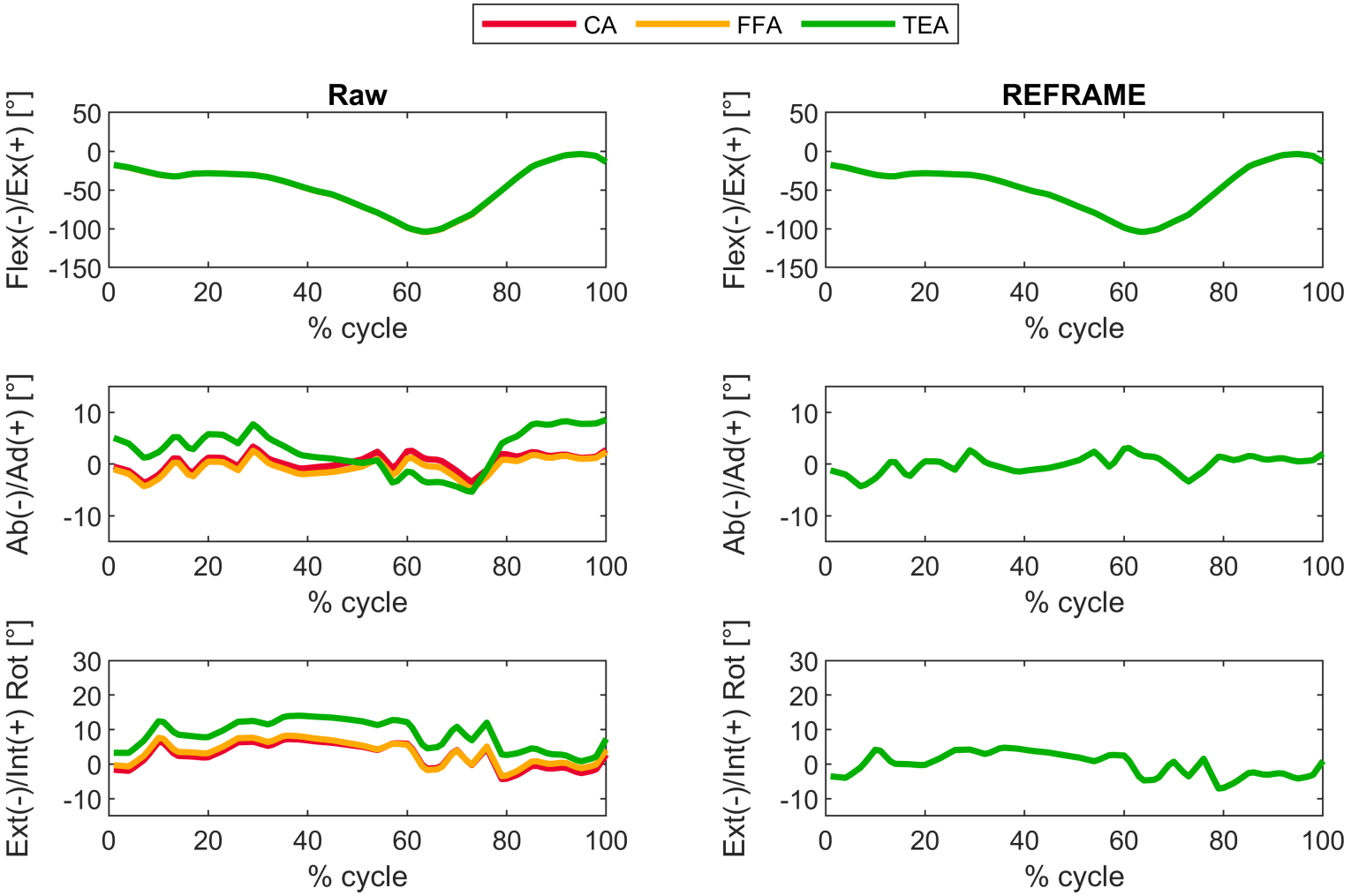

Supplementary Figure S9: Subject 1; Trial 3 – Rotational kinematics: Joint rotations (in degrees) of the tibial relative to the femoral segment frame for one cycle of stair descent, before (raw) and after REFRAME optimisation, for all three axis approaches (CA: cylindrical axis; FFA: functional flexion axis; TEA: transepicondylar axis). CA, FFA and TEA signals are shown in **all** subplots, but due to curve overlap in right-hand side plots, CA and FFA are covered by TEA. Note to readers from a clinical background: knee extension is illustrated here as **positive** because following the right-hand rule it corresponds with a positive rotation around the laterally pointing mediolateral axis for a right knee.

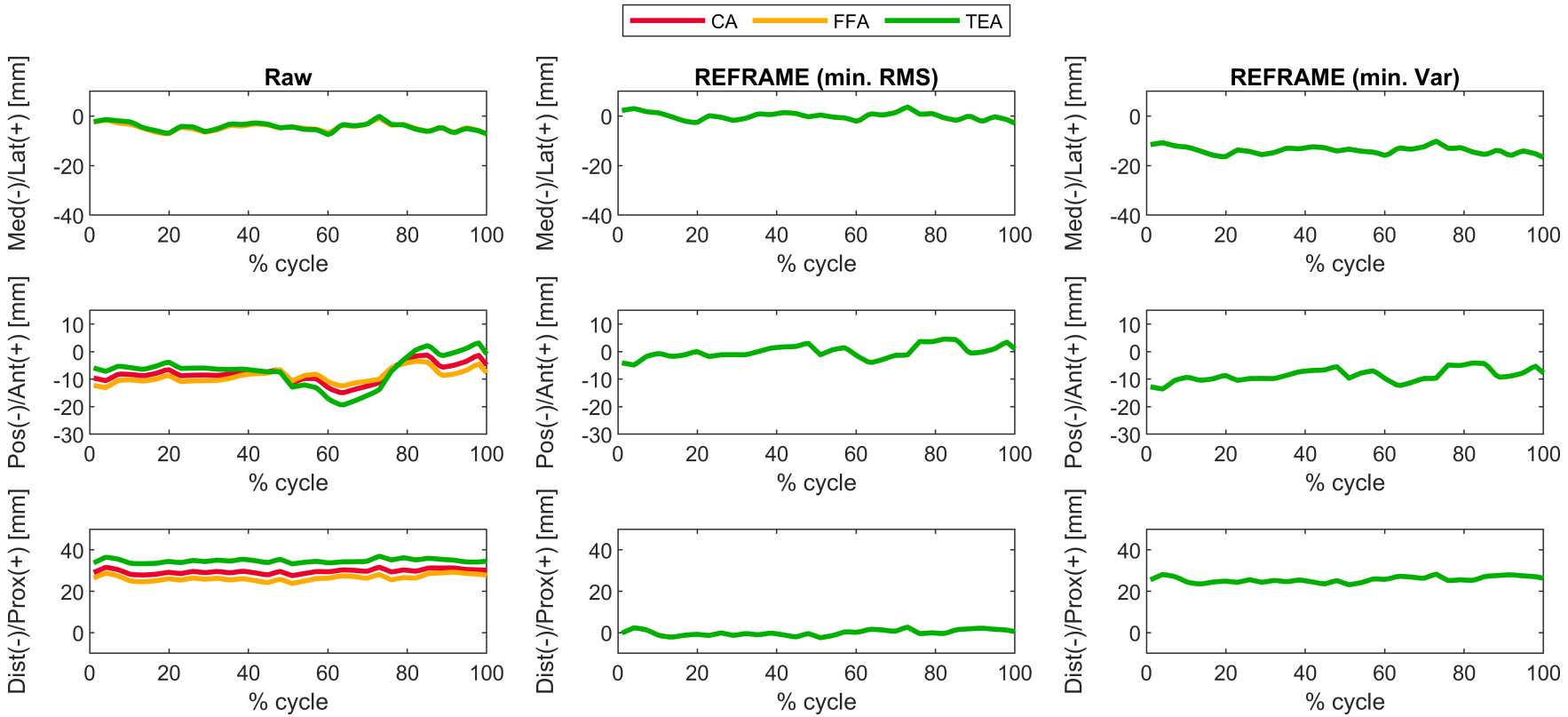

Supplementary Figure S10: Subject 1; Trial 3 – Translational kinematics: Joint translations (in mm) of the femoral relative to the tibial origin for one cycle of stair descent, before (raw, first column) and after application of the REFRAME optimisation (second column: based on the minimisation of translational root-mean-square; third column: based on the minimisation of translational variances), for all three axis approaches (CA: cylindrical axis; FFA: functional flexion axis; TEA: transepicondylar axis). CA, FFA and TEA signals are shown in **all** subplots, but due to curve overlap in the second and third columns, CA and FFA are covered by TEA.

3.1.4 Trial 4

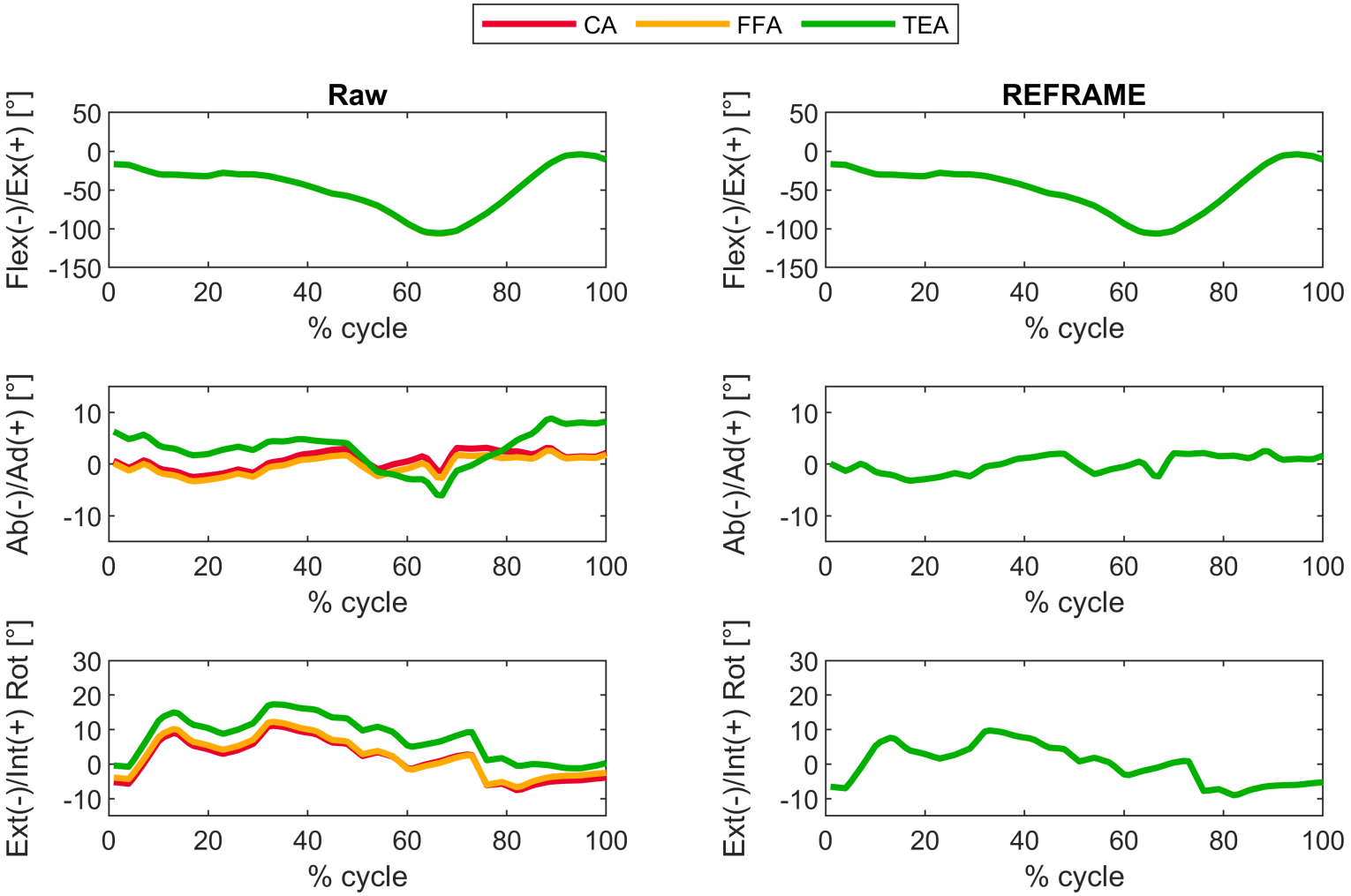

Supplementary Figure S11: Subject 1; Trial 4 – Rotational kinematics: Joint rotations (in degrees) of the tibial relative to the femoral segment frame for one cycle of stair descent, before (raw) and after REFRAME optimisation, for all three axis approaches (CA: cylindrical axis; FFA: functional flexion axis; TEA: transepicondylar axis). CA, FFA and TEA signals are shown in **all** subplots, but due to curve overlap in right-hand side plots, CA and FFA are covered by TEA. Note to readers from a clinical background: knee extension is illustrated here as **positive** because following the right-hand rule it corresponds with a positive rotation around the laterally pointing mediolateral axis for a right knee.

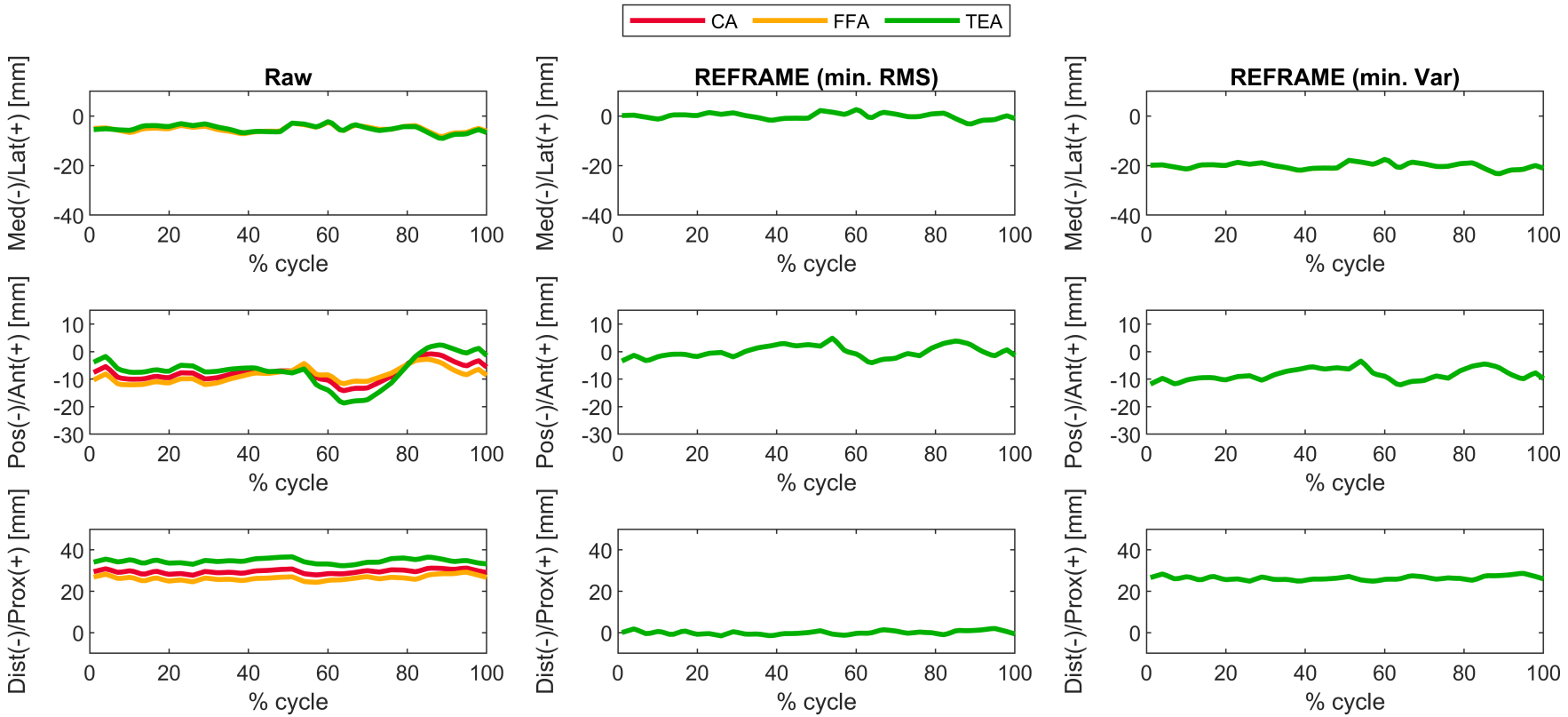

Supplementary Figure S12: Subject 1; Trial 4 – Translational kinematics: Joint translations (in mm) of the femoral relative to the tibial origin for one cycle of stair descent, before (raw, first column) and after application of the REFRAME optimisation (second column: based on the minimisation of translational root-mean-square; third column: based on the minimisation of translational variances), for all three axis approaches (CA: cylindrical axis; FFA: functional flexion axis; TEA: transepicondylar axis). CA, FFA and TEA signals are shown in **all** subplots, but due to curve overlap in the second and third columns, CA and FFA are covered by TEA.

3.1.5 Trial 5

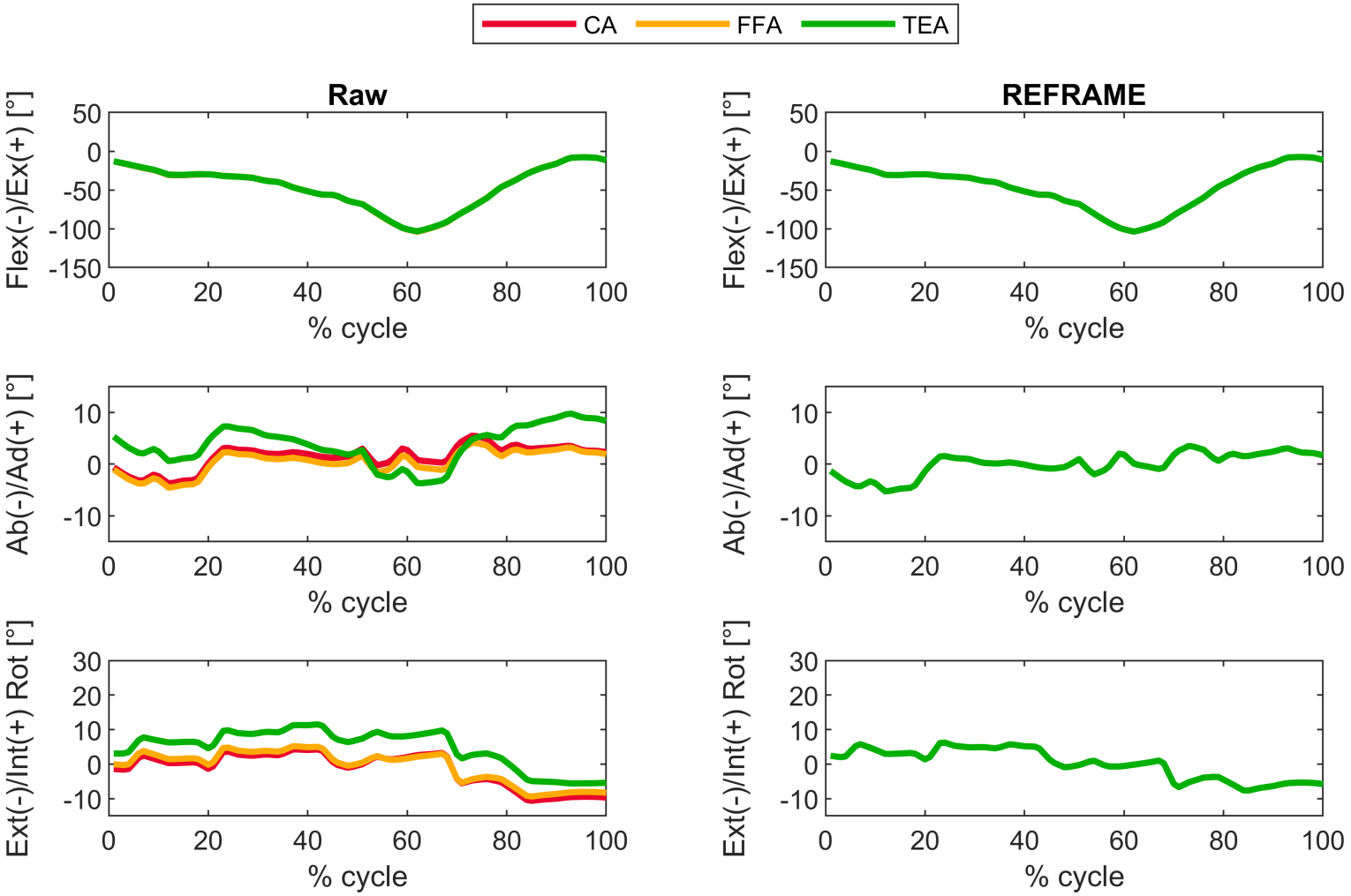

Supplementary Figure S13: Subject 1; Trial 5 – Rotational kinematics: Joint rotations (in degrees) of the tibial relative to the femoral segment frame for one cycle of stair descent, before (raw) and after REFRAME optimisation, for all three axis approaches (CA: cylindrical axis; FFA: functional flexion axis; TEA: transepicondylar axis). CA, FFA and TEA signals are shown in **all** subplots, but due to curve overlap in right-hand side plots, CA and FFA are covered by TEA. Note to readers from a clinical background: knee extension is illustrated here as **positive** because following the right-hand rule it corresponds with a positive rotation around the laterally pointing mediolateral axis for a right knee.

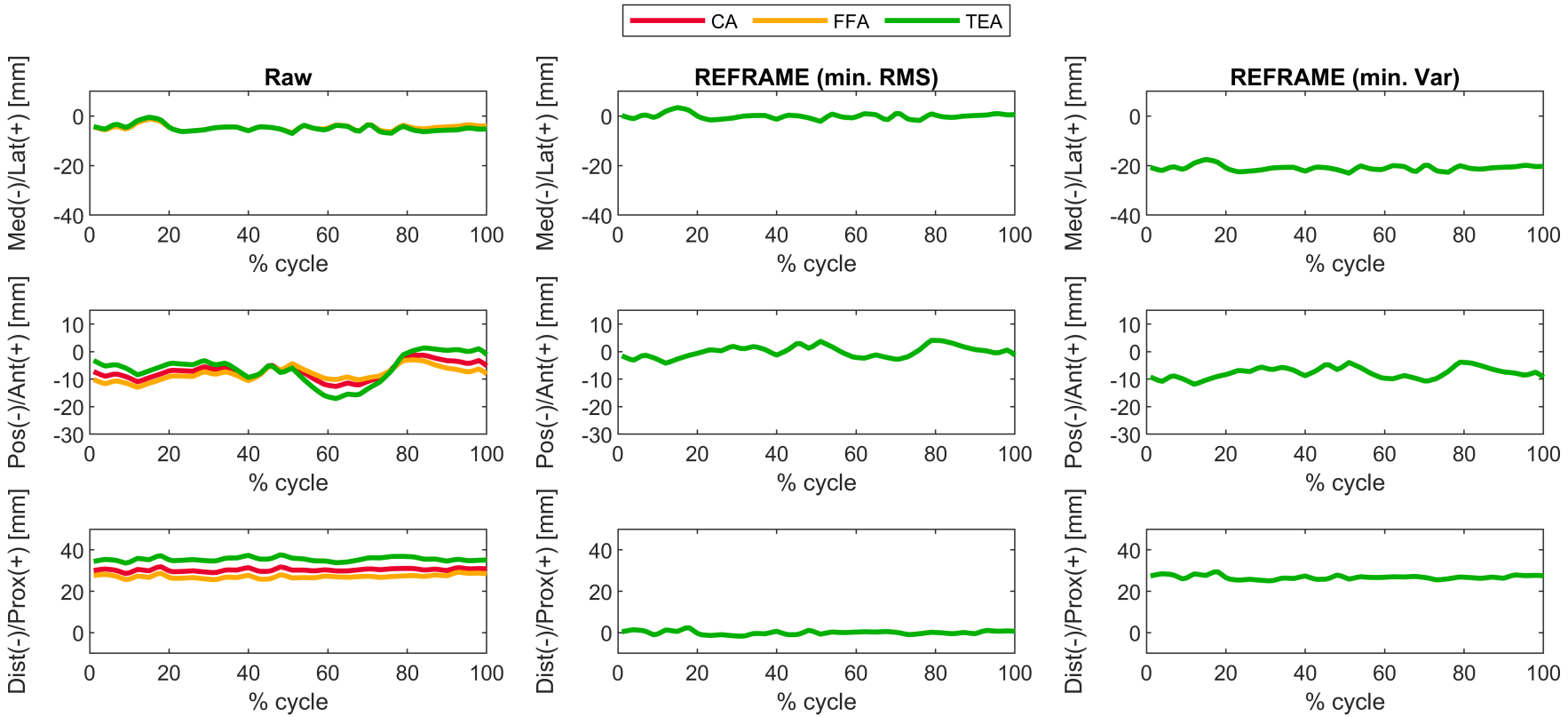

Supplementary Figure S14: Subject 1; Trial 5 – Translational kinematics: Joint translations (in mm) of the femoral relative to the tibial origin for one cycle of stair descent, before (raw, first column) and after application of the REFRAME optimisation (second column: based on the minimisation of translational root-mean-square; third column: based on the minimisation of translational variances), for all three axis approaches (CA: cylindrical axis; FFA: functional flexion axis; TEA: transepicondylar axis). CA, FFA and TEA signals are shown in **all** subplots, but due to curve overlap in the second and third columns, CA and FFA are covered by TEA.

3.2 Subject 2

3.2.1 Trial 1

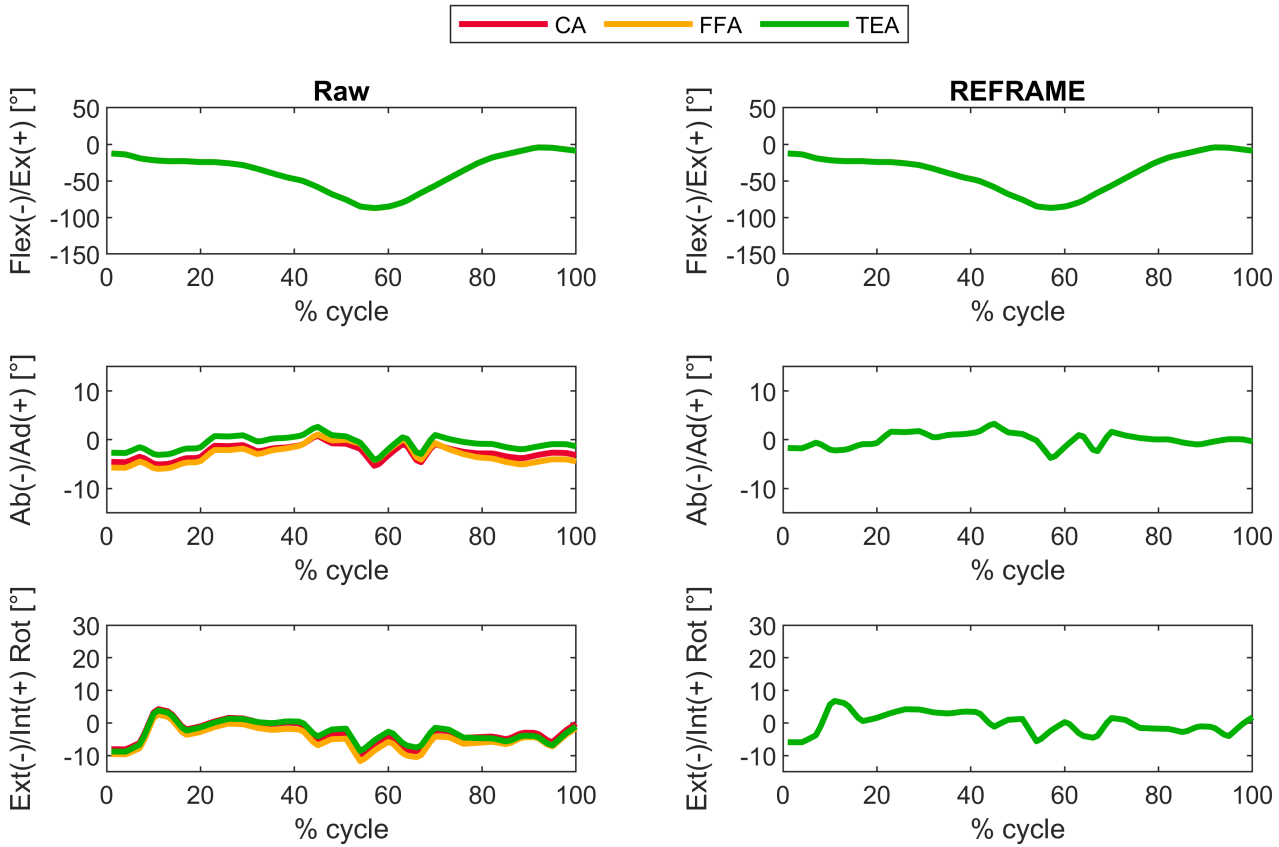

Supplementary Figure S15: Subject 2; Trial 1 – Rotational kinematics: Joint rotations (in degrees) of the tibial relative to the femoral segment frame for one cycle of stair descent, before (raw) and after REFRAME optimisation, for all three axis approaches (CA: cylindrical axis; FFA: functional flexion axis; TEA: transepicondylar axis). CA, FFA and TEA signals are shown in **all** subplots, but due to curve overlap in right-hand side plots, CA and FFA are covered by TEA. Note to readers from a clinical background: knee extension is illustrated here as **positive** because following the right-hand rule it corresponds with a positive rotation around the laterally pointing mediolateral axis for a right knee.

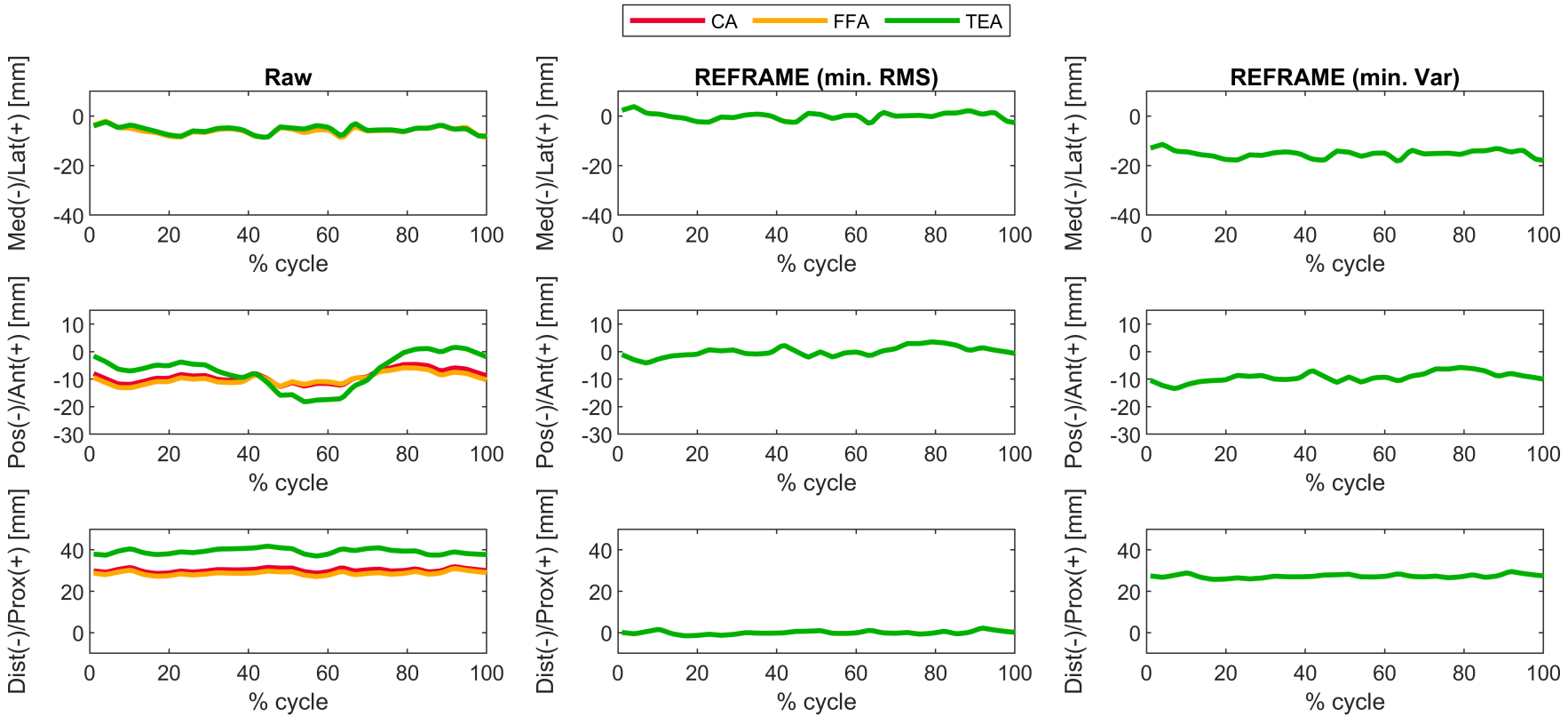

Supplementary Figure S16: Subject 2; Trial 1 – Translational kinematics: Joint translations (in mm) of the femoral relative to the tibial origin for one cycle of stair descent, before (raw, first column) and after application of the REFRAME optimisation (second column: based on the minimisation of translational root-mean-square; third column: based on the minimisation of translational variances), for all three axis approaches (CA: cylindrical axis; FFA: functional flexion axis; TEA: transepicondylar axis). CA, FFA and TEA signals are shown in **all** subplots, but due to curve overlap in the second and third columns, CA and FFA are covered by TEA.

3.2.2 Trial 2

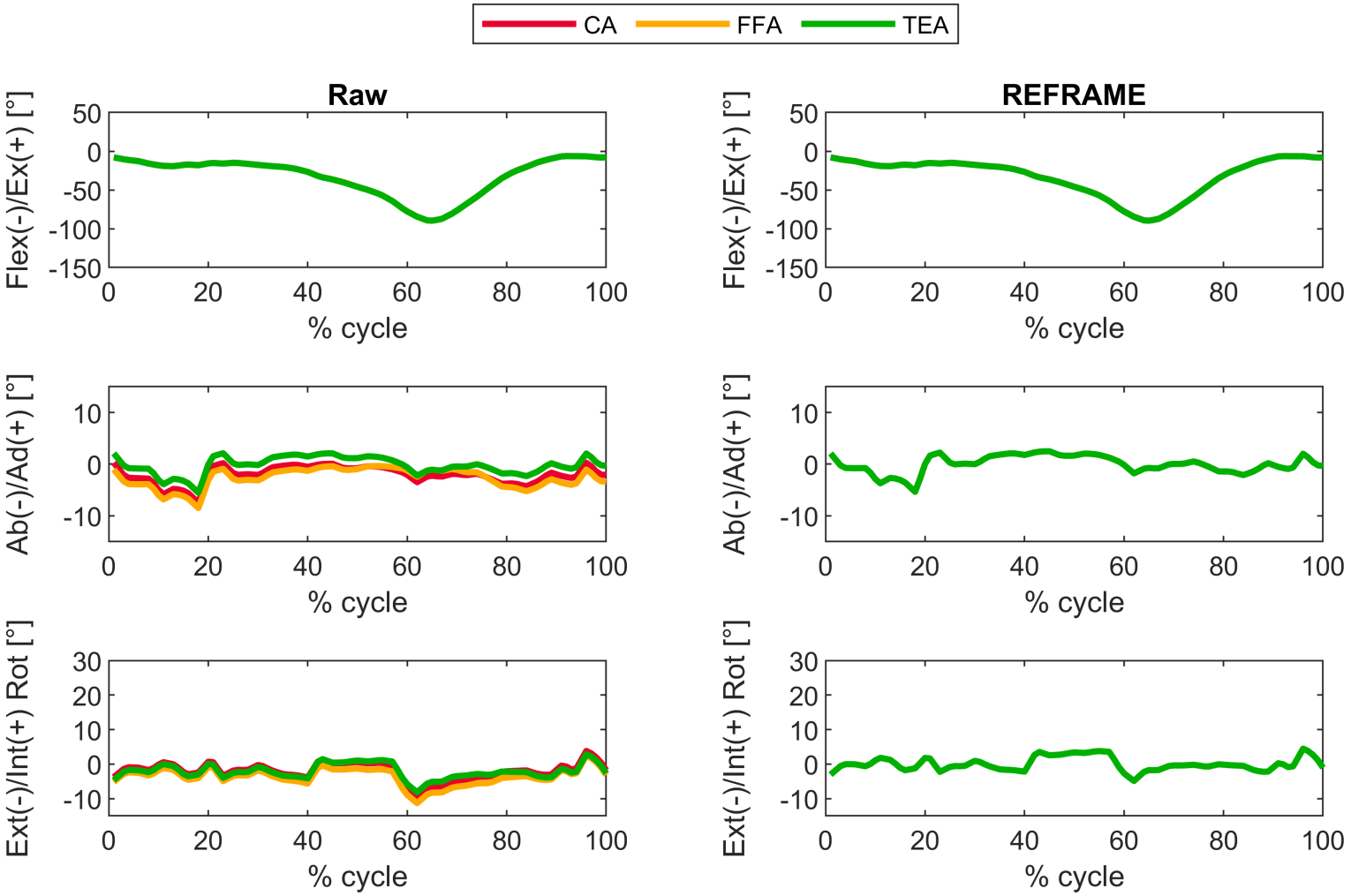

Supplementary Figure S17: Subject 2; Trial 2 – Rotational kinematics: Joint rotations (in degrees) of the tibial relative to the femoral segment frame for one cycle of stair descent, before (raw) and after REFRAME optimisation, for all three axis approaches (CA: cylindrical axis; FFA: functional flexion axis; TEA: transepicondylar axis). CA, FFA and TEA signals are shown in **all** subplots, but due to curve overlap in right-hand side plots, CA and FFA are covered by TEA. Note to readers from a clinical background: knee extension is illustrated here as **positive** because following the right-hand rule it corresponds with a positive rotation around the laterally pointing mediolateral axis for a right knee.

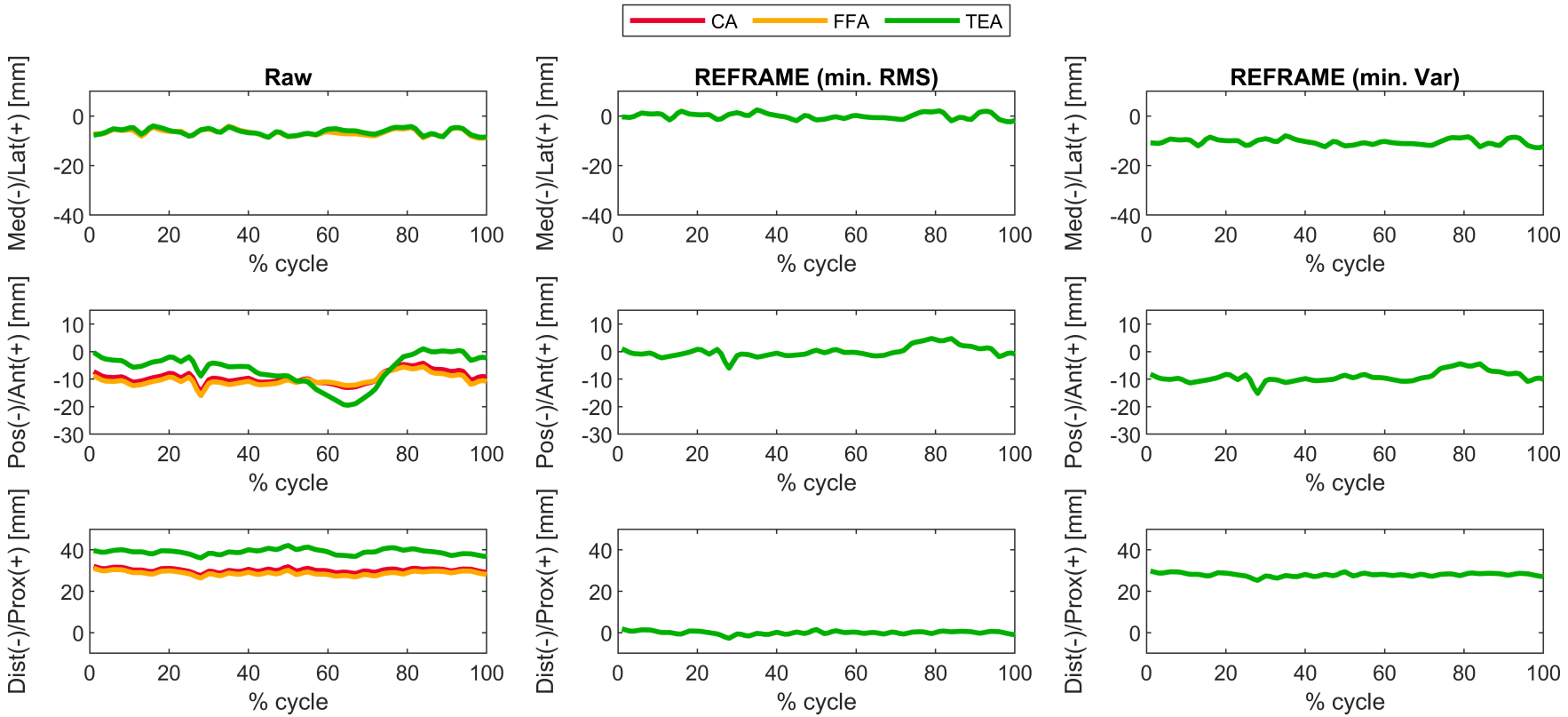

Supplementary Figure S18: Subject 2; Trial 2 – Translational kinematics: Joint translations (in mm) of the femoral relative to the tibial origin for one cycle of stair descent, before (raw, first column) and after application of the REFRAME optimisation (second column: based on the minimisation of translational root-mean-square; third column: based on the minimisation of translational variances), for all three axis approaches (CA: cylindrical axis; FFA: functional flexion axis; TEA: transepicondylar axis). CA, FFA and TEA signals are shown in **all** subplots, but due to curve overlap in the second and third columns, CA and FFA are covered by TEA.

3.2.3 Trial 3

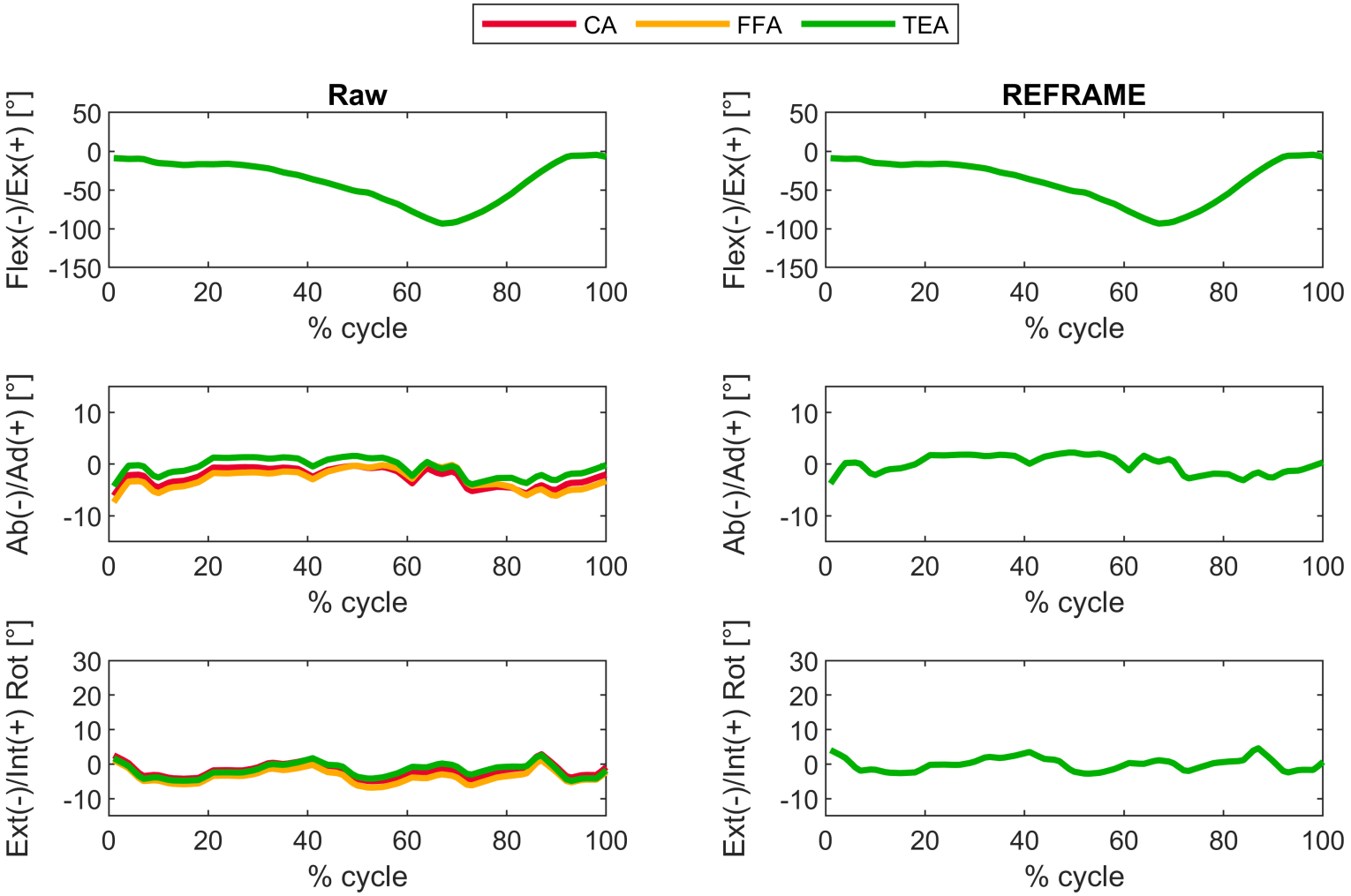

Supplementary Figure S19: Subject 2; Trial 3 – Rotational kinematics: Joint rotations (in degrees) of the tibial relative to the femoral segment frame for one cycle of stair descent, before (raw) and after REFRAME optimisation, for all three axis approaches (CA: cylindrical axis; FFA: functional flexion axis; TEA: transepicondylar axis). CA, FFA and TEA signals are shown in **all** subplots, but due to curve overlap in right-hand side plots, CA and FFA are covered by TEA. Note to readers from a clinical background: knee extension is illustrated here as **positive** because following the right-hand rule it corresponds with a positive rotation around the laterally pointing mediolateral axis for a right knee.

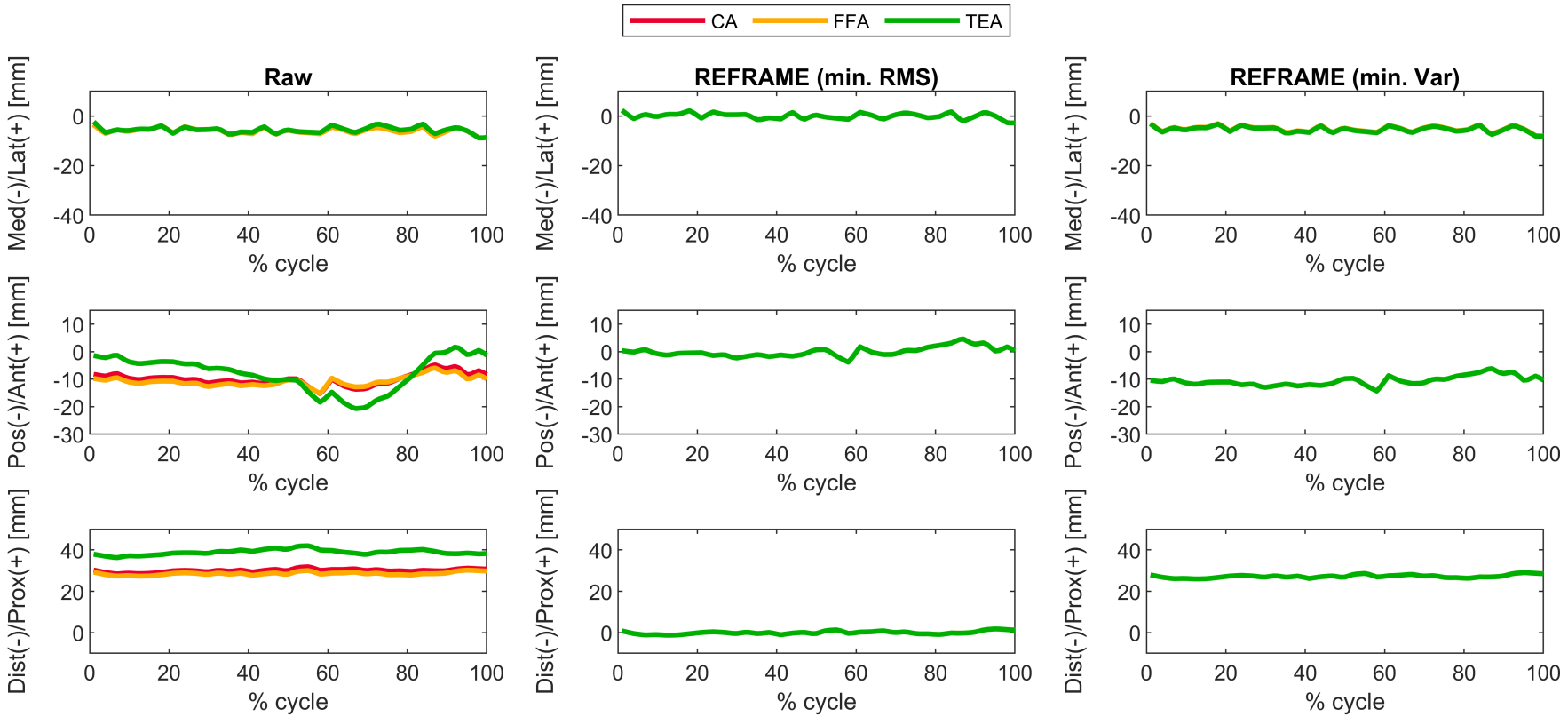

Supplementary Figure S20: Subject 2; Trial 3 – Translational kinematics: Joint translations (in mm) of the femoral relative to the tibial origin for one cycle of stair descent, before (raw, first column) and after application of the REFRAME optimisation (second column: based on the minimisation of translational root-mean-square; third column: based on the minimisation of translational variances), for all three axis approaches (CA: cylindrical axis; FFA: functional flexion axis; TEA: transepicondylar axis). CA, FFA and TEA signals are shown in **all** subplots, but due to curve overlap in the second and third columns, CA and FFA are covered by TEA.

3.2.4 Trial 4

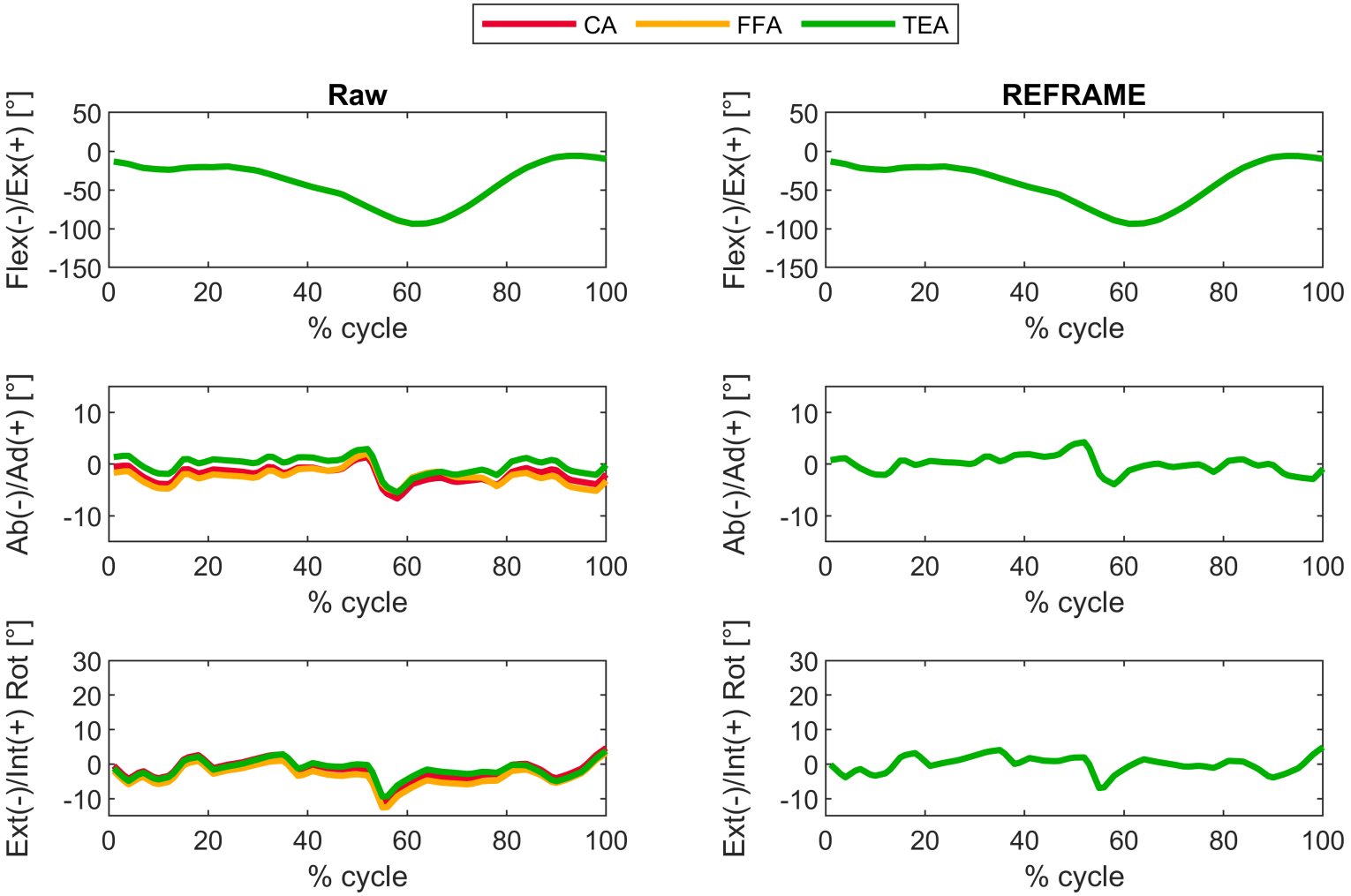

Supplementary Figure S21: Subject 2; Trial 4 – Rotational kinematics: Joint rotations (in degrees) of the tibial relative to the femoral segment frame for one cycle of stair descent, before (raw) and after REFRAME optimisation, for all three axis approaches (CA: cylindrical axis; FFA: functional flexion axis; TEA: transepicondylar axis). CA, FFA and TEA signals are shown in **all** subplots, but due to curve overlap in right-hand side plots, CA and FFA are covered by TEA. Note to readers from a clinical background: knee extension is illustrated here as **positive** because following the right-hand rule it corresponds with a positive rotation around the laterally pointing mediolateral axis for a right knee.

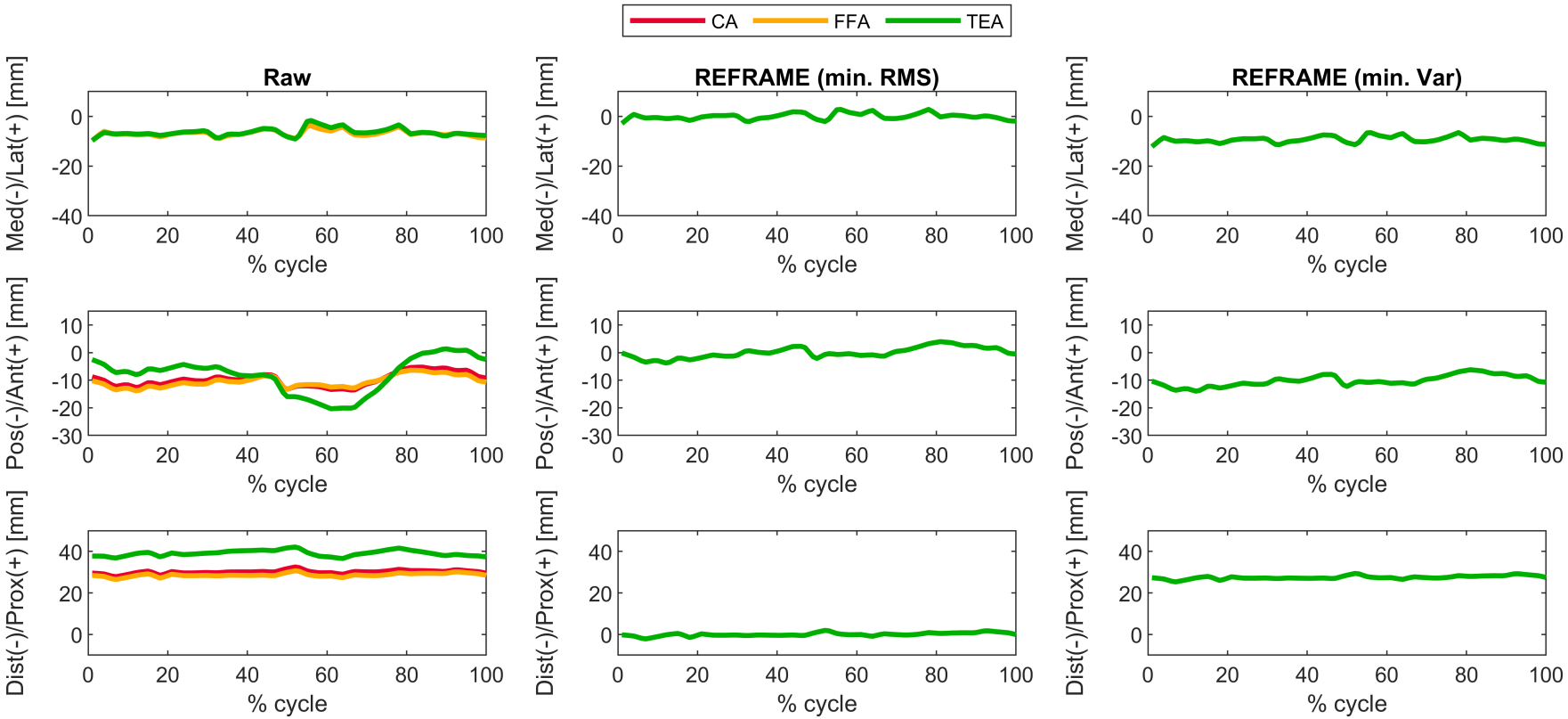

Supplementary Figure S22: Subject 2; Trial 4 – Translational kinematics: Joint translations (in mm) of the femoral relative to the tibial origin for one cycle of stair descent, before (raw, first column) and after application of the REFRAME optimisation (second column: based on the minimisation of translational root-mean-square; third column: based on the minimisation of translational variances), for all three axis approaches (CA: cylindrical axis; FFA: functional flexion axis; TEA: transepicondylar axis). CA, FFA and TEA signals are shown in **all** subplots, but due to curve overlap in the second and third columns, CA and FFA are covered by TEA.

3.2.5 Trial 5

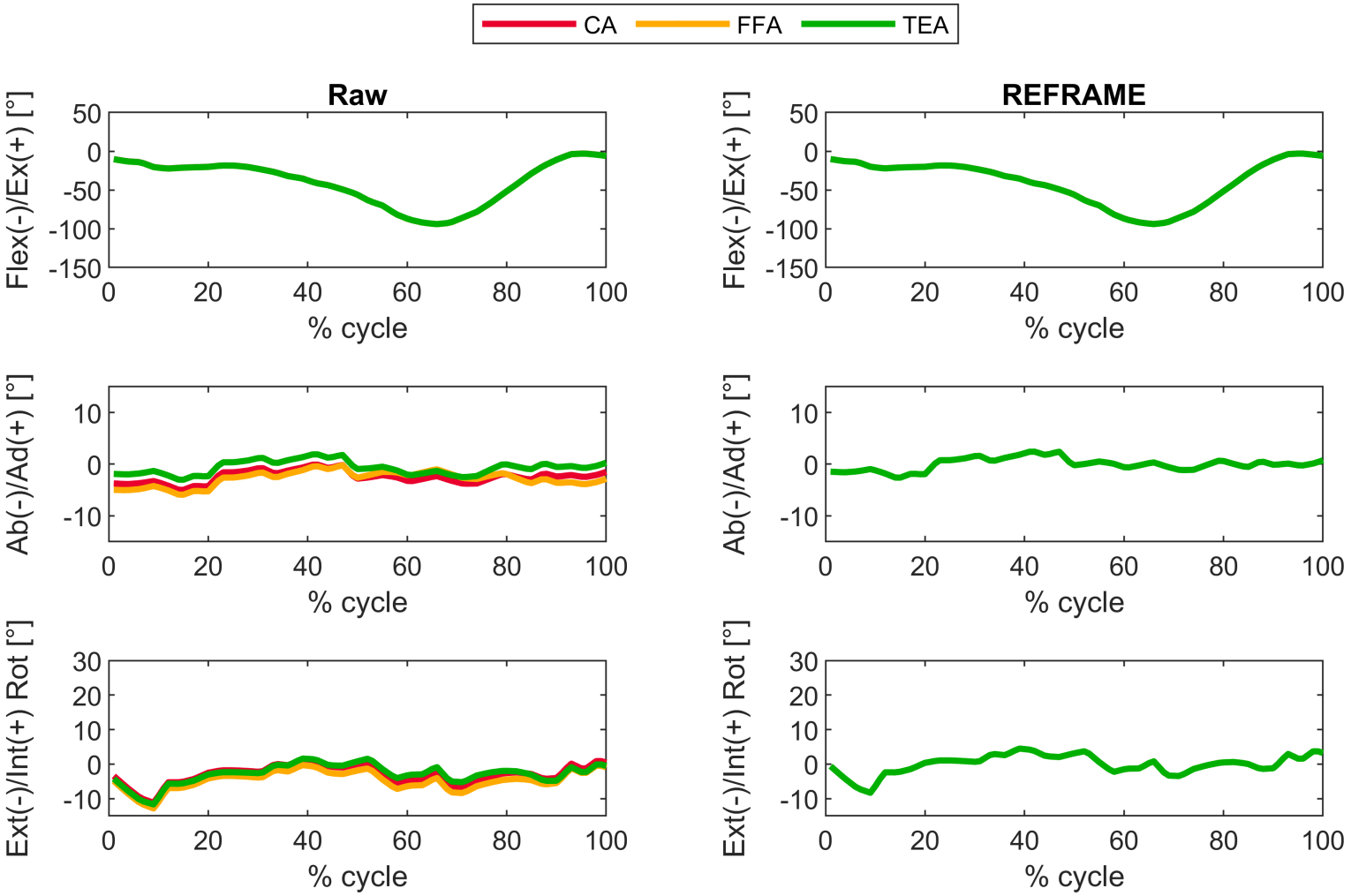

Supplementary Figure S23: Subject 2; Trial 5 – Rotational kinematics: Joint rotations (in degrees) of the tibial relative to the femoral segment frame for one cycle of stair descent, before (raw) and after REFRAME optimisation, for all three axis approaches (CA: cylindrical axis; FFA: functional flexion axis; TEA: transepicondylar axis). CA, FFA and TEA signals are shown in **all** subplots, but due to curve overlap in right-hand side plots, CA and FFA are covered by TEA. Note to readers from a clinical background: knee extension is illustrated here as **positive** because following the right-hand rule it corresponds with a positive rotation around the laterally pointing mediolateral axis for a right knee.

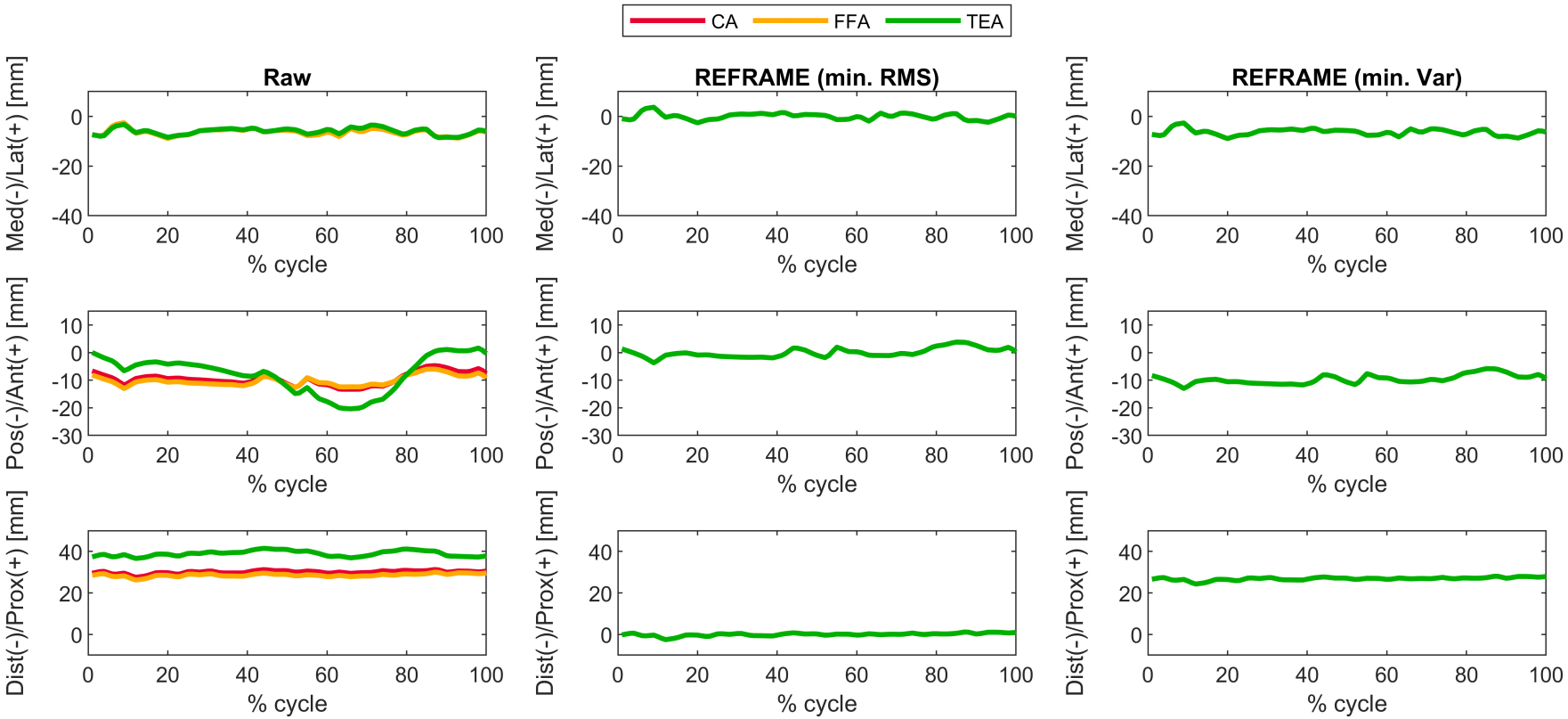

Supplementary Figure S24: Subject 2; Trial 5 – Translational kinematics: Joint translations (in mm) of the femoral relative to the tibial origin for one cycle of stair descent, before (raw, first column) and after application of the REFRAME optimisation (second column: based on the minimisation of translational root-mean-square; third column: based on the minimisation of translational variances), for all three axis approaches (CA: cylindrical axis; FFA: functional flexion axis; TEA: transepicondylar axis). CA, FFA and TEA signals are shown in **all** subplots, but due to curve overlap in the second and third columns, CA and FFA are covered by TEA.

3.3 Subject 3

3.3.1 Trial 1

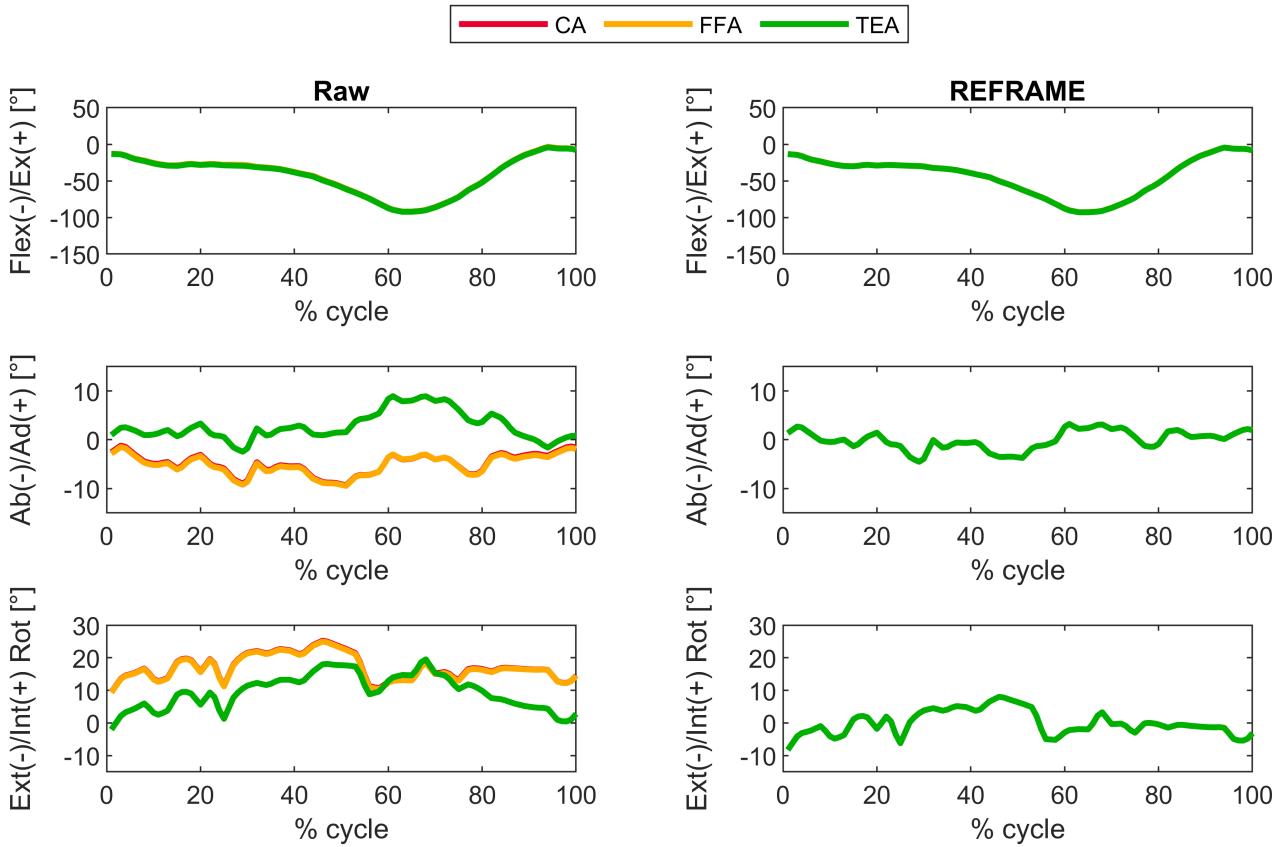

Supplementary Figure S25: Subject 3; Trial 1 – Rotational kinematics: Joint rotations (in degrees) of the tibial relative to the femoral segment frame for one cycle of stair descent, before (raw) and after REFRAME optimisation, for all three axis approaches (CA: cylindrical axis; FFA: functional flexion axis; TEA: transepicondylar axis). CA, FFA and TEA signals are shown in **all** subplots, but due to curve overlap in right-hand side plots, CA and FFA are covered by TEA. Note to readers from a clinical background: knee extension is illustrated here as **positive** because following the right-hand rule it corresponds with a positive rotation around the laterally pointing mediolateral axis for a right knee.

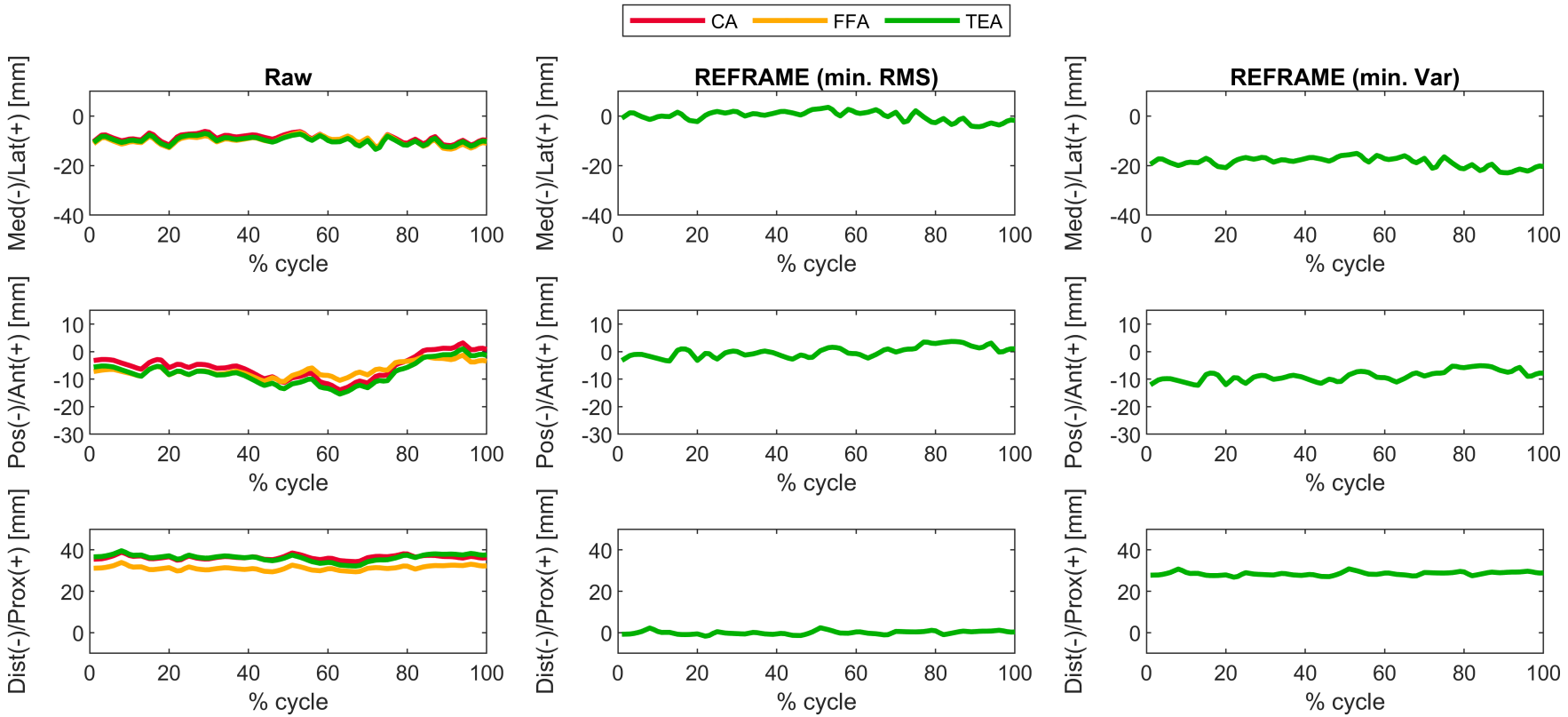

Supplementary Figure S26: Subject 3; Trial 1 – Translational kinematics: Joint translations (in mm) of the femoral relative to the tibial origin for one cycle of stair descent, before (raw, first column) and after application of the REFRAME optimisation (second column: based on the minimisation of translational root-mean-square; third column: based on the minimisation of translational variances), for all three axis approaches (CA: cylindrical axis; FFA: functional flexion axis; TEA: transepicondylar axis). CA, FFA and TEA signals are shown in **all** subplots, but due to curve overlap in the second and third columns, CA and FFA are covered by TEA.

3.3.2 Trial 2

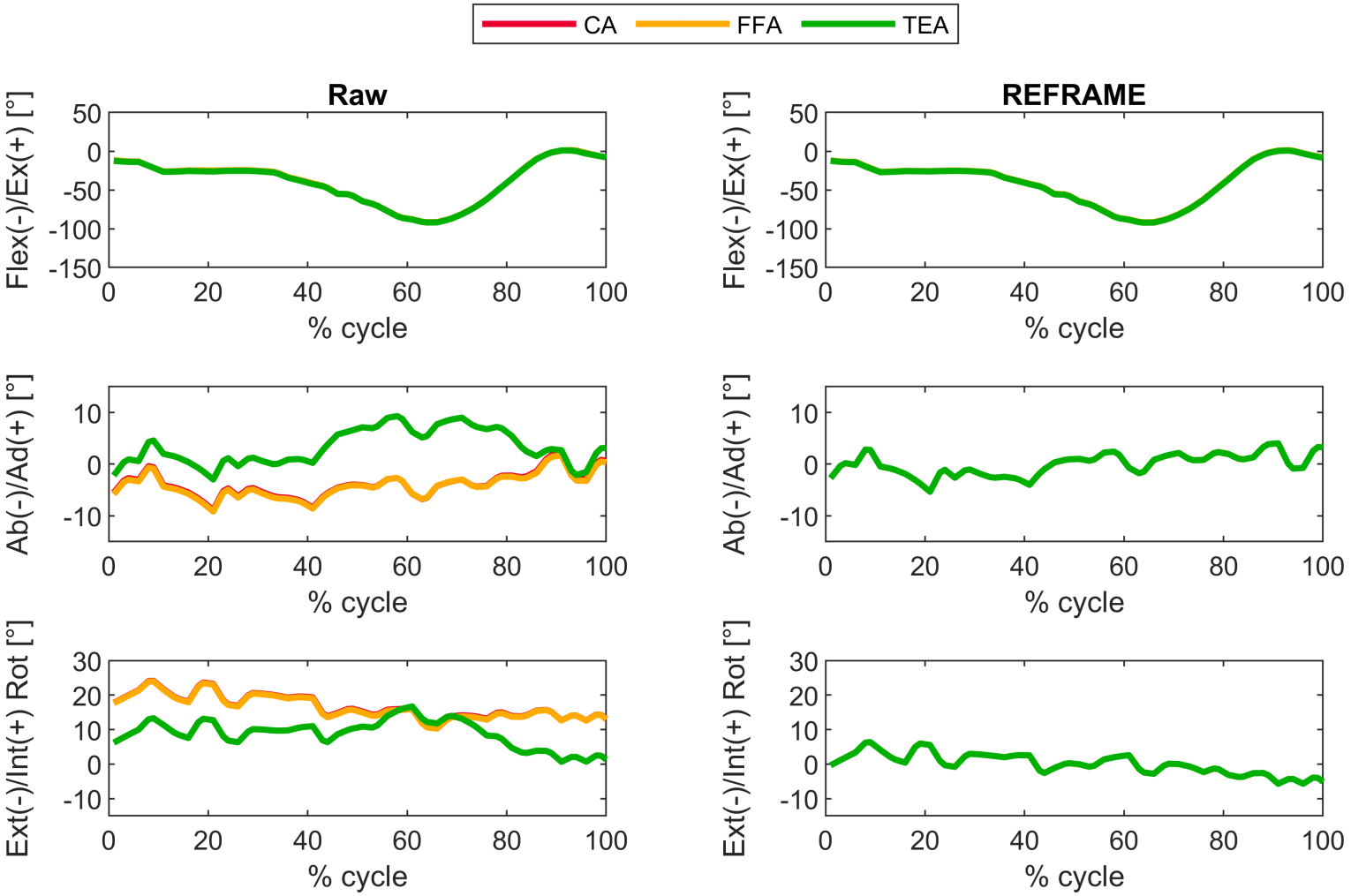

Supplementary Figure S27: Subject 3; Trial 2 – Rotational kinematics: Joint rotations (in degrees) of the tibial relative to the femoral segment frame for one cycle of stair descent, before (raw) and after REFRAME optimisation, for all three axis approaches (CA: cylindrical axis; FFA: functional flexion axis; TEA: transepicondylar axis). CA, FFA and TEA signals are shown in **all** subplots, but due to curve overlap in right-hand side plots, CA and FFA are covered by TEA. Note to readers from a clinical background: knee extension is illustrated here as **positive** because following the right-hand rule it corresponds with a positive rotation around the laterally pointing mediolateral axis for a right knee.

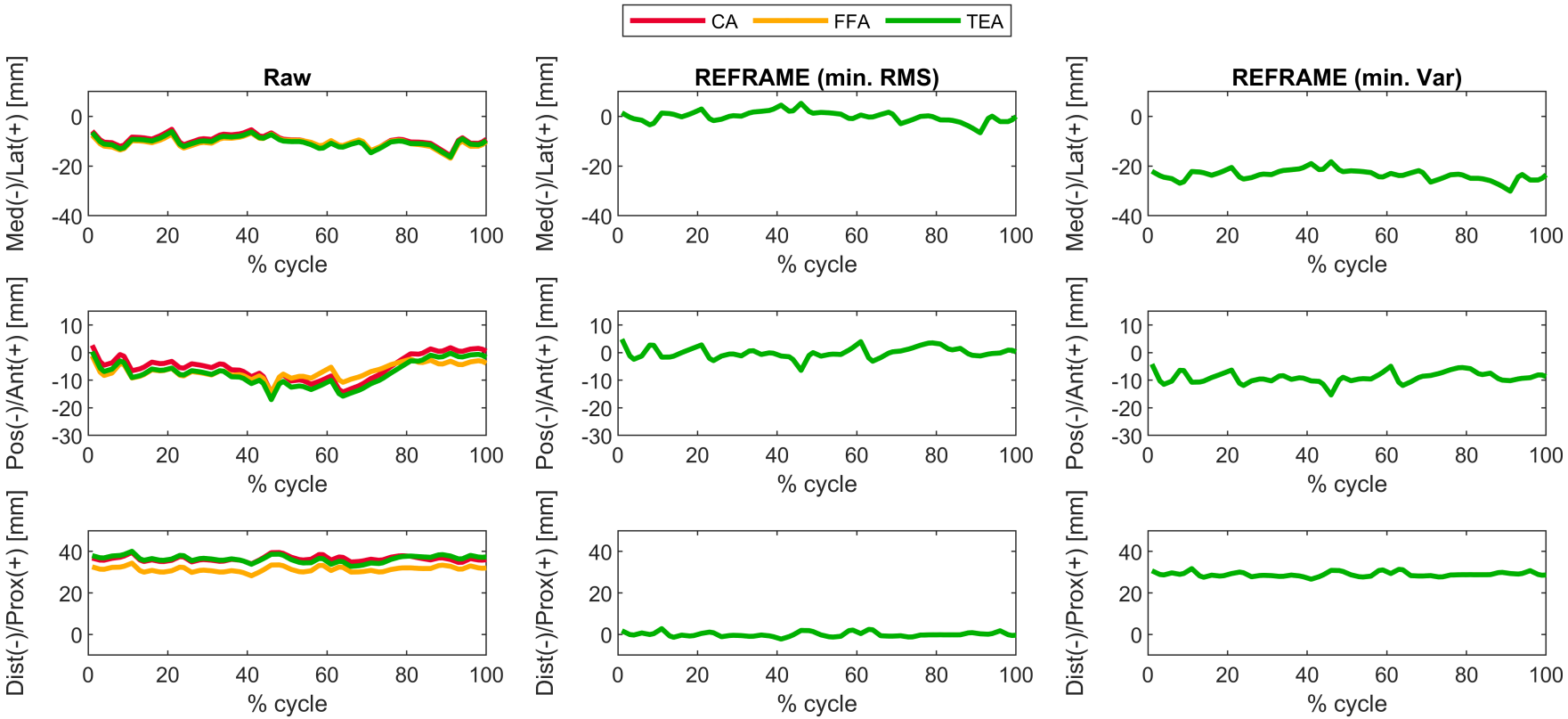

Supplementary Figure S28: Subject 3; Trial 2 – Translational kinematics: Joint translations (in mm) of the femoral relative to the tibial origin for one cycle of stair descent, before (raw, first column) and after application of the REFRAME optimisation (second column: based on the minimisation of translational root-mean-square; third column: based on the minimisation of translational variances), for all three axis approaches (CA: cylindrical axis; FFA: functional flexion axis; TEA: transepicondylar axis). CA, FFA and TEA signals are shown in **all** subplots, but due to curve overlap in the second and third columns, CA and FFA are covered by TEA.

3.3.3 Trial 3

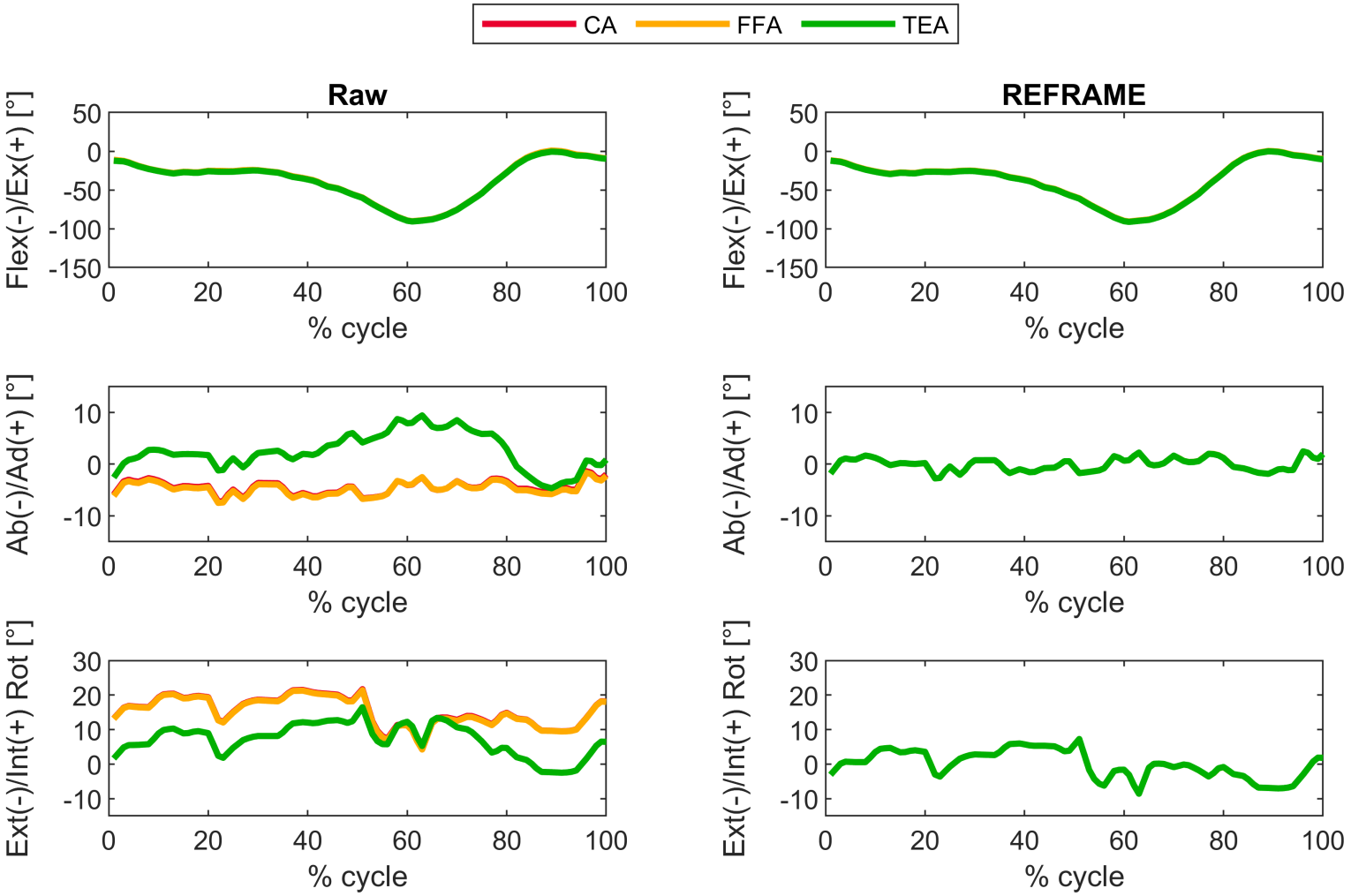

Supplementary Figure S29: Subject 3; Trial 3 – Rotational kinematics: Joint rotations (in degrees) of the tibial relative to the femoral segment frame for one cycle of stair descent, before (raw) and after REFRAME optimisation, for all three axis approaches (CA: cylindrical axis; FFA: functional flexion axis; TEA: transepicondylar axis). CA, FFA and TEA signals are shown in **all** subplots, but due to curve overlap in right-hand side plots, CA and FFA are covered by TEA. Note to readers from a clinical background: knee extension is illustrated here as **positive** because following the right-hand rule it corresponds with a positive rotation around the laterally pointing mediolateral axis for a right knee.

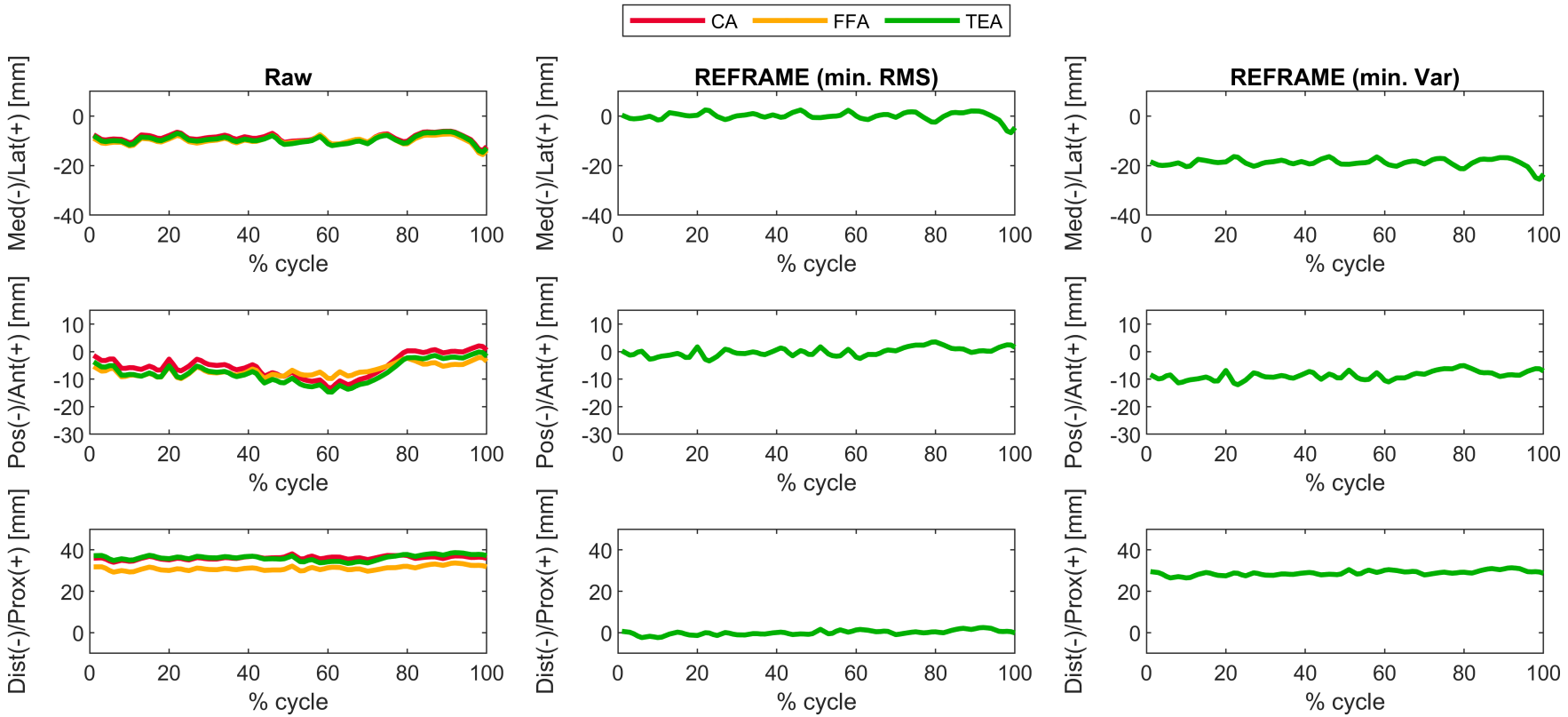

Supplementary Figure S30: Subject 3; Trial 3 – Translational kinematics: Joint translations (in mm) of the femoral relative to the tibial origin for one cycle of stair descent, before (raw, first column) and after application of the REFRAME optimisation (second column: based on the minimisation of translational root-mean-square; third column: based on the minimisation of translational variances), for all three axis approaches (CA: cylindrical axis; FFA: functional flexion axis; TEA: transepicondylar axis). CA, FFA and TEA signals are shown in **all** subplots, but due to curve overlap in the second and third columns, CA and FFA are covered by TEA.

3.3.4 Trial 4

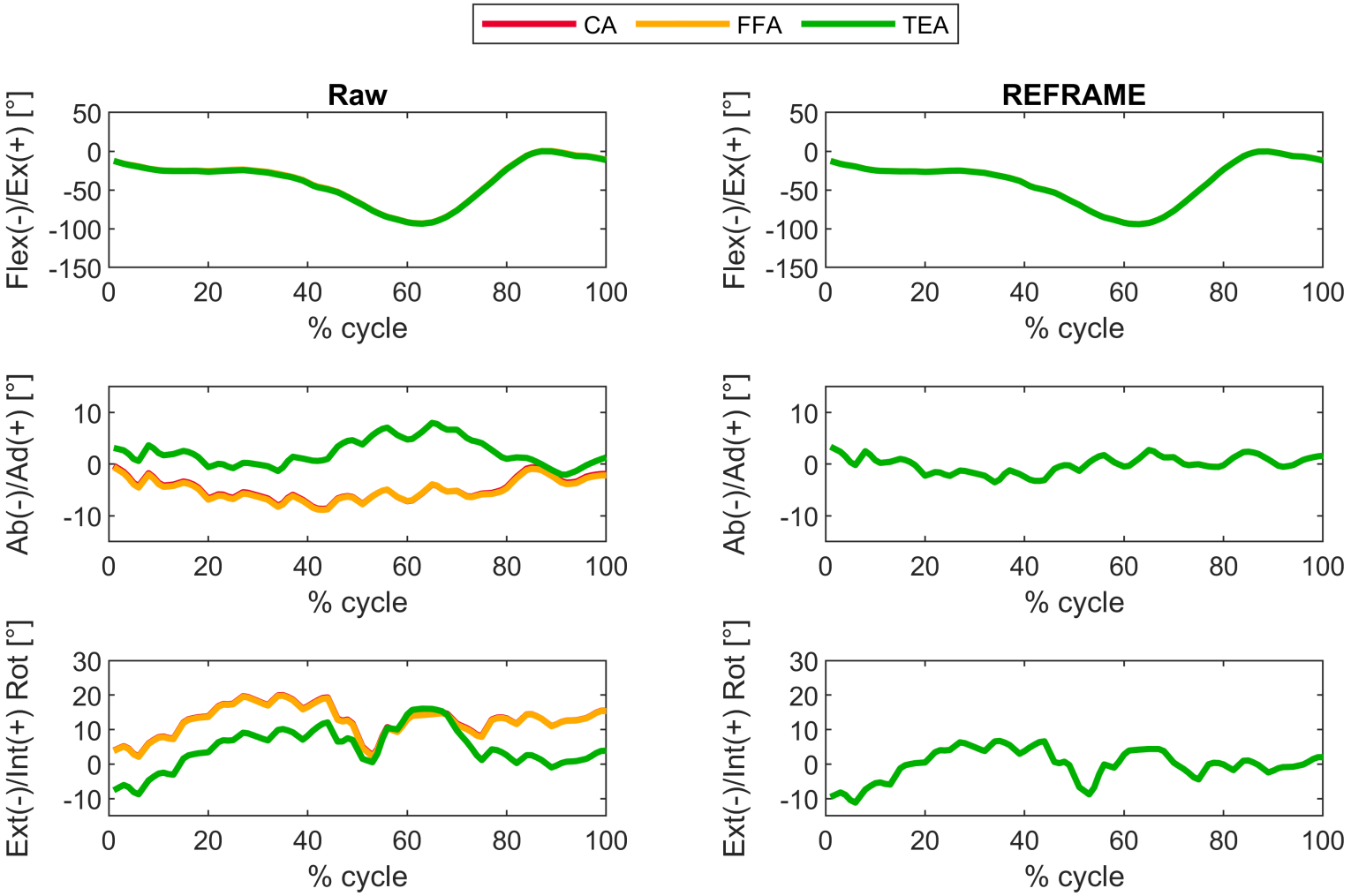

Supplementary Figure S31: Subject 3; Trial 4 – Rotational kinematics: Joint rotations (in degrees) of the tibial relative to the femoral segment frame for one cycle of stair descent, before (raw) and after REFRAME optimisation, for all three axis approaches (CA: cylindrical axis; FFA: functional flexion axis; TEA: transepicondylar axis). CA, FFA and TEA signals are shown in **all** subplots, but due to curve overlap in right-hand side plots, CA and FFA are covered by TEA. Note to readers from a clinical background: knee extension is illustrated here as **positive** because following the right-hand rule it corresponds with a positive rotation around the laterally pointing mediolateral axis for a right knee.

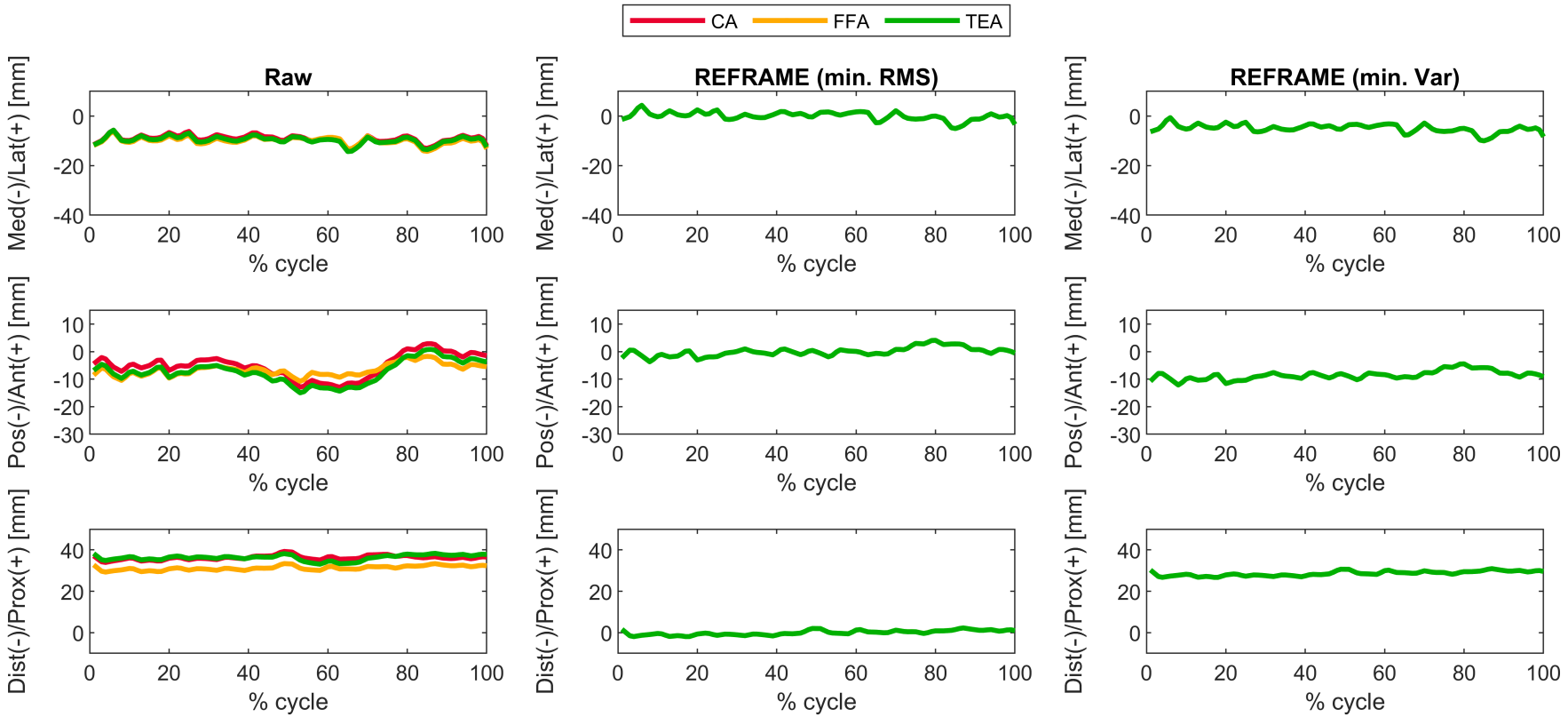

Supplementary Figure S32: Subject 3; Trial 4 – Translational kinematics: Joint translations (in mm) of the femoral relative to the tibial origin for one cycle of stair descent, before (raw, first column) and after application of the REFRAME optimisation (second column: based on the minimisation of translational root-mean-square; third column: based on the minimisation of translational variances), for all three axis approaches (CA: cylindrical axis; FFA: functional flexion axis; TEA: transepicondylar axis). CA, FFA and TEA signals are shown in **all** subplots, but due to curve overlap in the second and third columns, CA and FFA are covered by TEA.

3.3.5 Trial 5

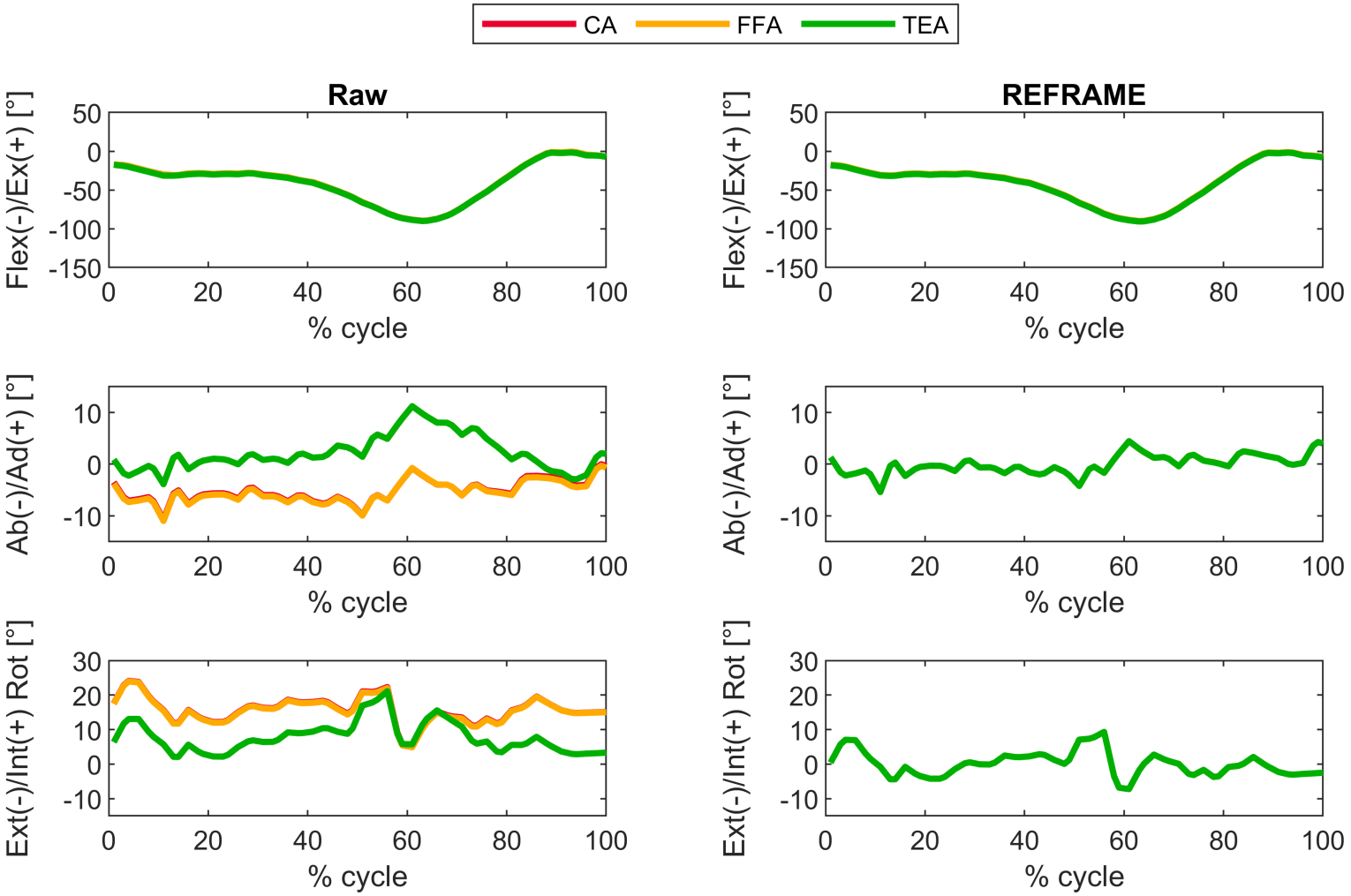

Supplementary Figure S33: Subject 3; Trial 5 – Rotational kinematics: Joint rotations (in degrees) of the tibial relative to the femoral segment frame for one cycle of stair descent, before (raw) and after REFRAME optimisation, for all three axis approaches (CA: cylindrical axis; FFA: functional flexion axis; TEA: transepicondylar axis). CA, FFA and TEA signals are shown in **all** subplots, but due to curve overlap in right-hand side plots, CA and FFA are covered by TEA. Note to readers from a clinical background: knee extension is illustrated here as **positive** because following the right-hand rule it corresponds with a positive rotation around the laterally pointing mediolateral axis for a right knee.

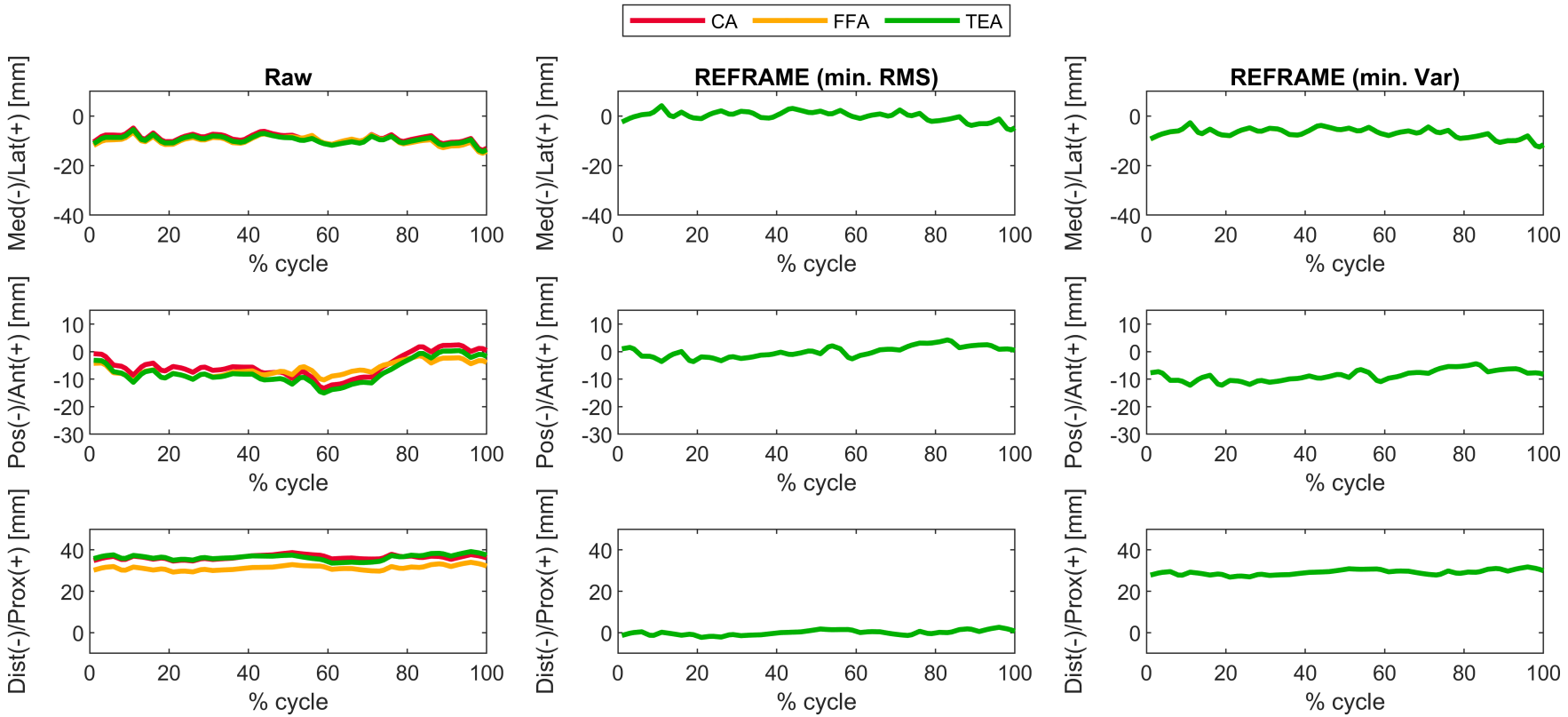

Supplementary Figure S34: Subject 3; Trial 5 – Translational kinematics: Joint translations (in mm) of the femoral relative to the tibial origin for one cycle of stair descent, before (raw, first column) and after application of the REFRAME optimisation (second column: based on the minimisation of translational root-mean-square; third column: based on the minimisation of translational variances), for all three axis approaches (CA: cylindrical axis; FFA: functional flexion axis; TEA: transepicondylar axis). CA, FFA and TEA signals are shown in **all** subplots, but due to curve overlap in the second and third columns, CA and FFA are covered by TEA.

3.4 Subject 4

3.4.1 Trial 1

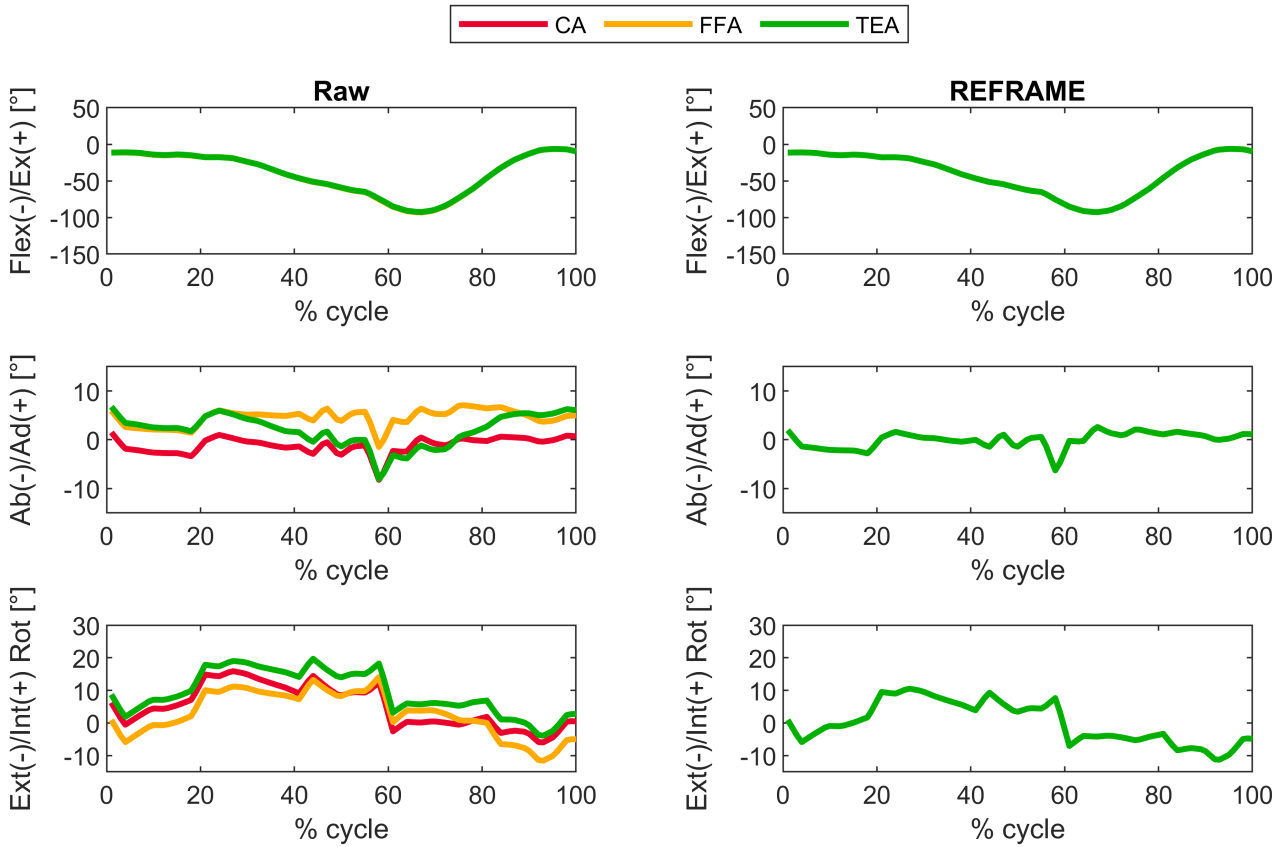

Supplementary Figure S35: Subject 4; Trial 1 – Rotational kinematics: Joint rotations (in degrees) of the tibial relative to the femoral segment frame for one cycle of stair descent, before (raw) and after REFRAME optimisation, for all three axis approaches (CA: cylindrical axis; FFA: functional flexion axis; TEA: transepicondylar axis). CA, FFA and TEA signals are shown in **all** subplots, but due to curve overlap in right-hand side plots, CA and FFA are covered by TEA. Note to readers from a clinical background: knee extension is illustrated here as **positive** because following the right-hand rule it corresponds with a positive rotation around the laterally pointing mediolateral axis for a right knee.

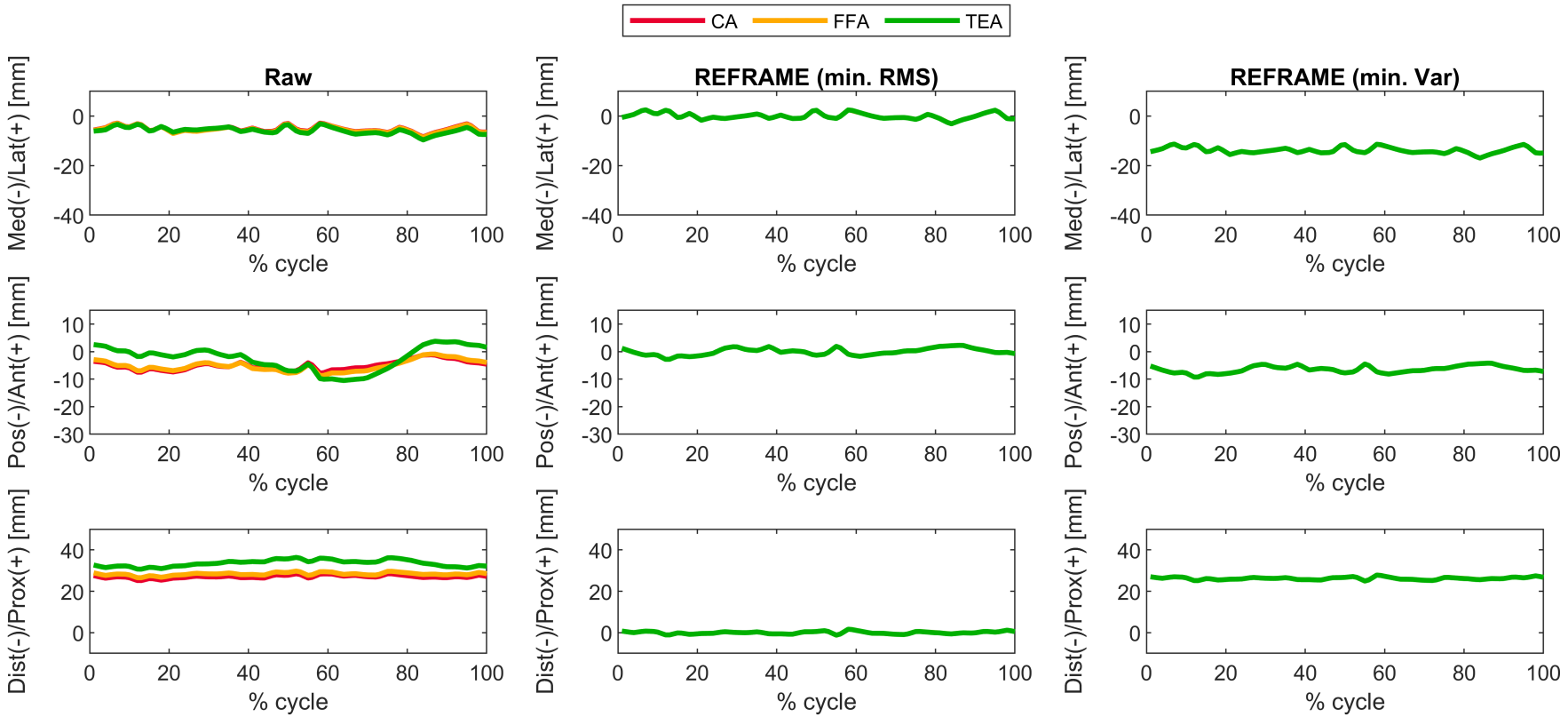

Supplementary Figure S36: Subject 4; Trial 1 – Translational kinematics: Joint translations (in mm) of the femoral relative to the tibial origin for one cycle of stair descent, before (raw, first column) and after application of the REFRAME optimisation (second column: based on the minimisation of translational root-mean-square; third column: based on the minimisation of translational variances), for all three axis approaches (CA: cylindrical axis; FFA: functional flexion axis; TEA: transepicondylar axis). CA, FFA and TEA signals are shown in **all** subplots, but due to curve overlap in the second and third columns, CA and FFA are covered by TEA.

3.4.2 Trial 2

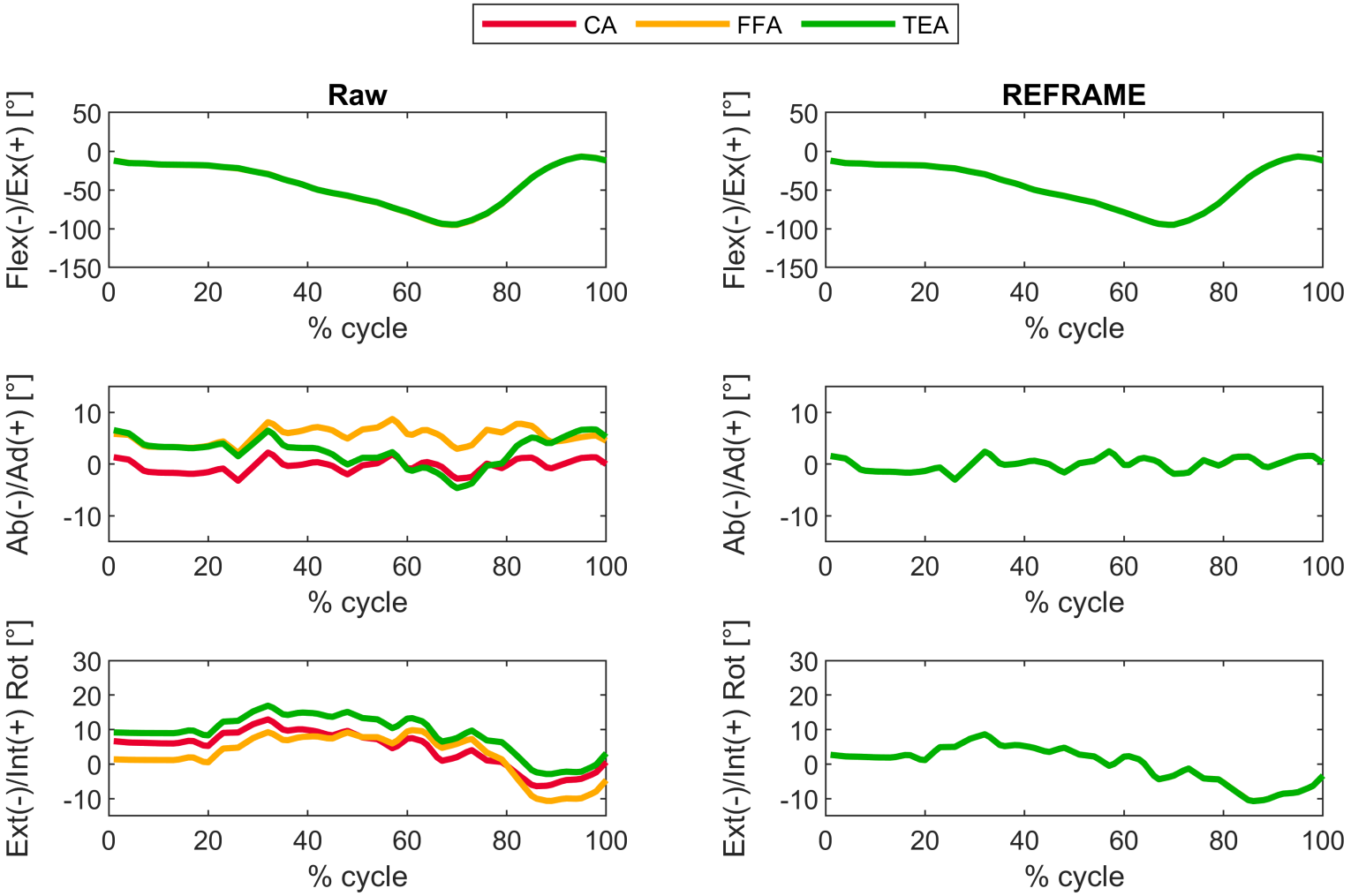

Supplementary Figure S37: Subject 4; Trial 2 – Rotational kinematics: Joint rotations (in degrees) of the tibial relative to the femoral segment frame for one cycle of stair descent, before (raw) and after REFRAME optimisation, for all three axis approaches (CA: cylindrical axis; FFA: functional flexion axis; TEA: transepicondylar axis). CA, FFA and TEA signals are shown in **all** subplots, but due to curve overlap in right-hand side plots, CA and FFA are covered by TEA. Note to readers from a clinical background: knee extension is illustrated here as **positive** because following the right-hand rule it corresponds with a positive rotation around the laterally pointing mediolateral axis for a right knee.

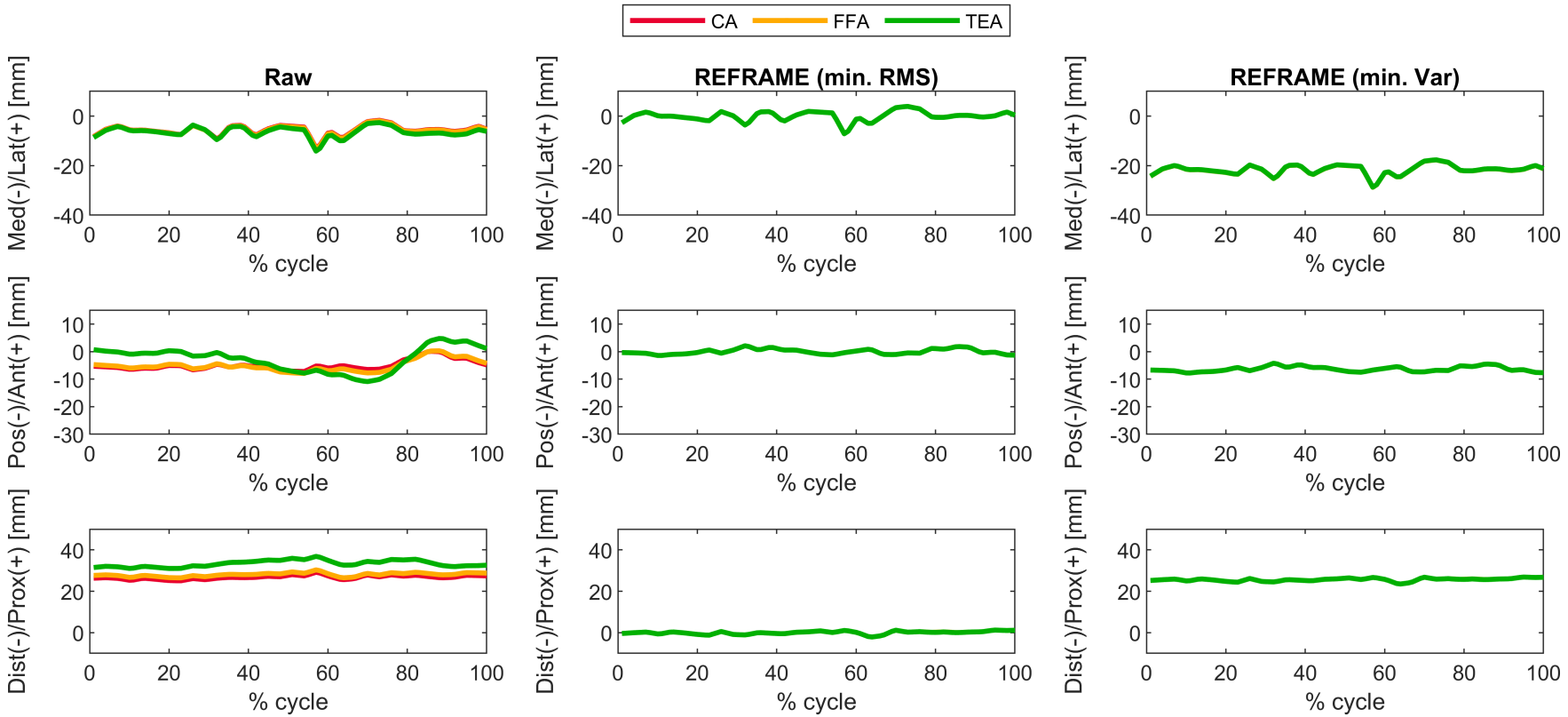

Supplementary Figure S38: Subject 4; Trial 2 – Translational kinematics: Joint translations (in mm) of the femoral relative to the tibial origin for one cycle of stair descent, before (raw, first column) and after application of the REFRAME optimisation (second column: based on the minimisation of translational root-mean-square; third column: based on the minimisation of translational variances), for all three axis approaches (CA: cylindrical axis; FFA: functional flexion axis; TEA: transepicondylar axis). CA, FFA and TEA signals are shown in **all** subplots, but due to curve overlap in the second and third columns, CA and FFA are covered by TEA.

3.4.3 Trial 3

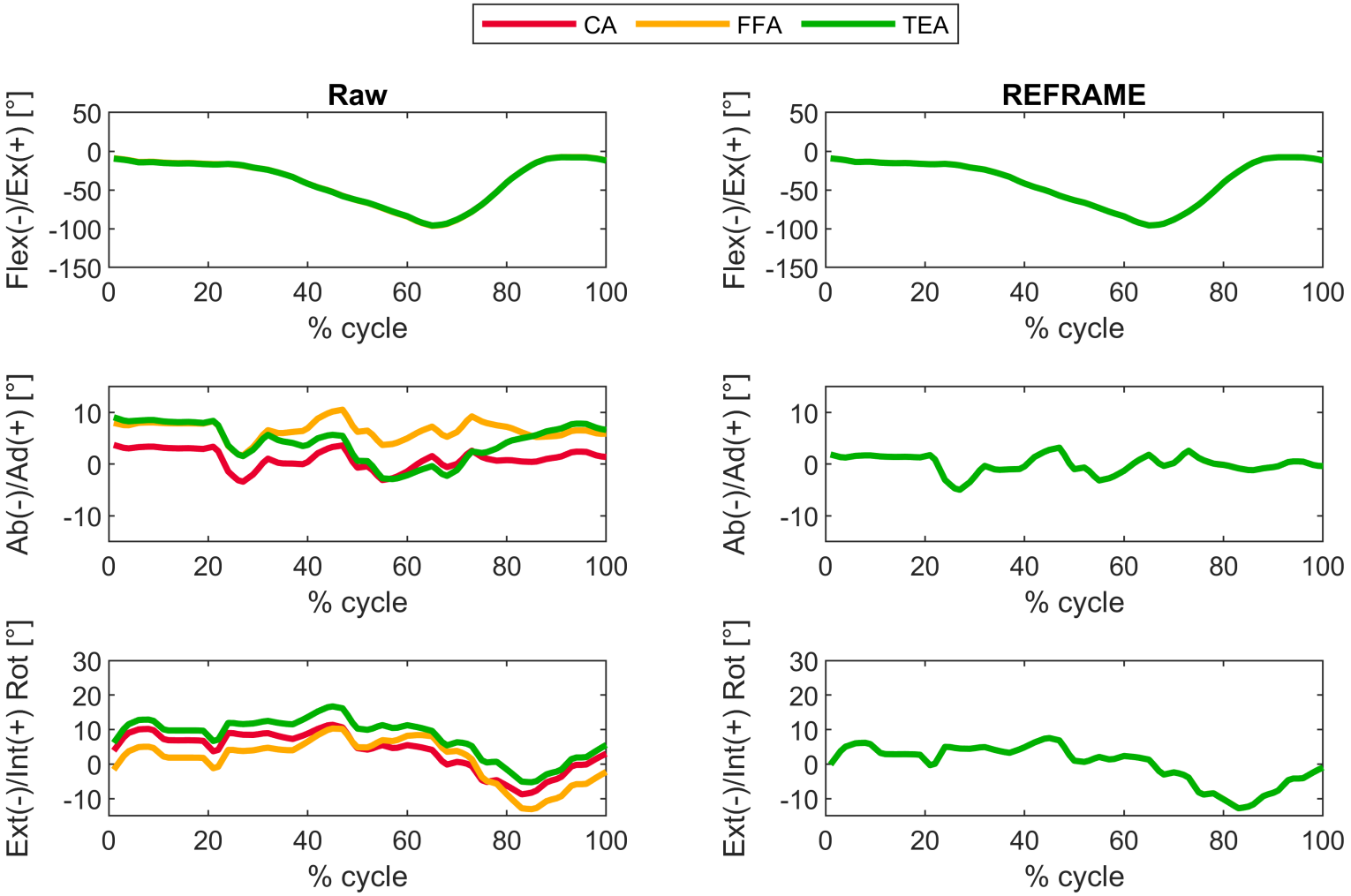

Supplementary Figure S39: Subject 4; Trial 3 – Rotational kinematics: Joint rotations (in degrees) of the tibial relative to the femoral segment frame for one cycle of stair descent, before (raw) and after REFRAME optimisation, for all three axis approaches (CA: cylindrical axis; FFA: functional flexion axis; TEA: transepicondylar axis). CA, FFA and TEA signals are shown in **all** subplots, but due to curve overlap in right-hand side plots, CA and FFA are covered by TEA. Note to readers from a clinical background: knee extension is illustrated here as **positive** because following the right-hand rule it corresponds with a positive rotation around the laterally pointing mediolateral axis for a right knee.

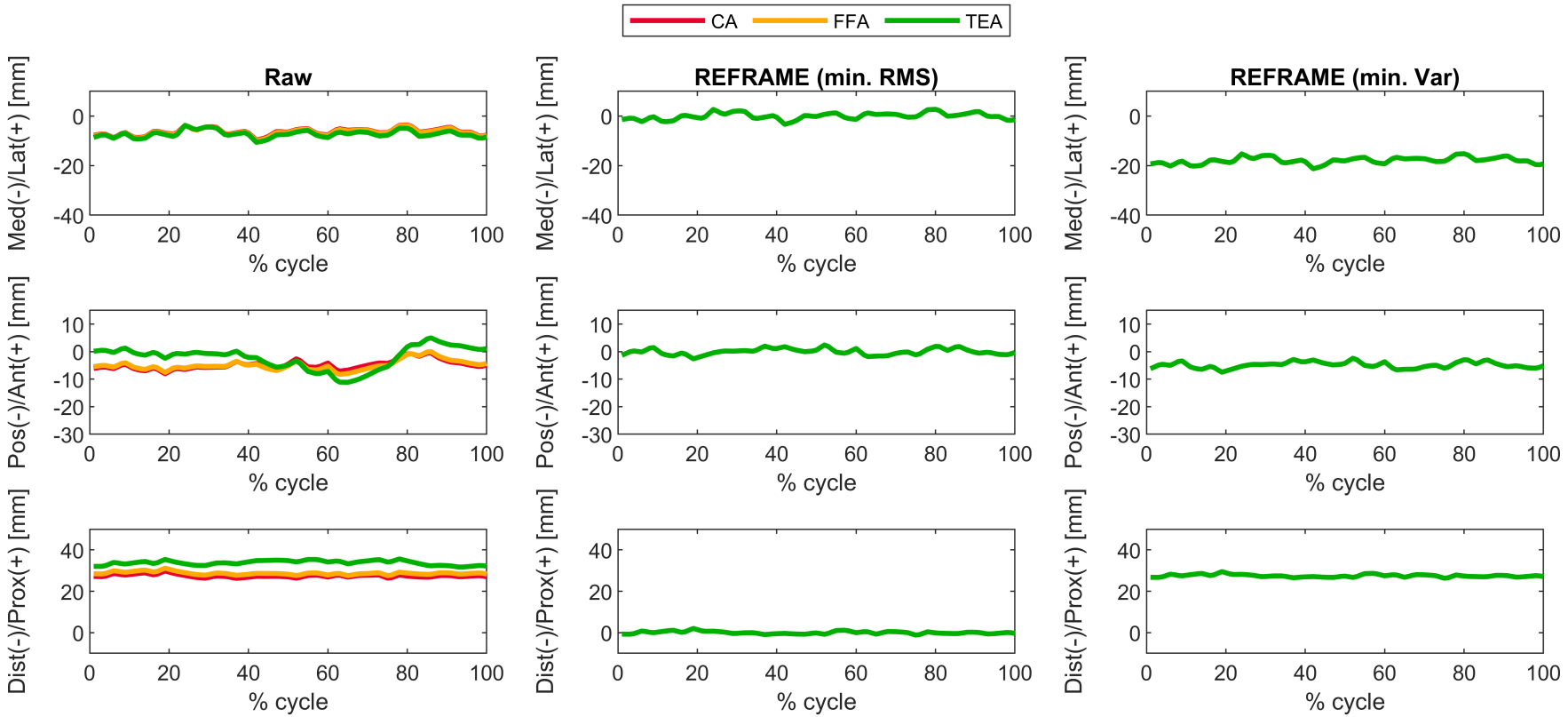

Supplementary Figure S40: Subject 4; Trial 3 – Translational kinematics: Joint translations (in mm) of the femoral relative to the tibial origin for one cycle of stair descent, before (raw, first column) and after application of the REFRAME optimisation (second column: based on the minimisation of translational root-mean-square; third column: based on the minimisation of translational variances), for all three axis approaches (CA: cylindrical axis; FFA: functional flexion axis; TEA: transepicondylar axis). CA, FFA and TEA signals are shown in **all** subplots, but due to curve overlap in the second and third columns, CA and FFA are covered by TEA.

3.4.4 Trial 4

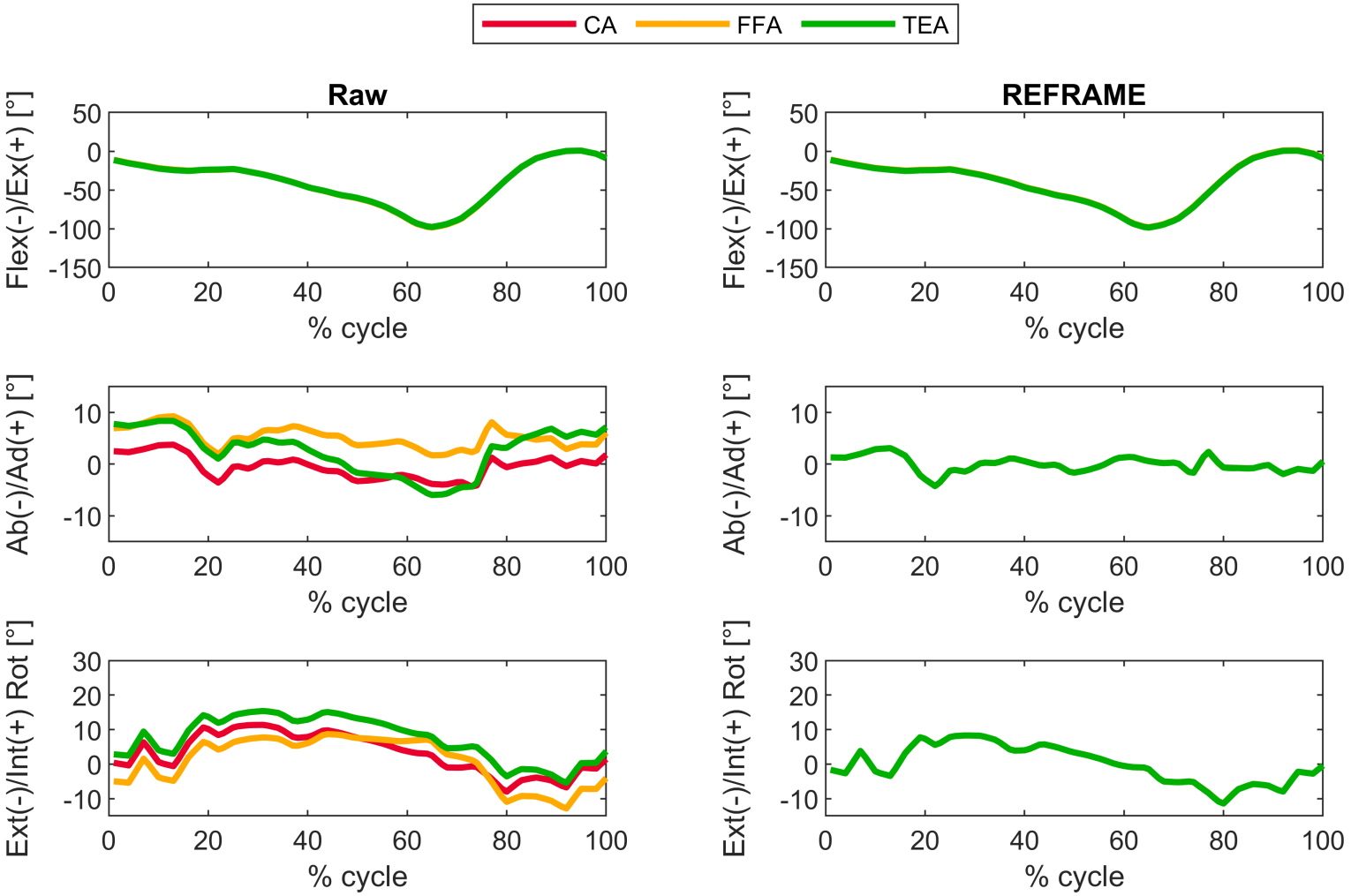

Supplementary Figure S41: Subject 4; Trial 4 – Rotational kinematics: Joint rotations (in degrees) of the tibial relative to the femoral segment frame for one cycle of stair descent, before (raw) and after REFRAME optimisation, for all three axis approaches (CA: cylindrical axis; FFA: functional flexion axis; TEA: transepicondylar axis). CA, FFA and TEA signals are shown in **all** subplots, but due to curve overlap in right-hand side plots, CA and FFA are covered by TEA. Note to readers from a clinical background: knee extension is illustrated here as **positive** because following the right-hand rule it corresponds with a positive rotation around the laterally pointing mediolateral axis for a right knee.

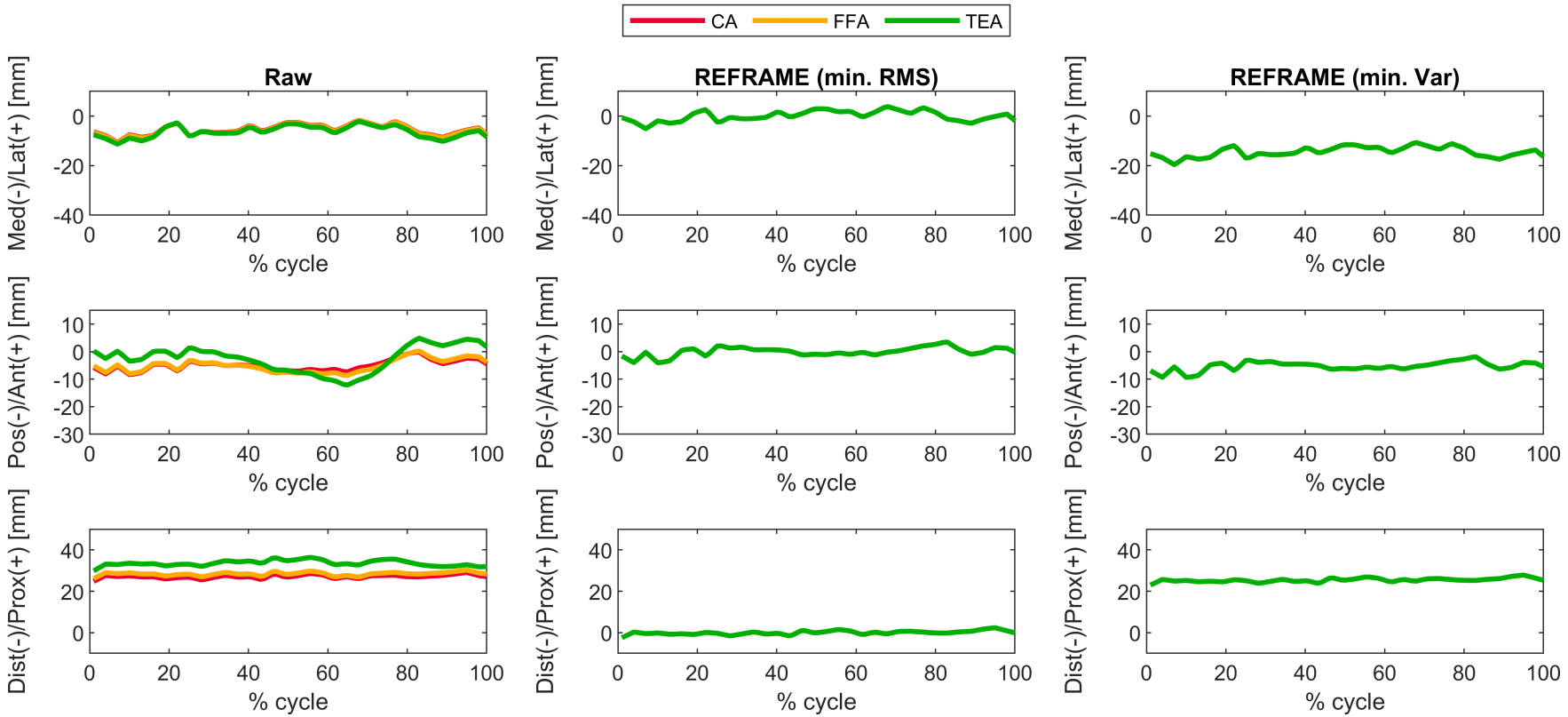

Supplementary Figure S42: Subject 4; Trial 4 – Translational kinematics: Joint translations (in mm) of the femoral relative to the tibial origin for one cycle of stair descent, before (raw, first column) and after application of the REFRAME optimisation (second column: based on the minimisation of translational root-mean-square; third column: based on the minimisation of translational variances), for all three axis approaches (CA: cylindrical axis; FFA: functional flexion axis; TEA: transepicondylar axis). CA, FFA and TEA signals are shown in **all** subplots, but due to curve overlap in the second and third columns, CA and FFA are covered by TEA.

3.4.5 Trial 5

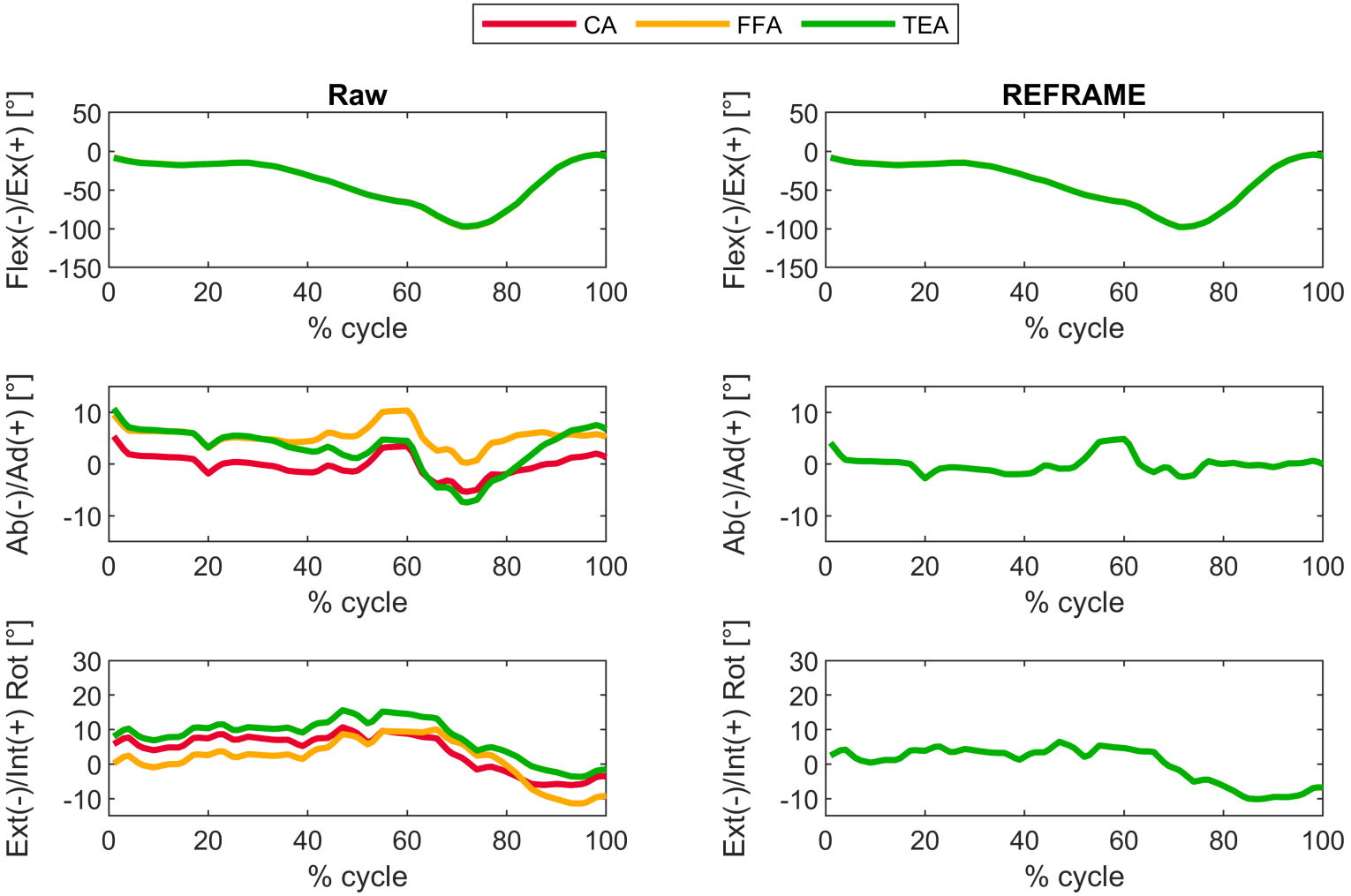

Supplementary Figure S43: Subject 4; Trial 5 – Rotational kinematics: Joint rotations (in degrees) of the tibial relative to the femoral segment frame for one cycle of stair descent, before (raw) and after REFRAME optimisation, for all three axis approaches (CA: cylindrical axis; FFA: functional flexion axis; TEA: transepicondylar axis). CA, FFA and TEA signals are shown in **all** subplots, but due to curve overlap in right-hand side plots, CA and FFA are covered by TEA. Note to readers from a clinical background: knee extension is illustrated here as **positive** because following the right-hand rule it corresponds with a positive rotation around the laterally pointing mediolateral axis for a right knee.

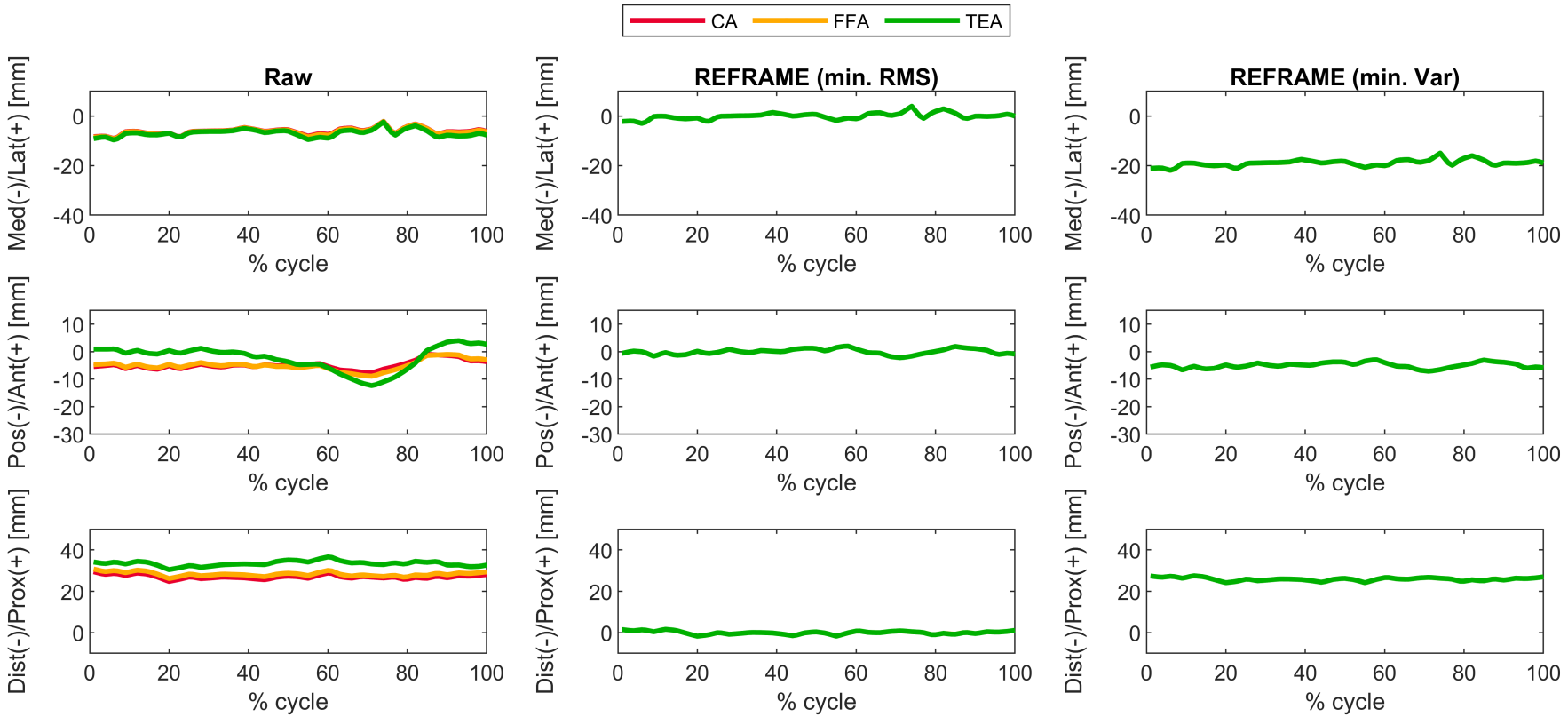

Supplementary Figure S44: Subject 4; Trial 5 – Translational kinematics: Joint translations (in mm) of the femoral relative to the tibial origin for one cycle of stair descent, before (raw, first column) and after application of the REFRAME optimisation (second column: based on the minimisation of translational root-mean-square; third column: based on the minimisation of translational variances), for all three axis approaches (CA: cylindrical axis; FFA: functional flexion axis; TEA: transepicondylar axis). CA, FFA and TEA signals are shown in **all** subplots, but due to curve overlap in the second and third columns, CA and FFA are covered by TEA.

3.5 Subject 5

3.5.1 Trial 1

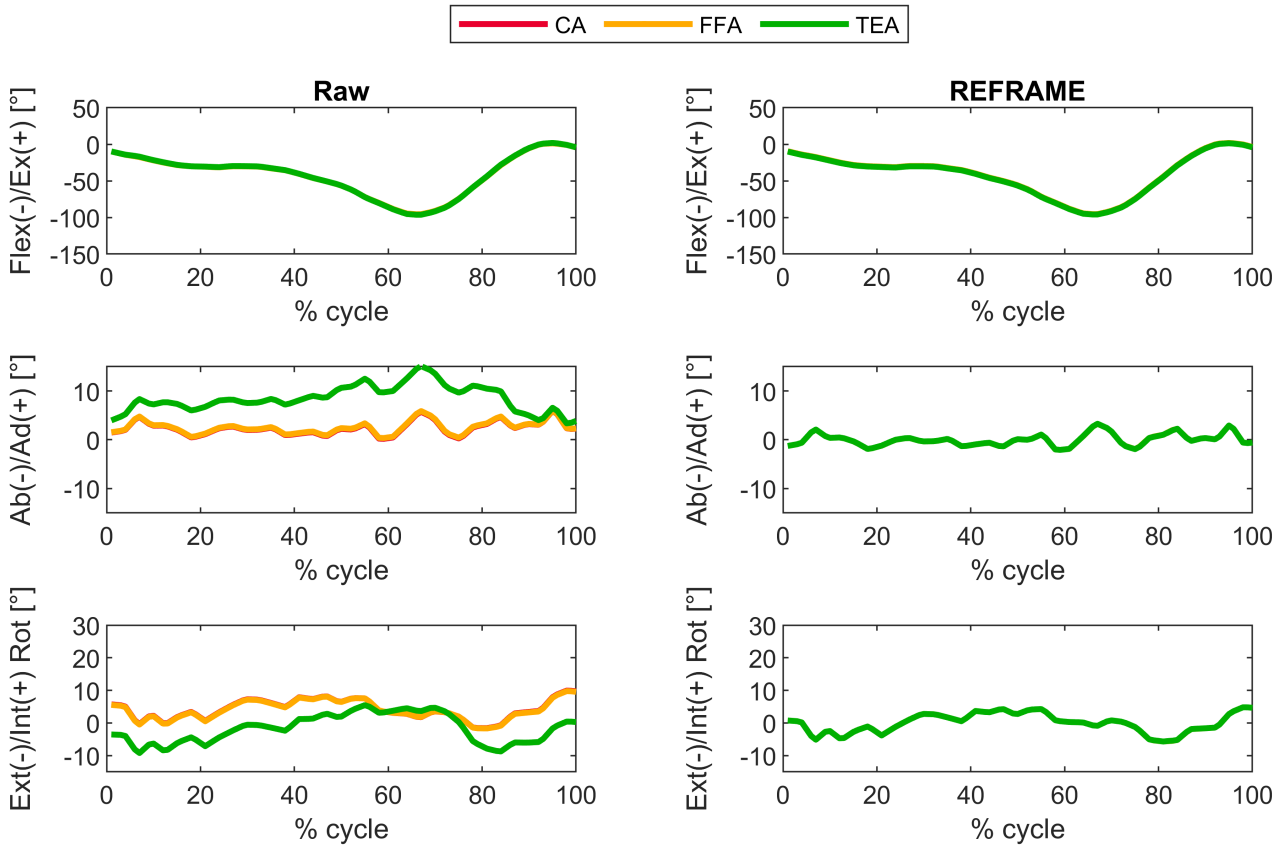

Supplementary Figure S45: Subject 5; Trial 1 – Rotational kinematics: Joint rotations (in degrees) of the tibial relative to the femoral segment frame for one cycle of stair descent, before (raw) and after REFRAME optimisation, for all three axis approaches (CA: cylindrical axis; FFA: functional flexion axis; TEA: transepicondylar axis). CA, FFA and TEA signals are shown in **all** subplots, but due to curve overlap in right-hand side plots, CA and FFA are covered by TEA. Note to readers from a clinical background: knee extension is illustrated here as **positive** because following the right-hand rule it corresponds with a positive rotation around the laterally pointing mediolateral axis for a right knee.

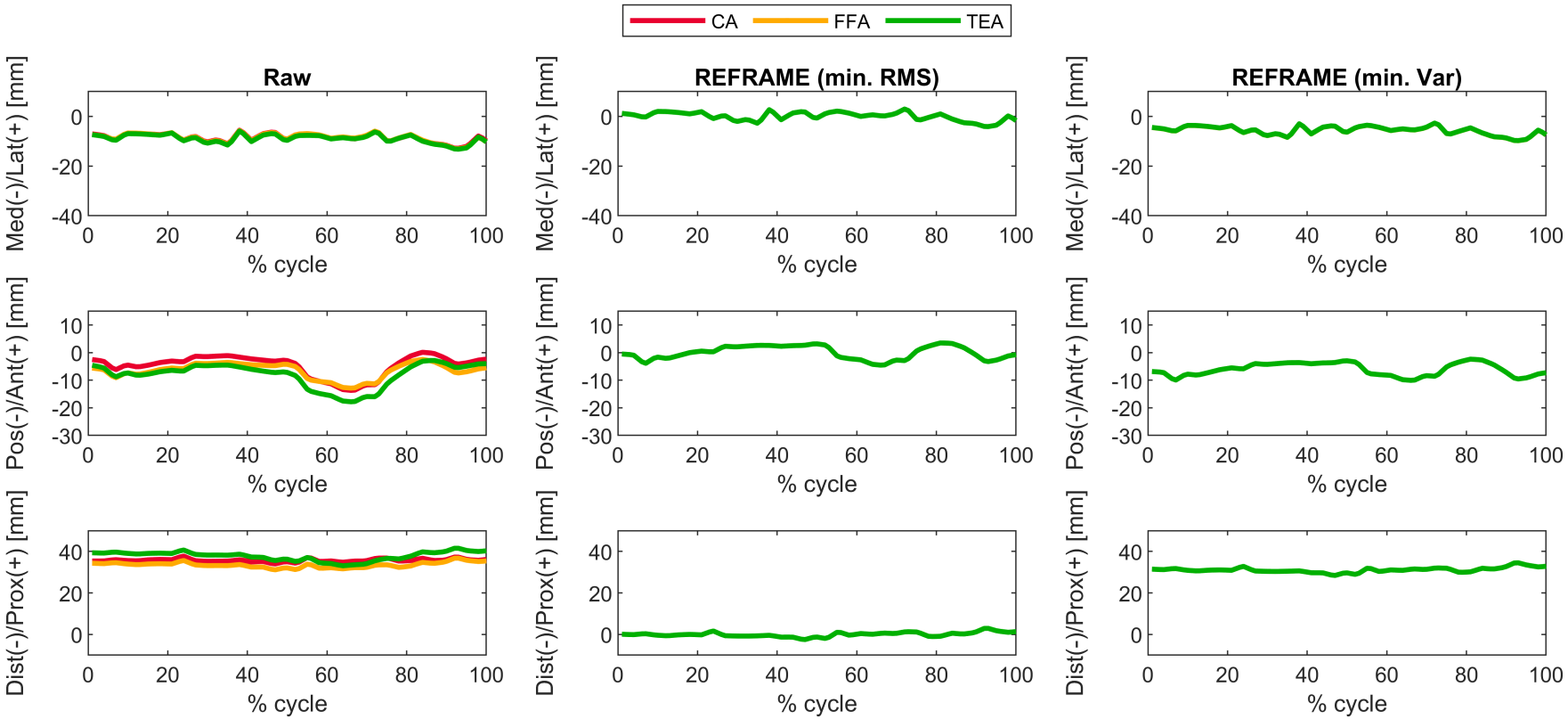

Supplementary Figure S46: Subject 5; Trial 1 – Translational kinematics: Joint translations (in mm) of the femoral relative to the tibial origin for one cycle of stair descent, before (raw, first column) and after application of the REFRAME optimisation (second column: based on the minimisation of translational root-mean-square; third column: based on the minimisation of translational variances), for all three axis approaches (CA: cylindrical axis; FFA: functional flexion axis; TEA: transepicondylar axis). CA, FFA and TEA signals are shown in **all** subplots, but due to curve overlap in the second and third columns, CA and FFA are covered by TEA.

3.5.2 Trial 2

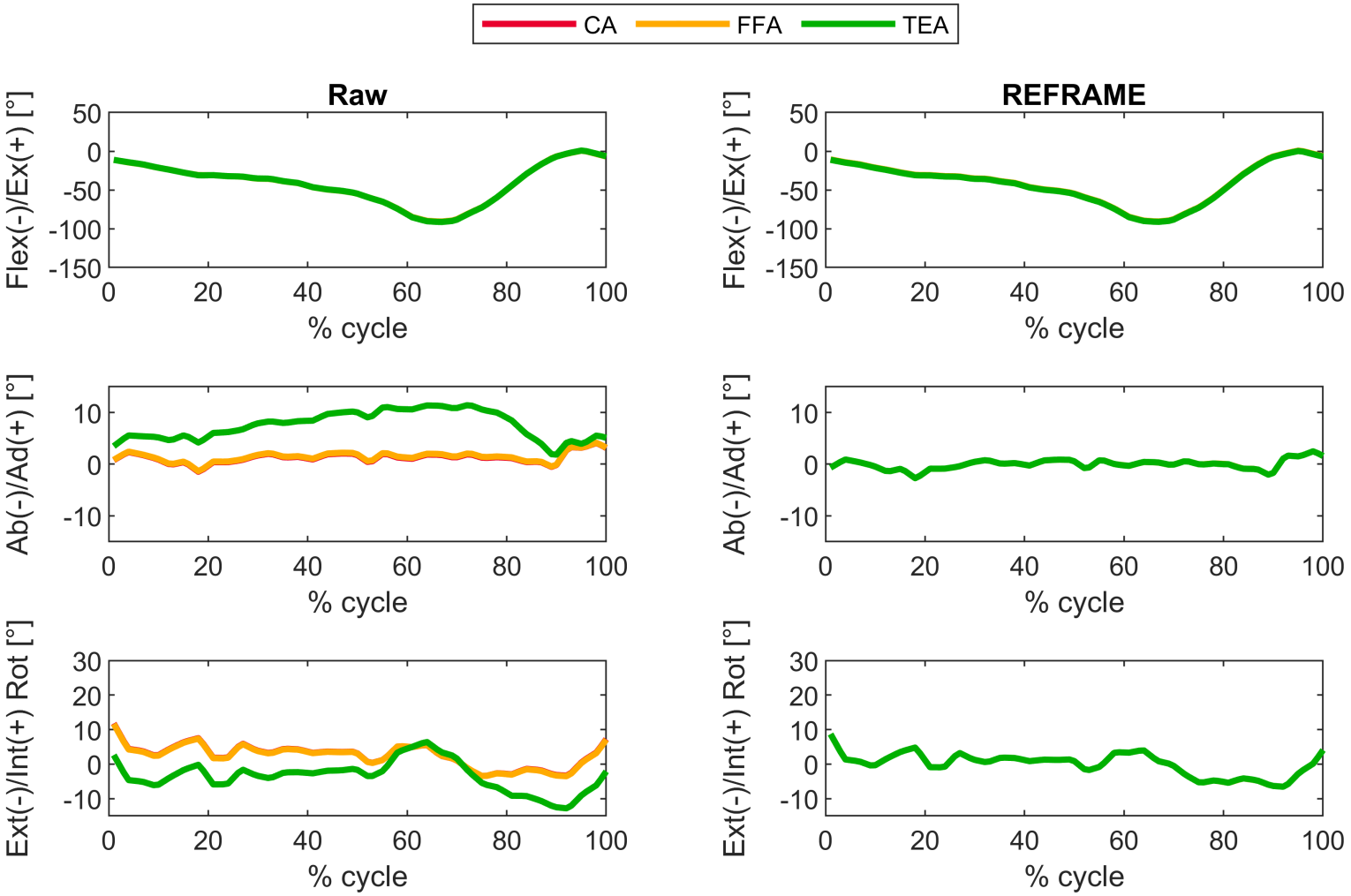

Supplementary Figure S47: Subject 5; Trial 2 – Rotational kinematics: Joint rotations (in degrees) of the tibial relative to the femoral segment frame for one cycle of stair descent, before (raw) and after REFRAME optimisation, for all three axis approaches (CA: cylindrical axis; FFA: functional flexion axis; TEA: transepicondylar axis). CA, FFA and TEA signals are shown in **all** subplots, but due to curve overlap in right-hand side plots, CA and FFA are covered by TEA. Note to readers from a clinical background: knee extension is illustrated here as **positive** because following the right-hand rule it corresponds with a positive rotation around the laterally pointing mediolateral axis for a right knee.

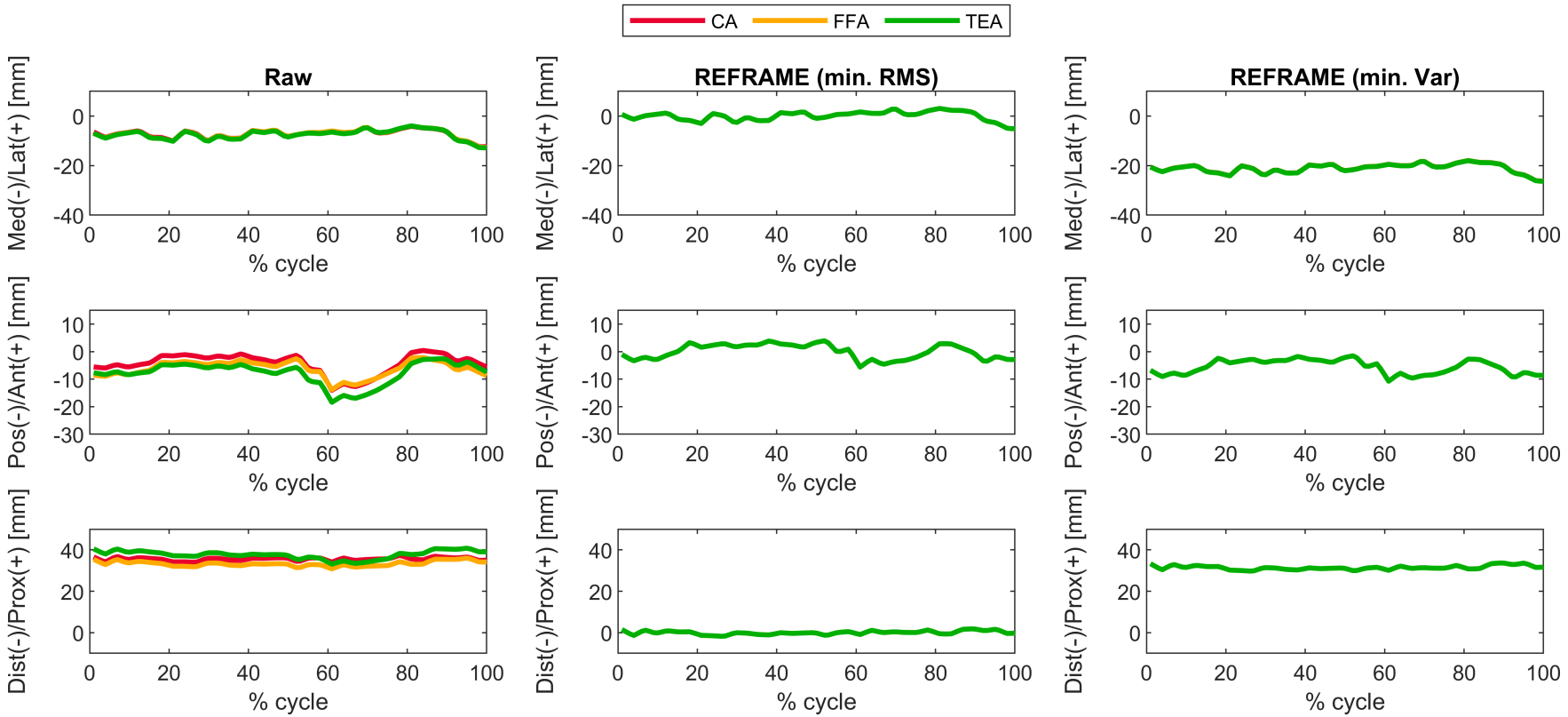

Supplementary Figure S48: Subject 5; Trial 2 – Translational kinematics: Joint translations (in mm) of the femoral relative to the tibial origin for one cycle of stair descent, before (raw, first column) and after application of the REFRAME optimisation (second column: based on the minimisation of translational root-mean-square; third column: based on the minimisation of translational variances), for all three axis approaches (CA: cylindrical axis; FFA: functional flexion axis; TEA: transepicondylar axis). CA, FFA and TEA signals are shown in **all** subplots, but due to curve overlap in the second and third columns, CA and FFA are covered by TEA.

3.5.3 Trial 3

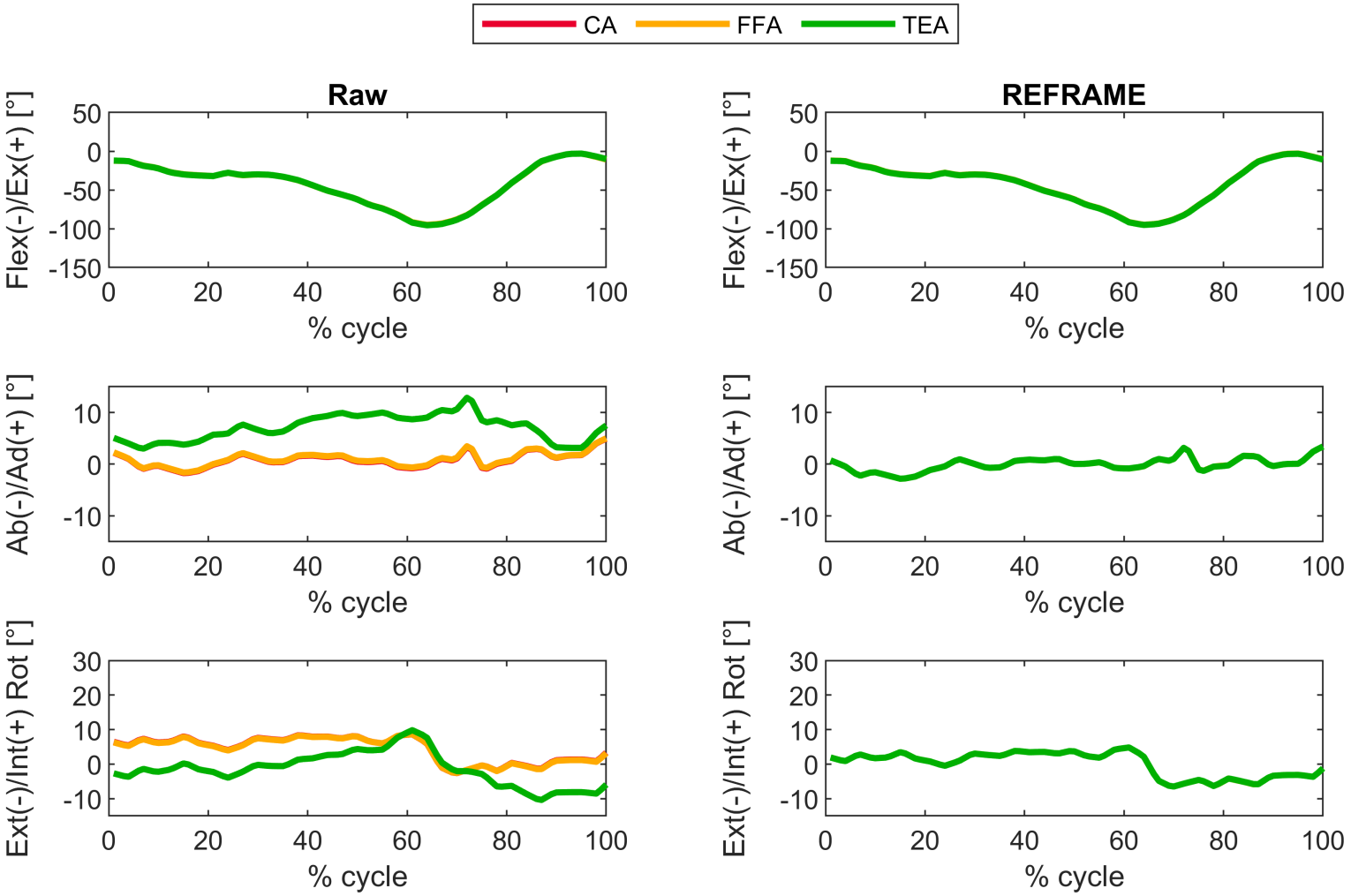

Supplementary Figure S49: Subject 5; Trial 3 – Rotational kinematics: Joint rotations (in degrees) of the tibial relative to the femoral segment frame for one cycle of stair descent, before (raw) and after REFRAME optimisation, for all three axis approaches (CA: cylindrical axis; FFA: functional flexion axis; TEA: transepicondylar axis). CA, FFA and TEA signals are shown in **all** subplots, but due to curve overlap in right-hand side plots, CA and FFA are covered by TEA. Note to readers from a clinical background: knee extension is illustrated here as **positive** because following the right-hand rule it corresponds with a positive rotation around the laterally pointing mediolateral axis for a right knee.

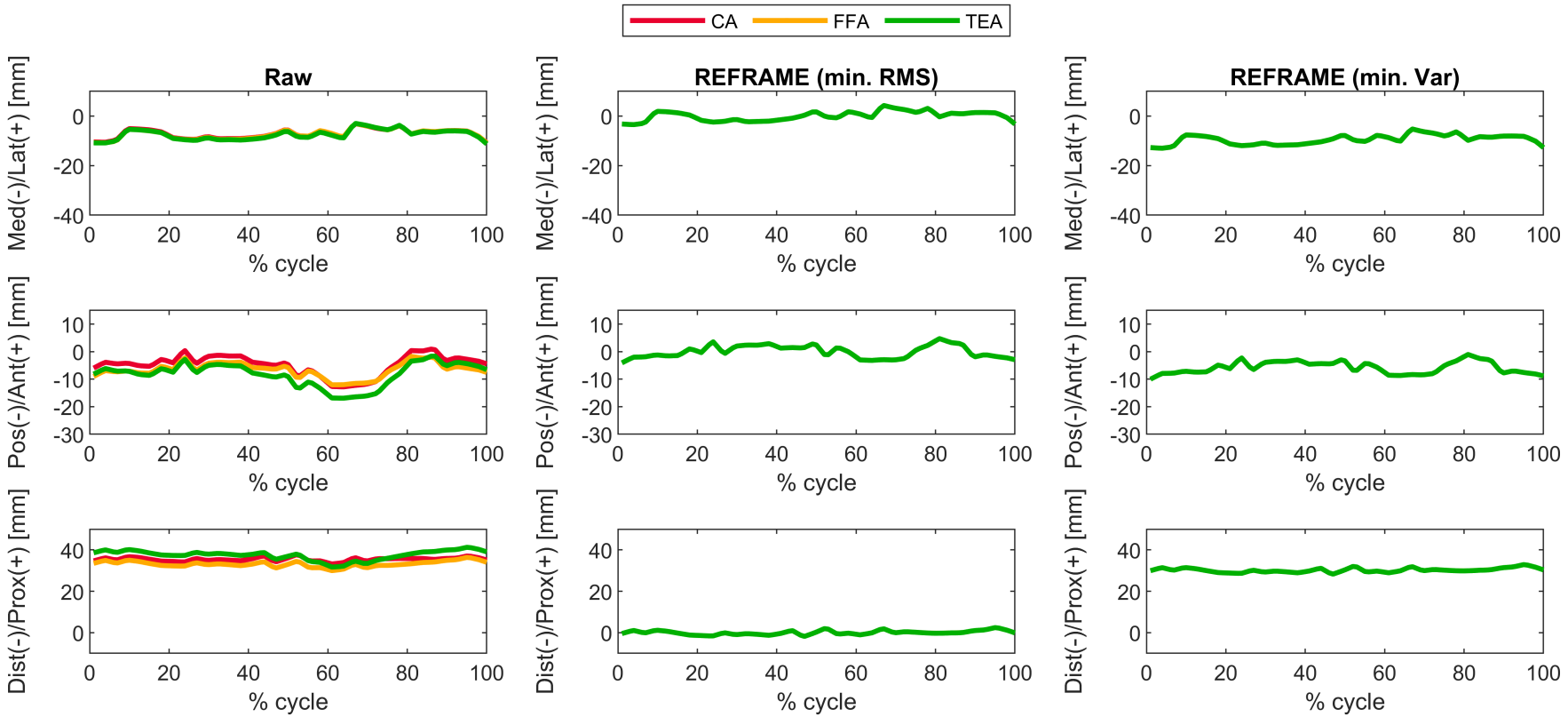

Supplementary Figure S50: Subject 5; Trial 3 – Translational kinematics: Joint translations (in mm) of the femoral relative to the tibial origin for one cycle of stair descent, before (raw, first column) and after application of the REFRAME optimisation (second column: based on the minimisation of translational root-mean-square; third column: based on the minimisation of translational variances), for all three axis approaches (CA: cylindrical axis; FFA: functional flexion axis; TEA: transepicondylar axis). CA, FFA and TEA signals are shown in **all** subplots, but due to curve overlap in the second and third columns, CA and FFA are covered by TEA.

3.5.4 Trial 4

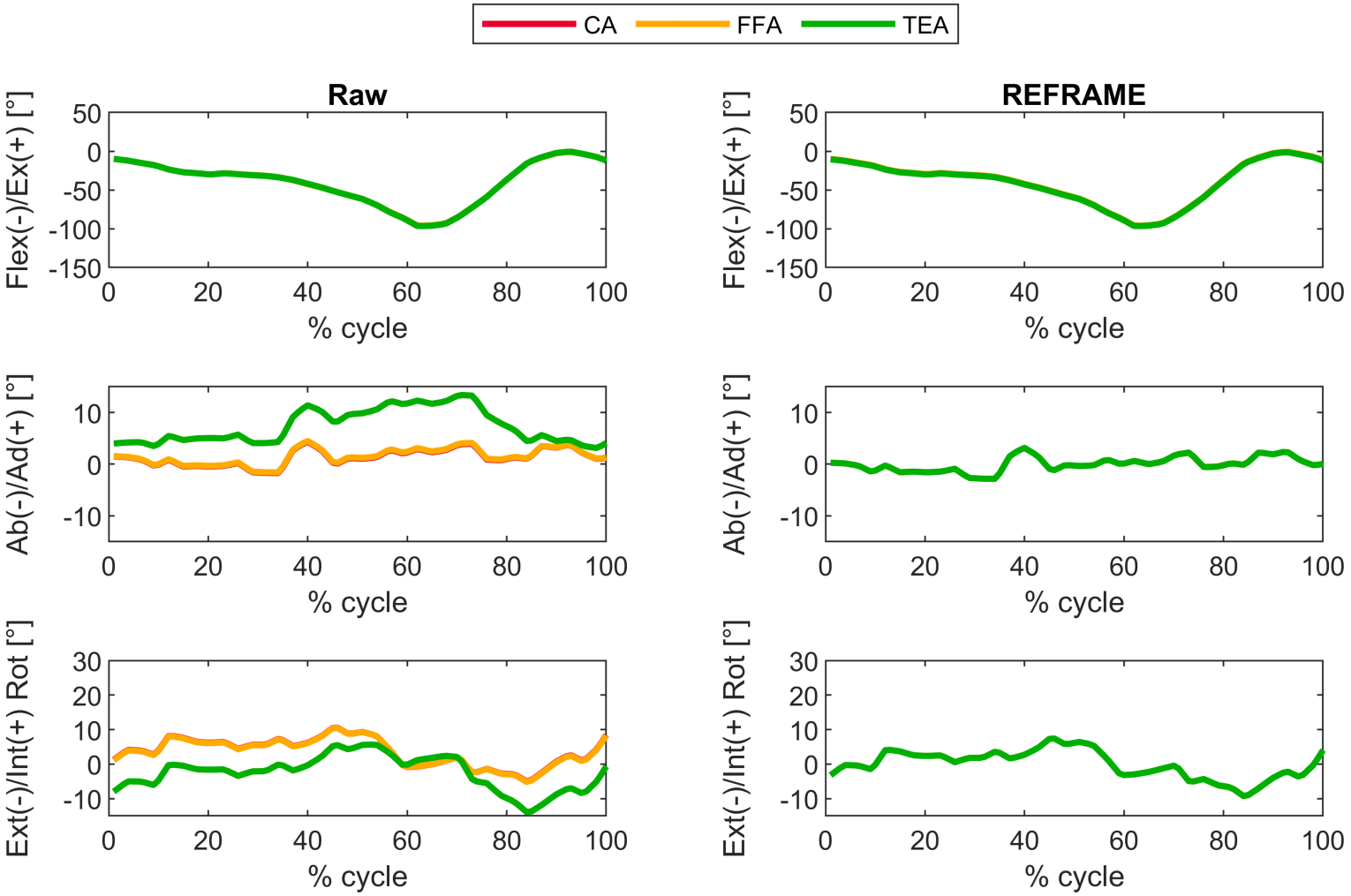

Supplementary Figure S51: Subject 5; Trial 4 – Rotational kinematics: Joint rotations (in degrees) of the tibial relative to the femoral segment frame for one cycle of stair descent, before (raw) and after REFRAME optimisation, for all three axis approaches (CA: cylindrical axis; FFA: functional flexion axis; TEA: transepicondylar axis). CA, FFA and TEA signals are shown in **all** subplots, but due to curve overlap in right-hand side plots, CA and FFA are covered by TEA. Note to readers from a clinical background: knee extension is illustrated here as **positive** because following the right-hand rule it corresponds with a positive rotation around the laterally pointing mediolateral axis for a right knee.

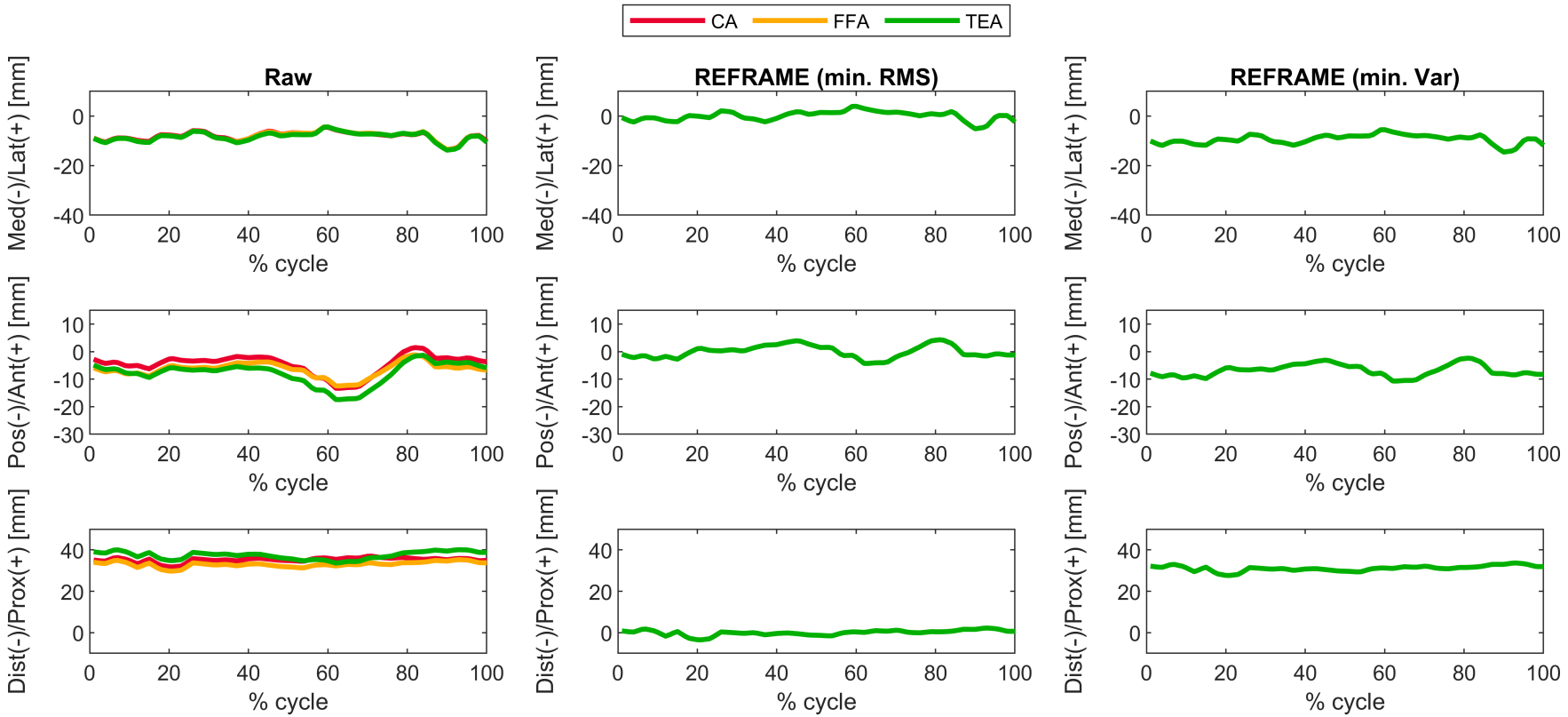

Supplementary Figure S52: Subject 5; Trial 4 – Translational kinematics: Joint translations (in mm) of the femoral relative to the tibial origin for one cycle of stair descent, before (raw, first column) and after application of the REFRAME optimisation (second column: based on the minimisation of translational root-mean-square; third column: based on the minimisation of translational variances), for all three axis approaches (CA: cylindrical axis; FFA: functional flexion axis; TEA: transepicondylar axis). CA, FFA and TEA signals are shown in **all** subplots, but due to curve overlap in the second and third columns, CA and FFA are covered by TEA.

3.5.5 Trial 5

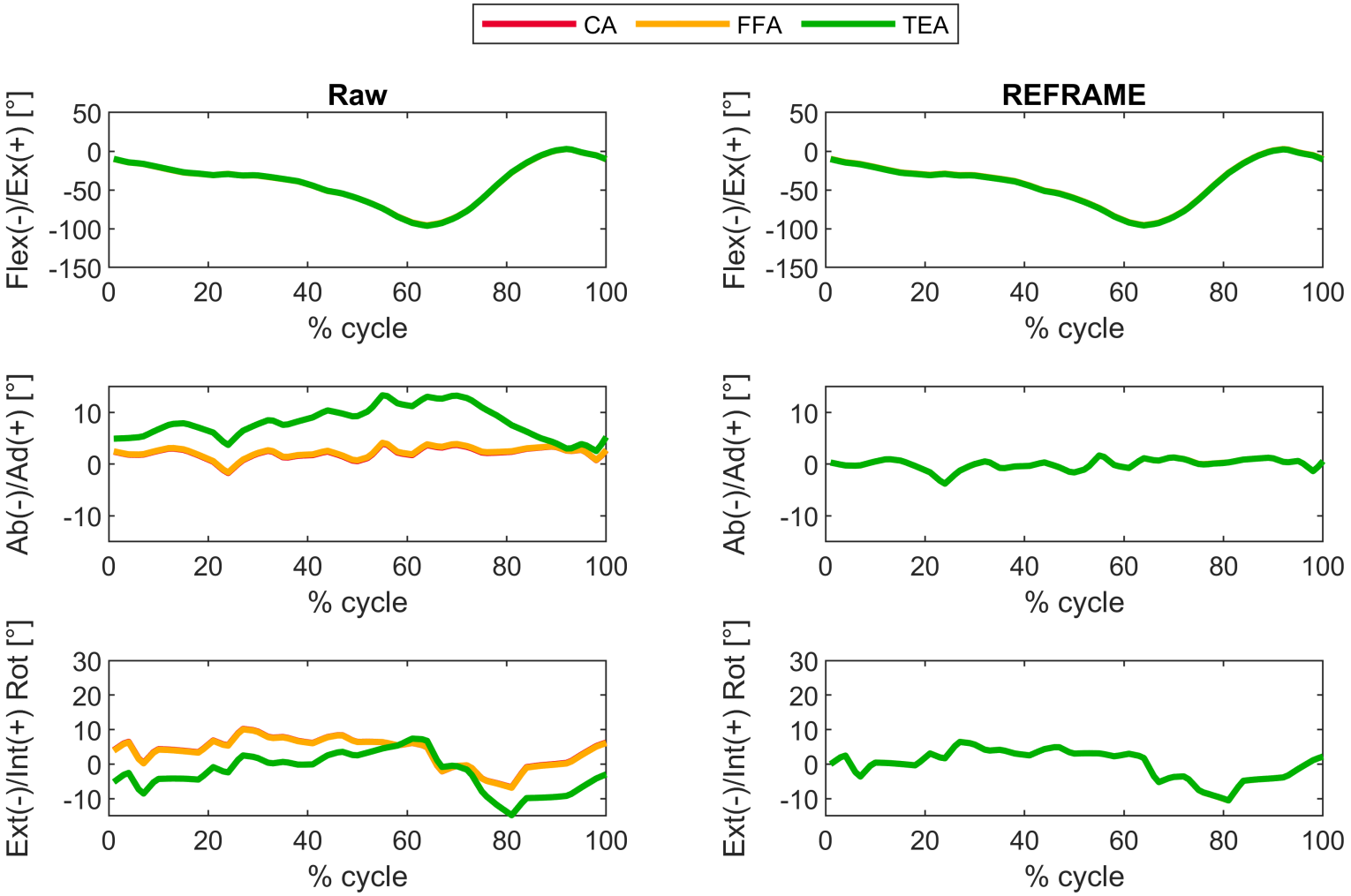

Supplementary Figure S53: Subject 5; Trial 5 – Rotational kinematics: Joint rotations (in degrees) of the tibial relative to the femoral segment frame for one cycle of stair descent, before (raw) and after REFRAME optimisation, for all three axis approaches (CA: cylindrical axis; FFA: functional flexion axis; TEA: transepicondylar axis). CA, FFA and TEA signals are shown in **all** subplots, but due to curve overlap in right-hand side plots, CA and FFA are covered by TEA. Note to readers from a clinical background: knee extension is illustrated here as **positive** because following the right-hand rule it corresponds with a positive rotation around the laterally pointing mediolateral axis for a right knee.

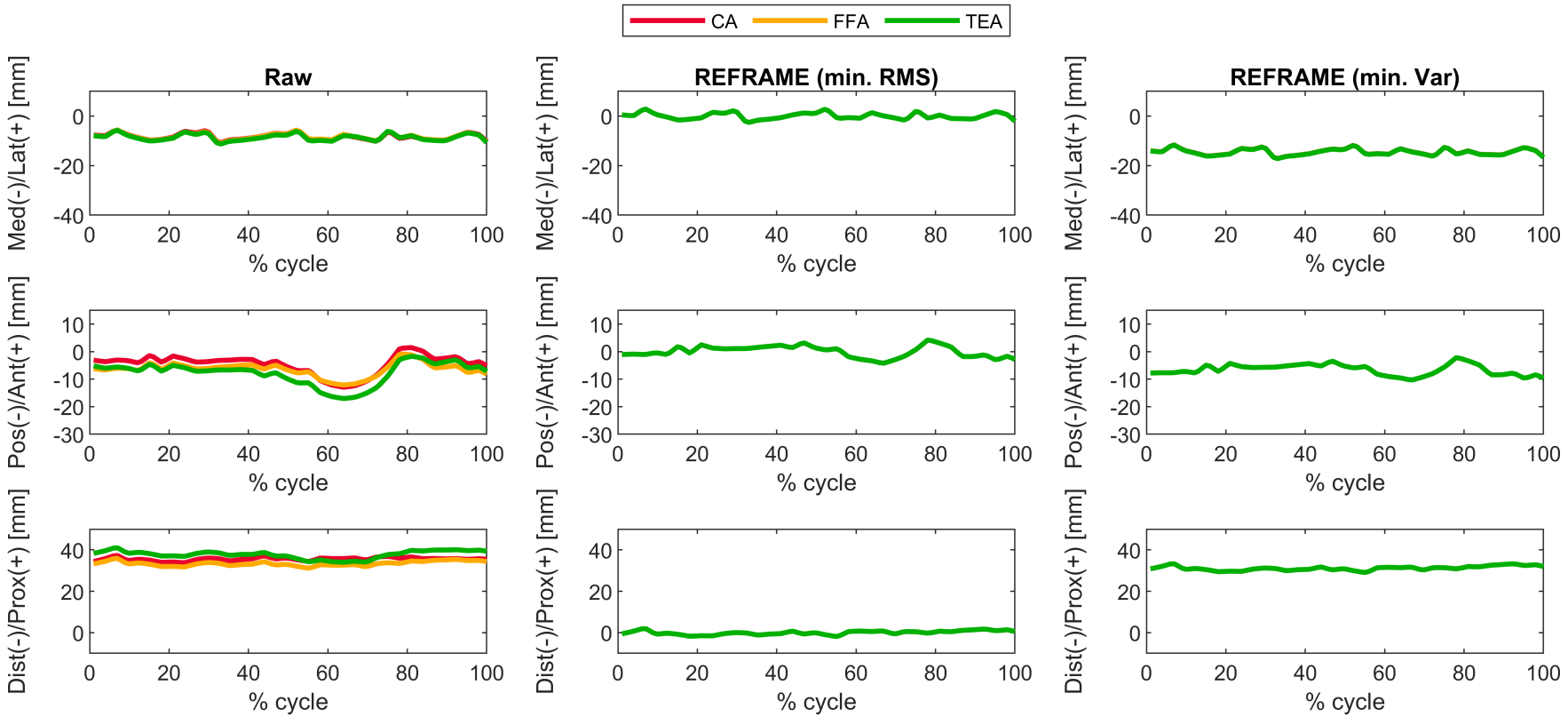

Supplementary Figure S54: Subject 5; Trial 5 – Translational kinematics: Joint translations (in mm) of the femoral relative to the tibial origin for one cycle of stair descent, before (raw, first column) and after application of the REFRAME optimisation (second column: based on the minimisation of translational root-mean-square; third column: based on the minimisation of translational variances), for all three axis approaches (CA: cylindrical axis; FFA: functional flexion axis; TEA: transepicondylar axis). CA, FFA and TEA signals are shown in **all** subplots, but due to curve overlap in the second and third columns, CA and FFA are covered by TEA.

3.6 Subject 6

3.6.1 Trial 1

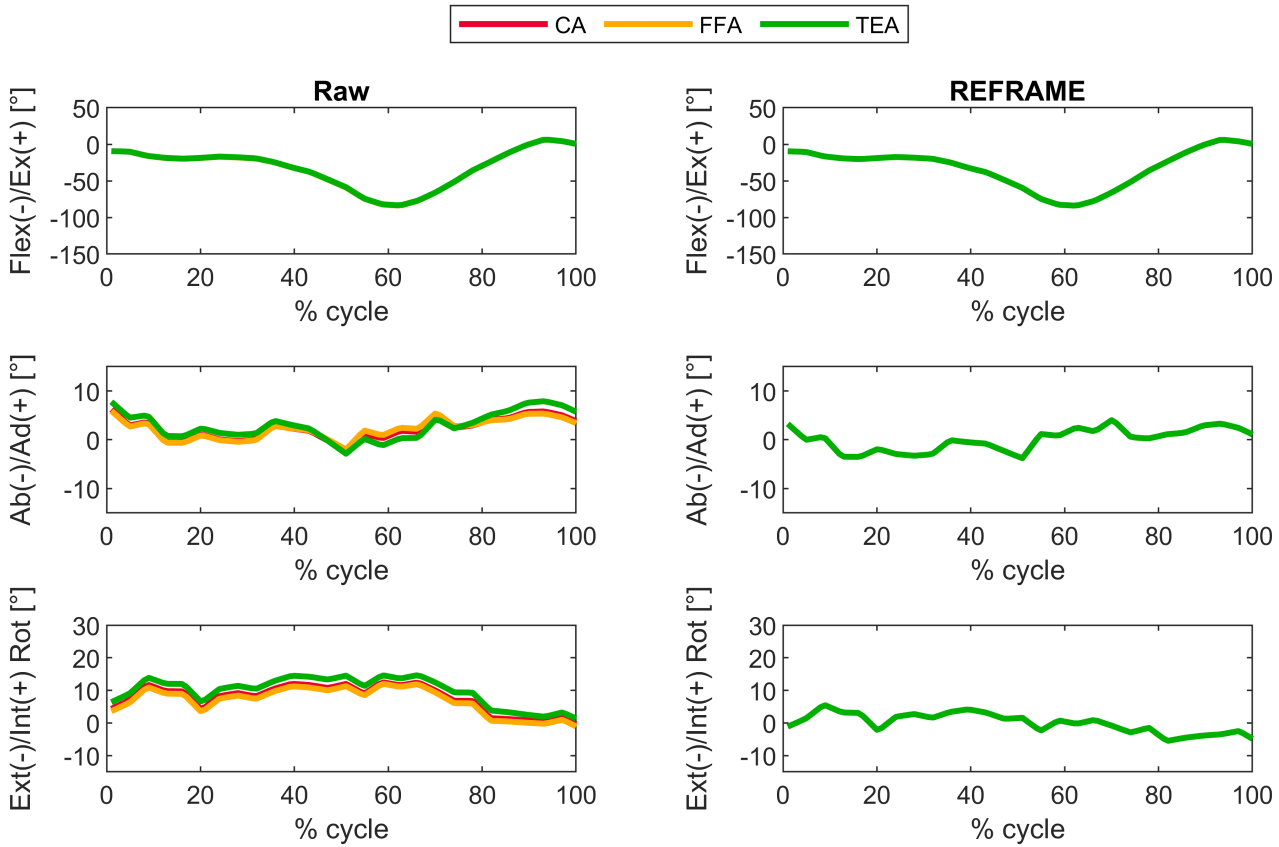

Supplementary Figure S55: Subject 6; Trial 1 – Rotational kinematics: Joint rotations (in degrees) of the tibial relative to the femoral segment frame for one cycle of stair descent, before (raw) and after REFRAME optimisation, for all three axis approaches (CA: cylindrical axis; FFA: functional flexion axis; TEA: transepicondylar axis). CA, FFA and TEA signals are shown in **all** subplots, but due to curve overlap in right-hand side plots, CA and FFA are covered by TEA. Note to readers from a clinical background: knee extension is illustrated here as **positive** because following the right-hand rule it corresponds with a positive rotation around the laterally pointing mediolateral axis for a right knee.

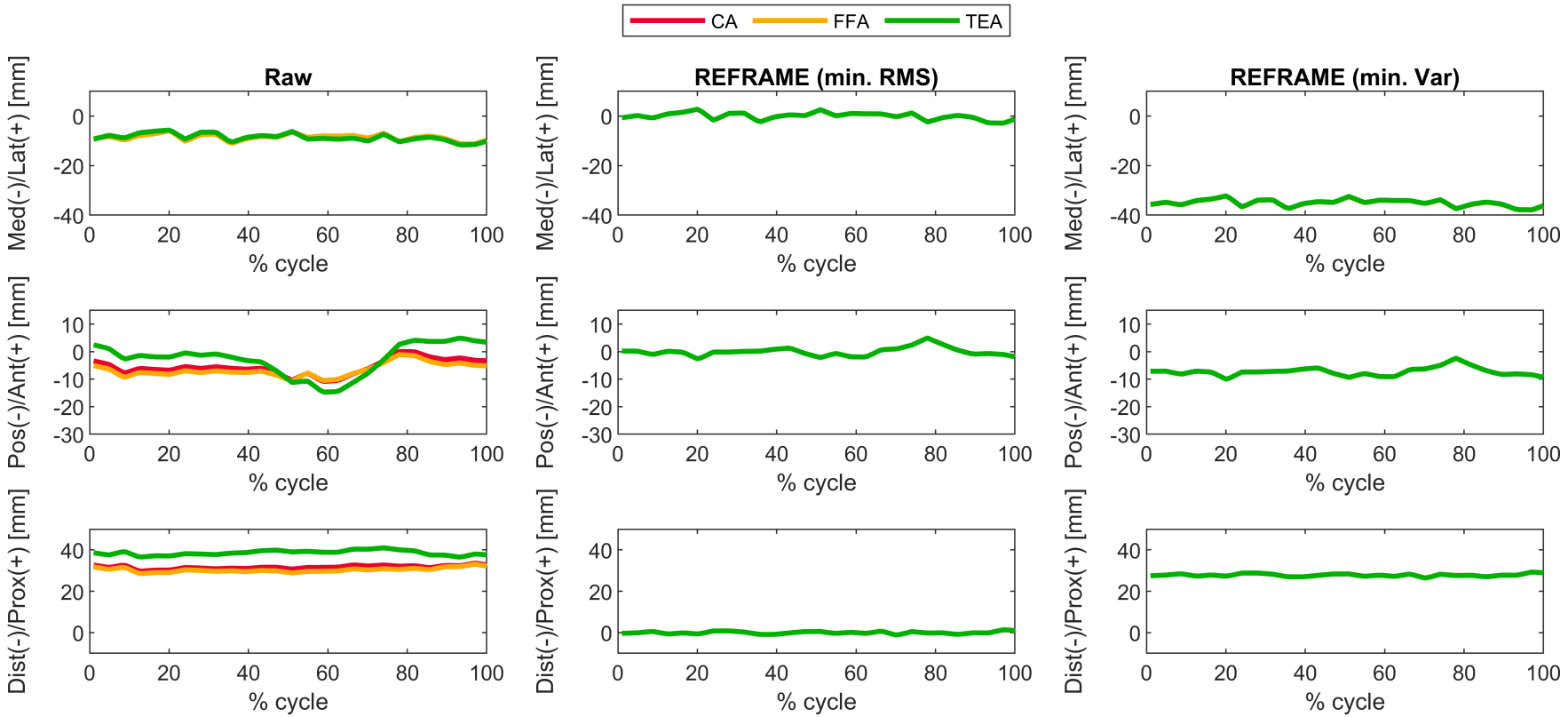

Supplementary Figure S56: Subject 6; Trial 1 – Translational kinematics: Joint translations (in mm) of the femoral relative to the tibial origin for one cycle of stair descent, before (raw, first column) and after application of the REFRAME optimisation (second column: based on the minimisation of translational root-mean-square; third column: based on the minimisation of translational variances), for all three axis approaches (CA: cylindrical axis; FFA: functional flexion axis; TEA: transepicondylar axis). CA, FFA and TEA signals are shown in **all** subplots, but due to curve overlap in the second and third columns, CA and FFA are covered by TEA.

3.6.2 Trial 2

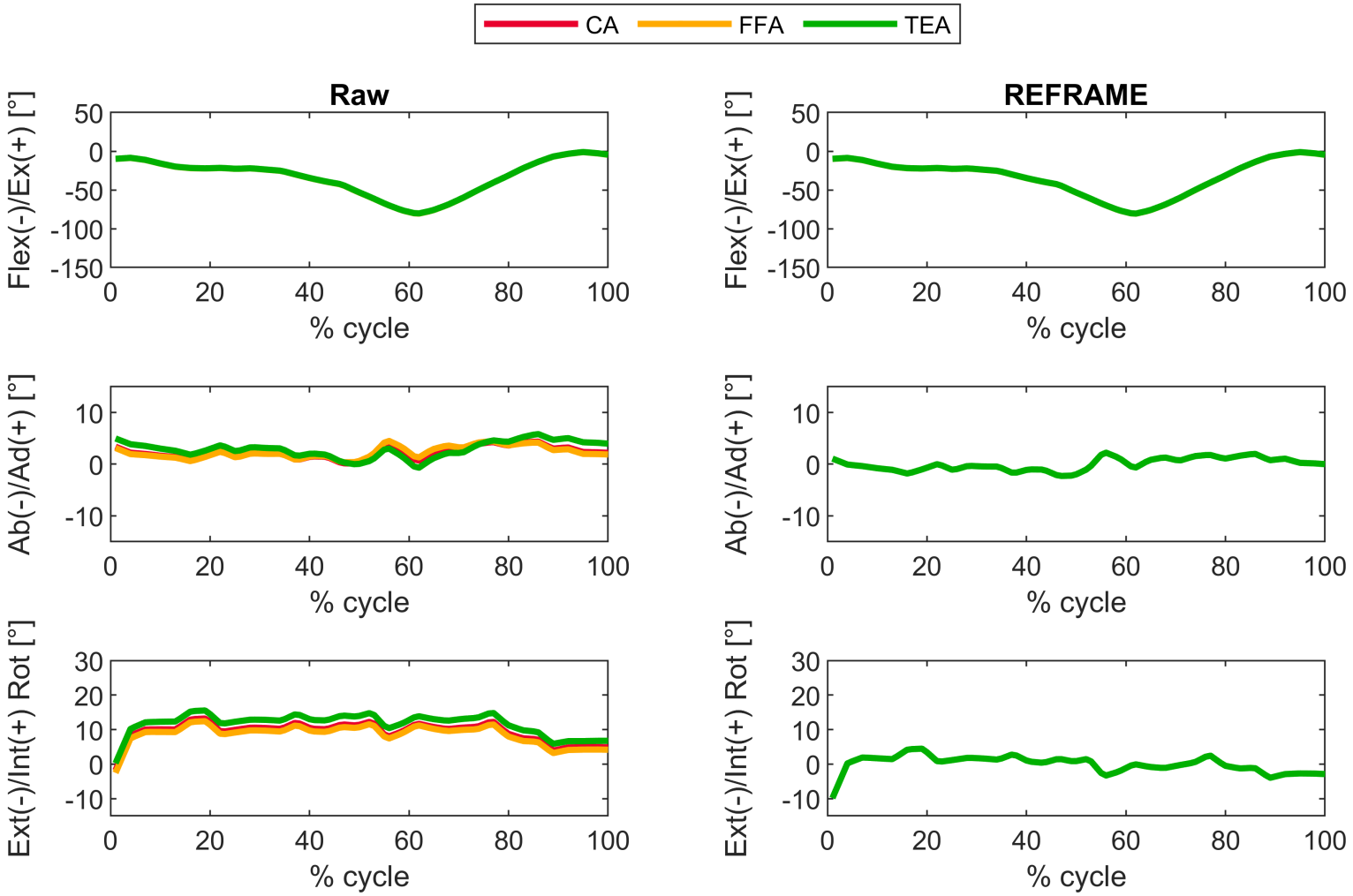

Supplementary Figure S57: Subject 6; Trial 2 – Rotational kinematics: Joint rotations (in degrees) of the tibial relative to the femoral segment frame for one cycle of stair descent, before (raw) and after REFRAME optimisation, for all three axis approaches (CA: cylindrical axis; FFA: functional flexion axis; TEA: transepicondylar axis). CA, FFA and TEA signals are shown in **all** subplots, but due to curve overlap in right-hand side plots, CA and FFA are covered by TEA. Note to readers from a clinical background: knee extension is illustrated here as **positive** because following the right-hand rule it corresponds with a positive rotation around the laterally pointing mediolateral axis for a right knee.

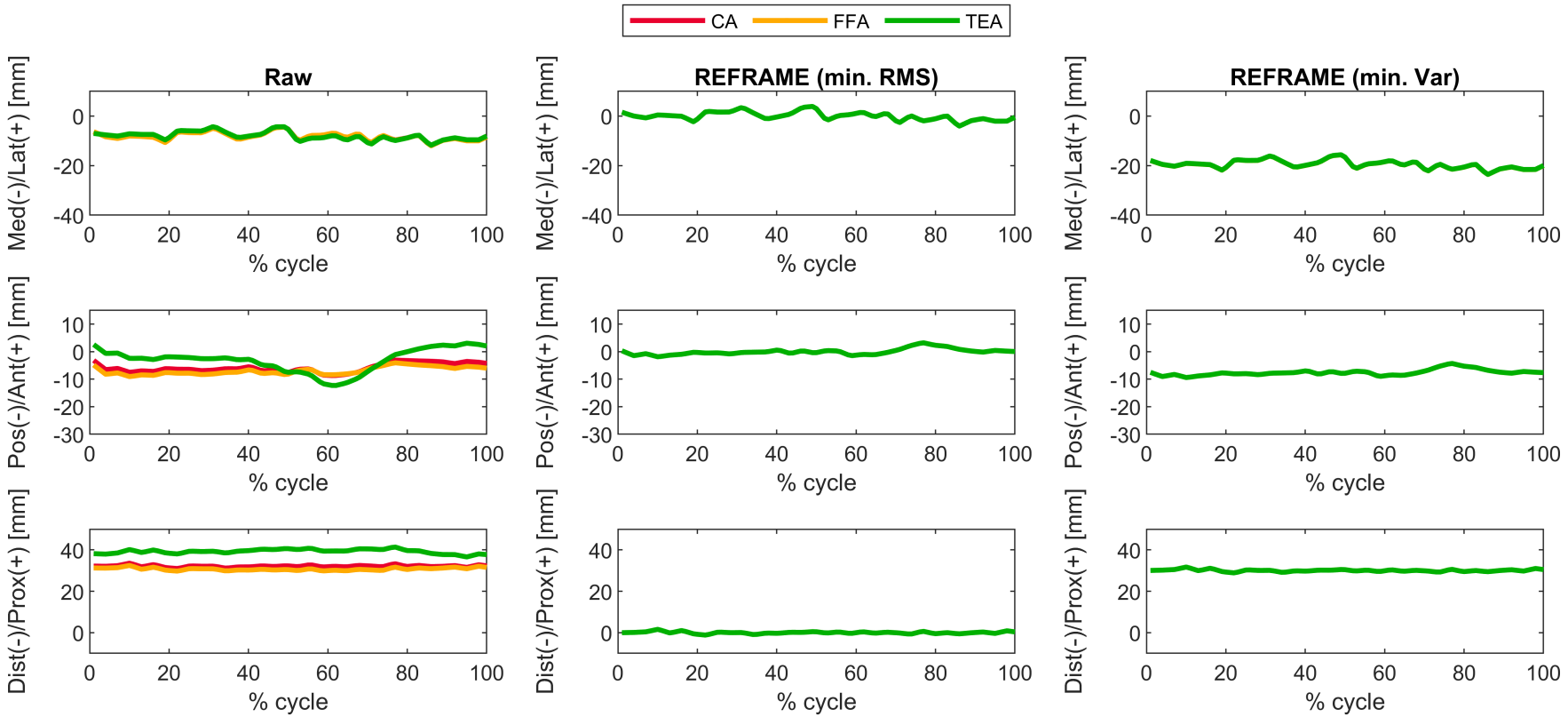

Supplementary Figure S58: Subject 6; Trial 2 – Translational kinematics: Joint translations (in mm) of the femoral relative to the tibial origin for one cycle of stair descent, before (raw, first column) and after application of the REFRAME optimisation (second column: based on the minimisation of translational root-mean-square; third column: based on the minimisation of translational variances), for all three axis approaches (CA: cylindrical axis; FFA: functional flexion axis; TEA: transepicondylar axis). CA, FFA and TEA signals are shown in **all** subplots, but due to curve overlap in the second and third columns, CA and FFA are covered by TEA.

3.6.3 Trial 3

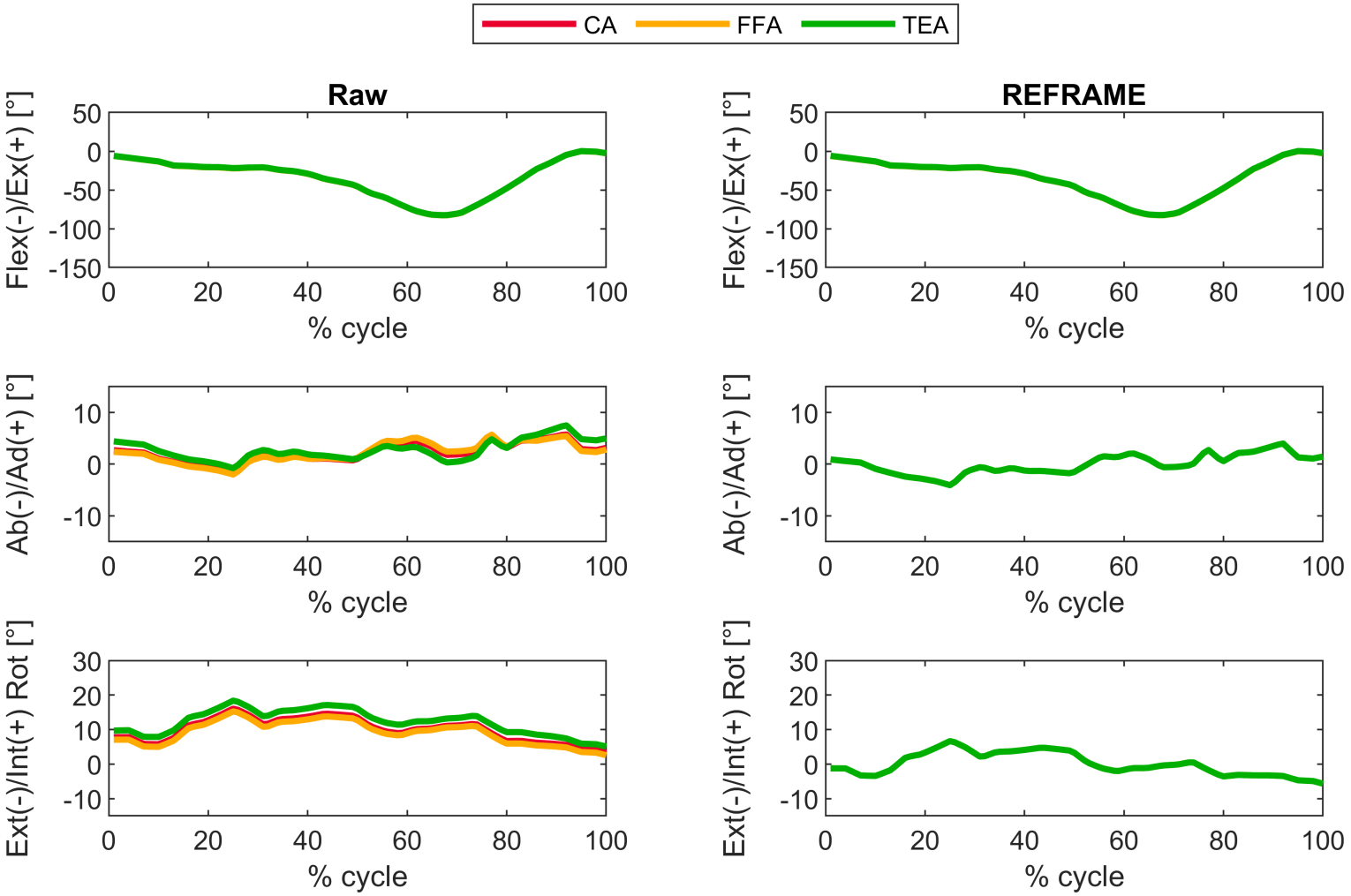

Supplementary Figure S59: Subject 6; Trial 3 – Rotational kinematics: Joint rotations (in degrees) of the tibial relative to the femoral segment frame for one cycle of stair descent, before (raw) and after REFRAME optimisation, for all three axis approaches (CA: cylindrical axis; FFA: functional flexion axis; TEA: transepicondylar axis). CA, FFA and TEA signals are shown in **all** subplots, but due to curve overlap in right-hand side plots, CA and FFA are covered by TEA. Note to readers from a clinical background: knee extension is illustrated here as **positive** because following the right-hand rule it corresponds with a positive rotation around the laterally pointing mediolateral axis for a right knee.

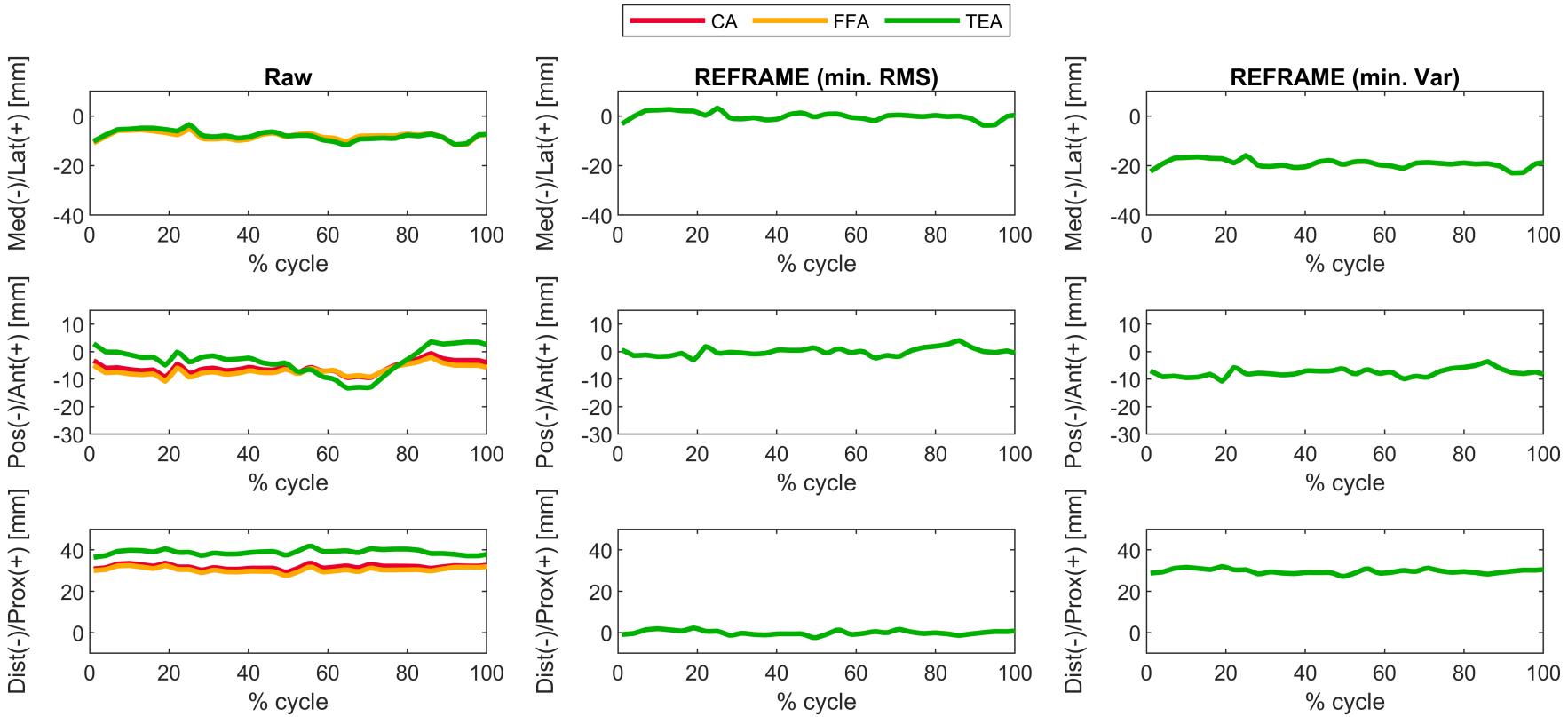

Supplementary Figure S60: Subject 6; Trial 3 – Translational kinematics: Joint translations (in mm) of the femoral relative to the tibial origin for one cycle of stair descent, before (raw, first column) and after application of the REFRAME optimisation (second column: based on the minimisation of translational root-mean-square; third column: based on the minimisation of translational variances), for all three axis approaches (CA: cylindrical axis; FFA: functional flexion axis; TEA: transepicondylar axis). CA, FFA and TEA signals are shown in **all** subplots, but due to curve overlap in the second and third columns, CA and FFA are covered by TEA.

3.6.4 Trial 4

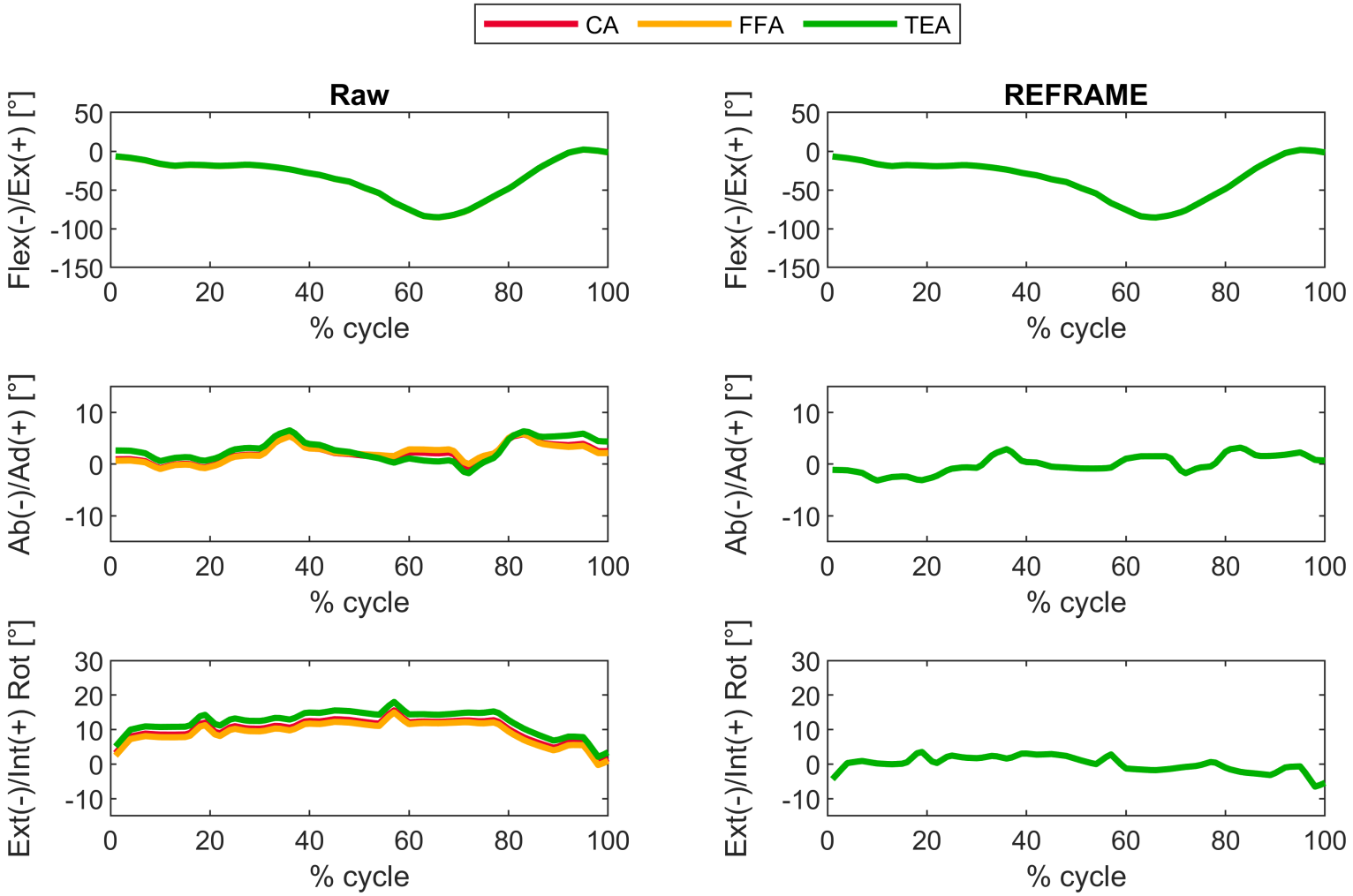

Supplementary Figure S61: Subject 6; Trial 4 – Rotational kinematics: Joint rotations (in degrees) of the tibial relative to the femoral segment frame for one cycle of stair descent, before (raw) and after REFRAME optimisation, for all three axis approaches (CA: cylindrical axis; FFA: functional flexion axis; TEA: transepicondylar axis). CA, FFA and TEA signals are shown in **all** subplots, but due to curve overlap in right-hand side plots, CA and FFA are covered by TEA. Note to readers from a clinical background: knee extension is illustrated here as **positive** because following the right-hand rule it corresponds with a positive rotation around the laterally pointing mediolateral axis for a right knee.

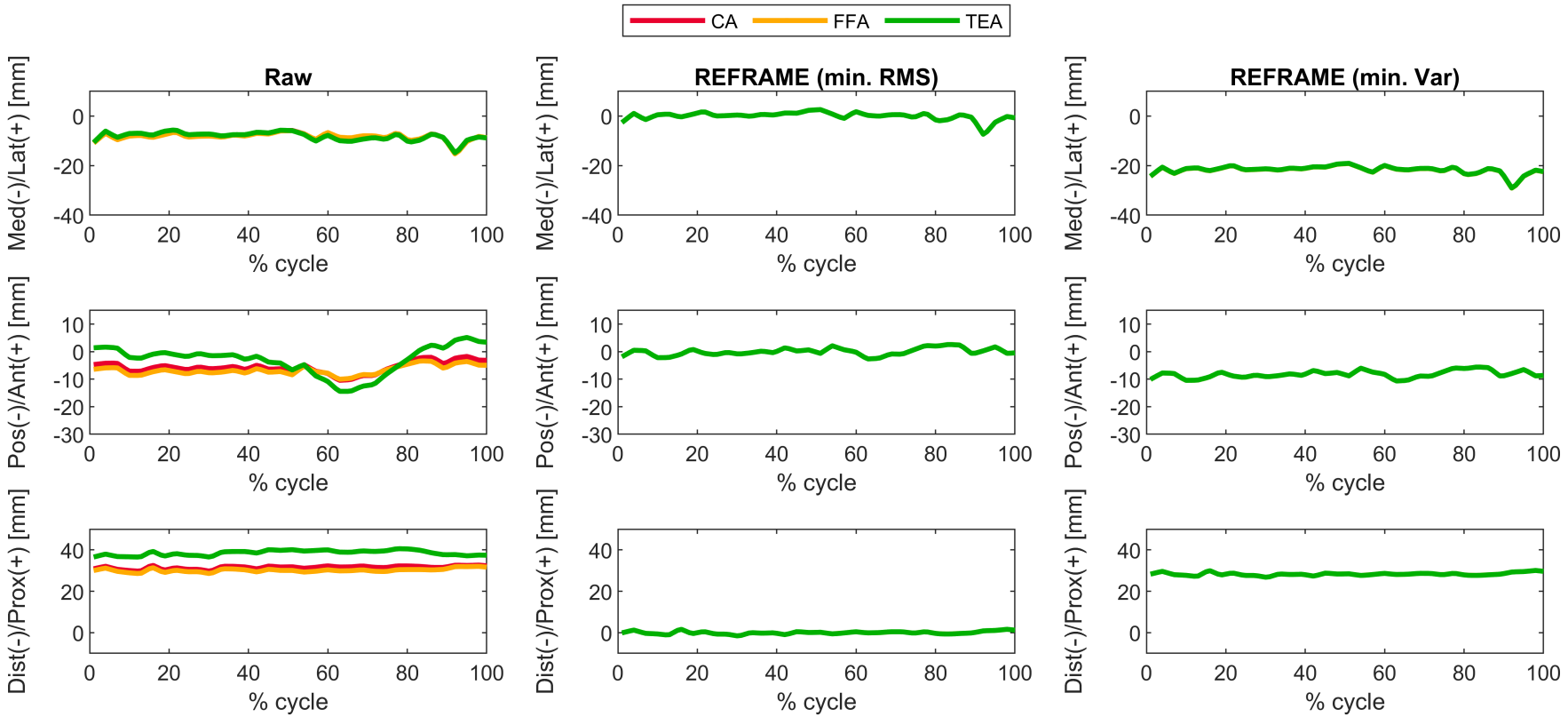

Supplementary Figure S62: Subject 6; Trial 4 – Translational kinematics: Joint translations (in mm) of the femoral relative to the tibial origin for one cycle of stair descent, before (raw, first column) and after application of the REFRAME optimisation (second column: based on the minimisation of translational root-mean-square; third column: based on the minimisation of translational variances), for all three axis approaches (CA: cylindrical axis; FFA: functional flexion axis; TEA: transepicondylar axis). CA, FFA and TEA signals are shown in **all** subplots, but due to curve overlap in the second and third columns, CA and FFA are covered by TEA.

3.6.5 Trial 5

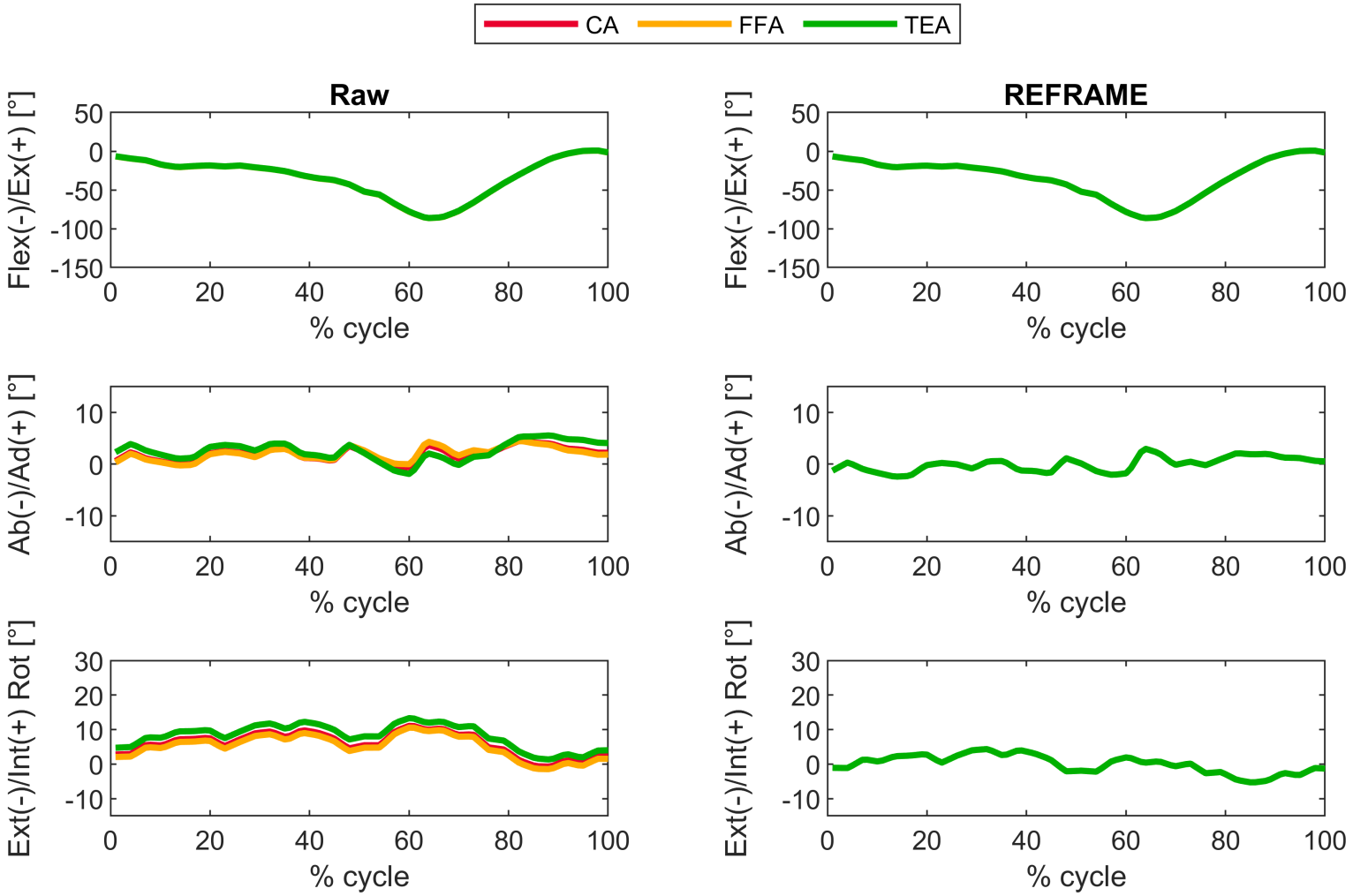

Supplementary Figure S63: Subject 6; Trial 5 – Rotational kinematics: Joint rotations (in degrees) of the tibial relative to the femoral segment frame for one cycle of stair descent, before (raw) and after REFRAME optimisation, for all three axis approaches (CA: cylindrical axis; FFA: functional flexion axis; TEA: transepicondylar axis). CA, FFA and TEA signals are shown in **all** subplots, but due to curve overlap in right-hand side plots, CA and FFA are covered by TEA. Note to readers from a clinical background: knee extension is illustrated here as **positive** because following the right-hand rule it corresponds with a positive rotation around the laterally pointing mediolateral axis for a right knee.

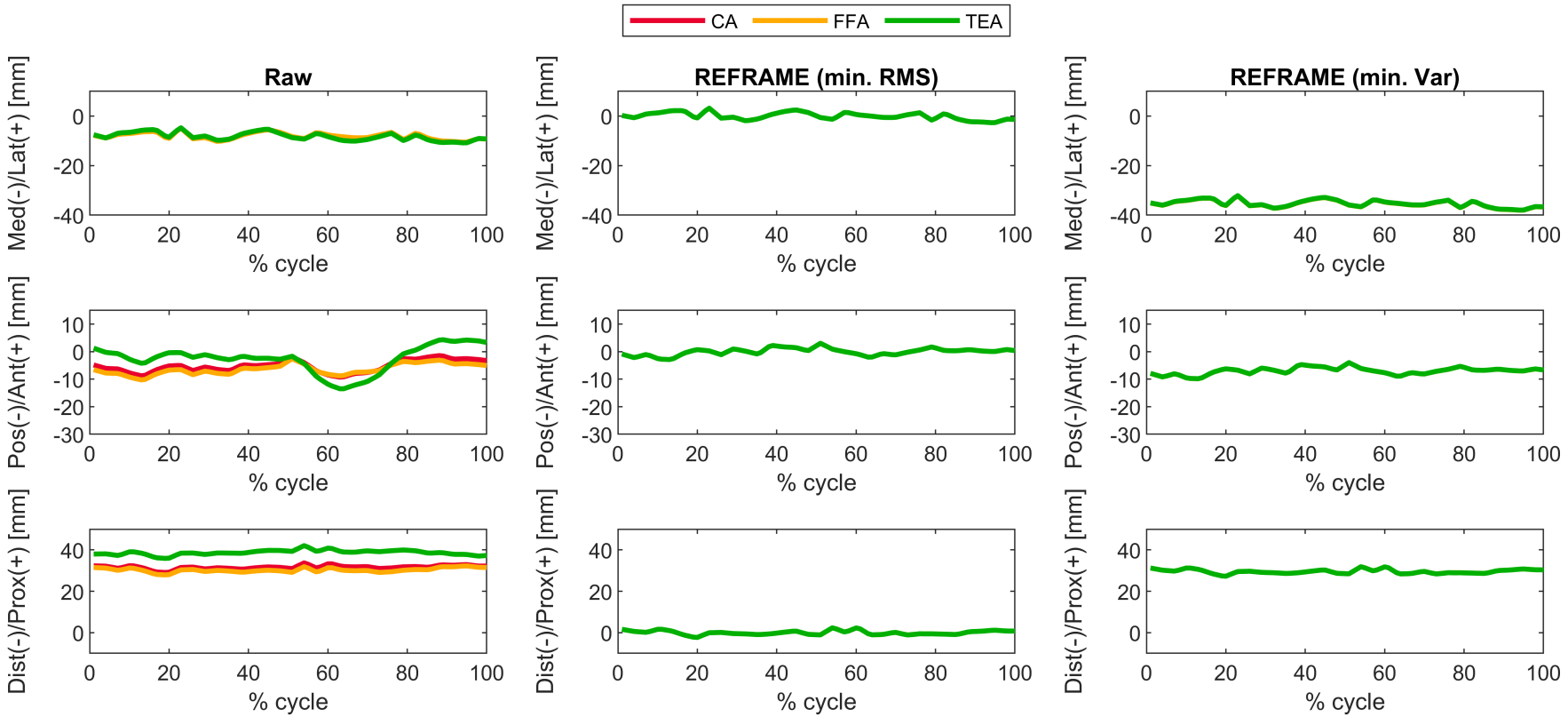

Supplementary Figure S64: Subject 6; Trial 5 – Translational kinematics: Joint translations (in mm) of the femoral relative to the tibial origin for one cycle of stair descent, before (raw, first column) and after application of the REFRAME optimisation (second column: based on the minimisation of translational root-mean-square; third column: based on the minimisation of translational variances), for all three axis approaches (CA: cylindrical axis; FFA: functional flexion axis; TEA: transepicondylar axis). CA, FFA and TEA signals are shown in **all** subplots, but due to curve overlap in the second and third columns, CA and FFA are covered by TEA.

3.7 Subject 7

3.7.1 Trial 1

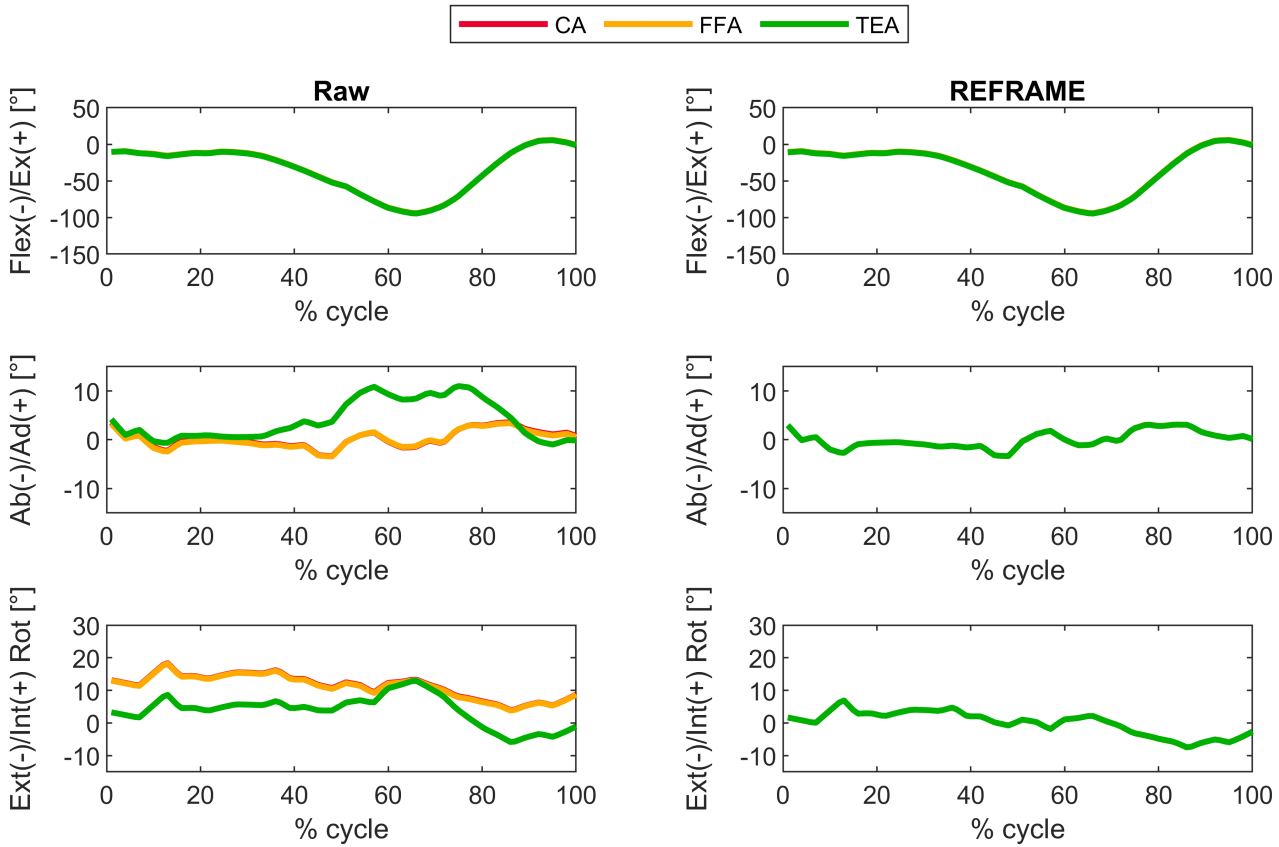

Supplementary Figure S65: Subject 7; Trial 1 – Rotational kinematics: Joint rotations (in degrees) of the tibial relative to the femoral segment frame for one cycle of stair descent, before (raw) and after REFRAME optimisation, for all three axis approaches (CA: cylindrical axis; FFA: functional flexion axis; TEA: transepicondylar axis). CA, FFA and TEA signals are shown in **all** subplots, but due to curve overlap in right-hand side plots, CA and FFA are covered by TEA. Note to readers from a clinical background: knee extension is illustrated here as **positive** because following the right-hand rule it corresponds with a positive rotation around the laterally pointing mediolateral axis for a right knee.

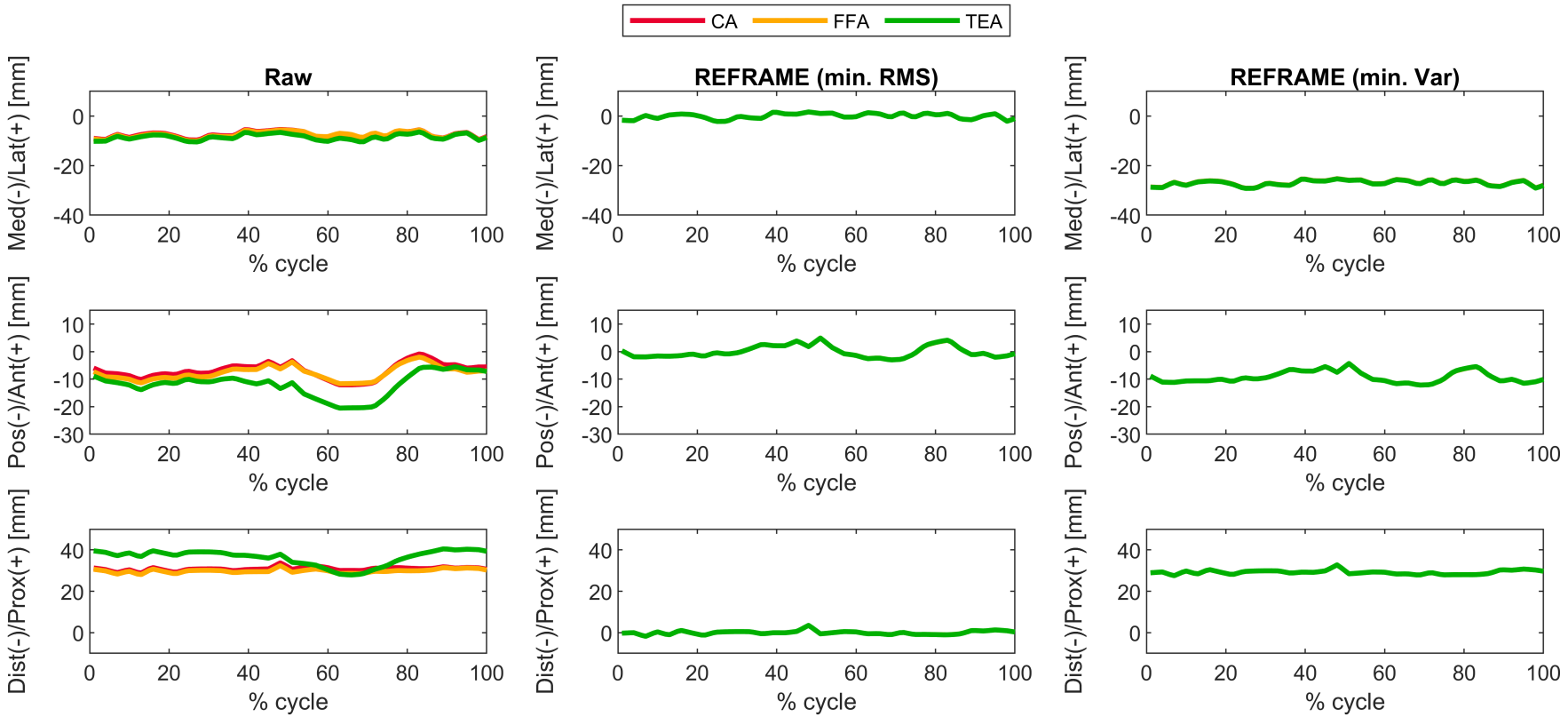

Supplementary Figure S66: Subject 7; Trial 1 – Translational kinematics: Joint translations (in mm) of the femoral relative to the tibial origin for one cycle of stair descent, before (raw, first column) and after application of the REFRAME optimisation (second column: based on the minimisation of translational root-mean-square; third column: based on the minimisation of translational variances), for all three axis approaches (CA: cylindrical axis; FFA: functional flexion axis; TEA: transepicondylar axis). CA, FFA and TEA signals are shown in **all** subplots, but due to curve overlap in the second and third columns, CA and FFA are covered by TEA.

3.7.2 Trial 2

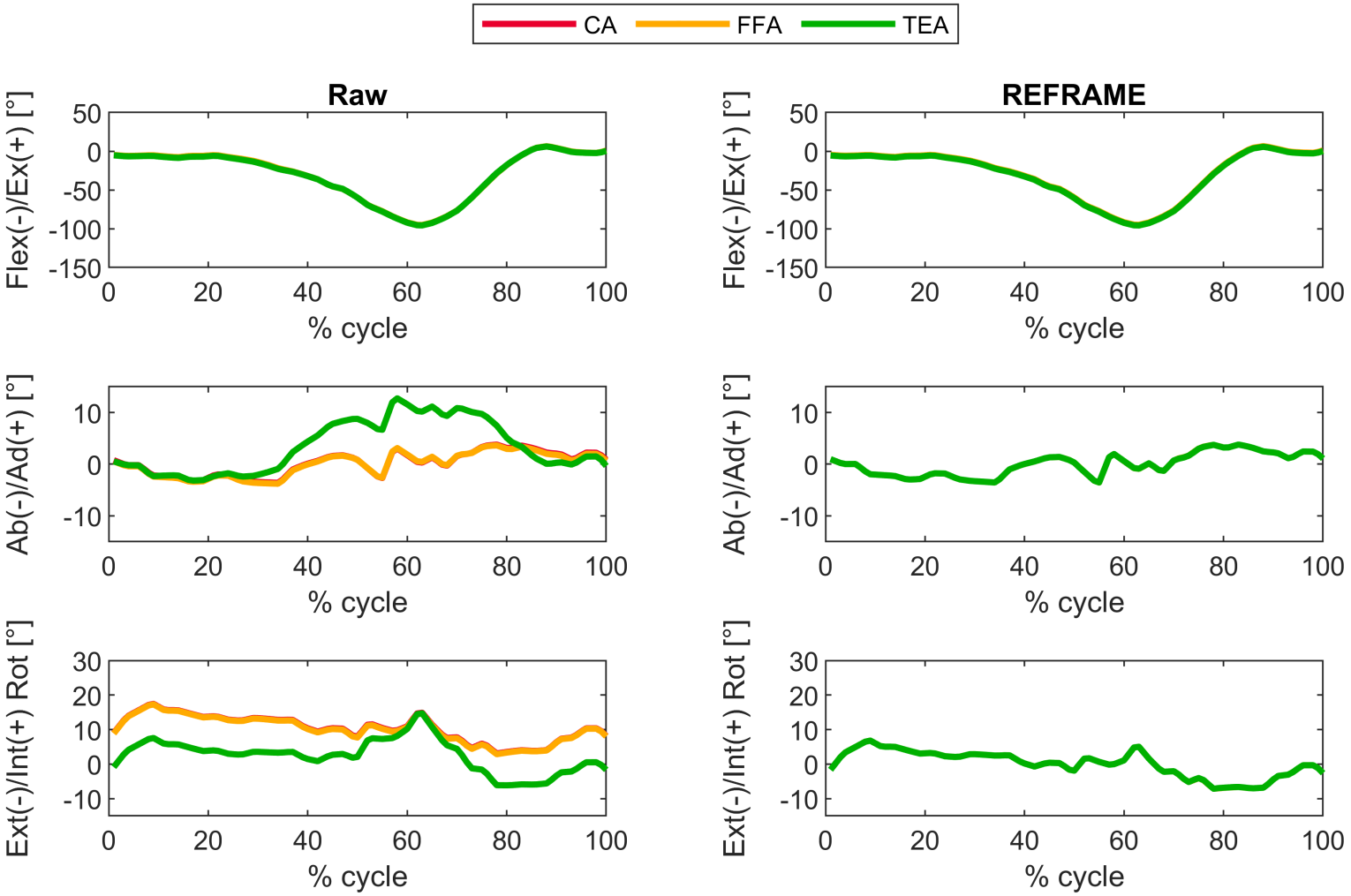

Supplementary Figure S67: Subject 7; Trial 2 – Rotational kinematics: Joint rotations (in degrees) of the tibial relative to the femoral segment frame for one cycle of stair descent, before (raw) and after REFRAME optimisation, for all three axis approaches (CA: cylindrical axis; FFA: functional flexion axis; TEA: transepicondylar axis). CA, FFA and TEA signals are shown in **all** subplots, but due to curve overlap in right-hand side plots, CA and FFA are covered by TEA. Note to readers from a clinical background: knee extension is illustrated here as **positive** because following the right-hand rule it corresponds with a positive rotation around the laterally pointing mediolateral axis for a right knee.

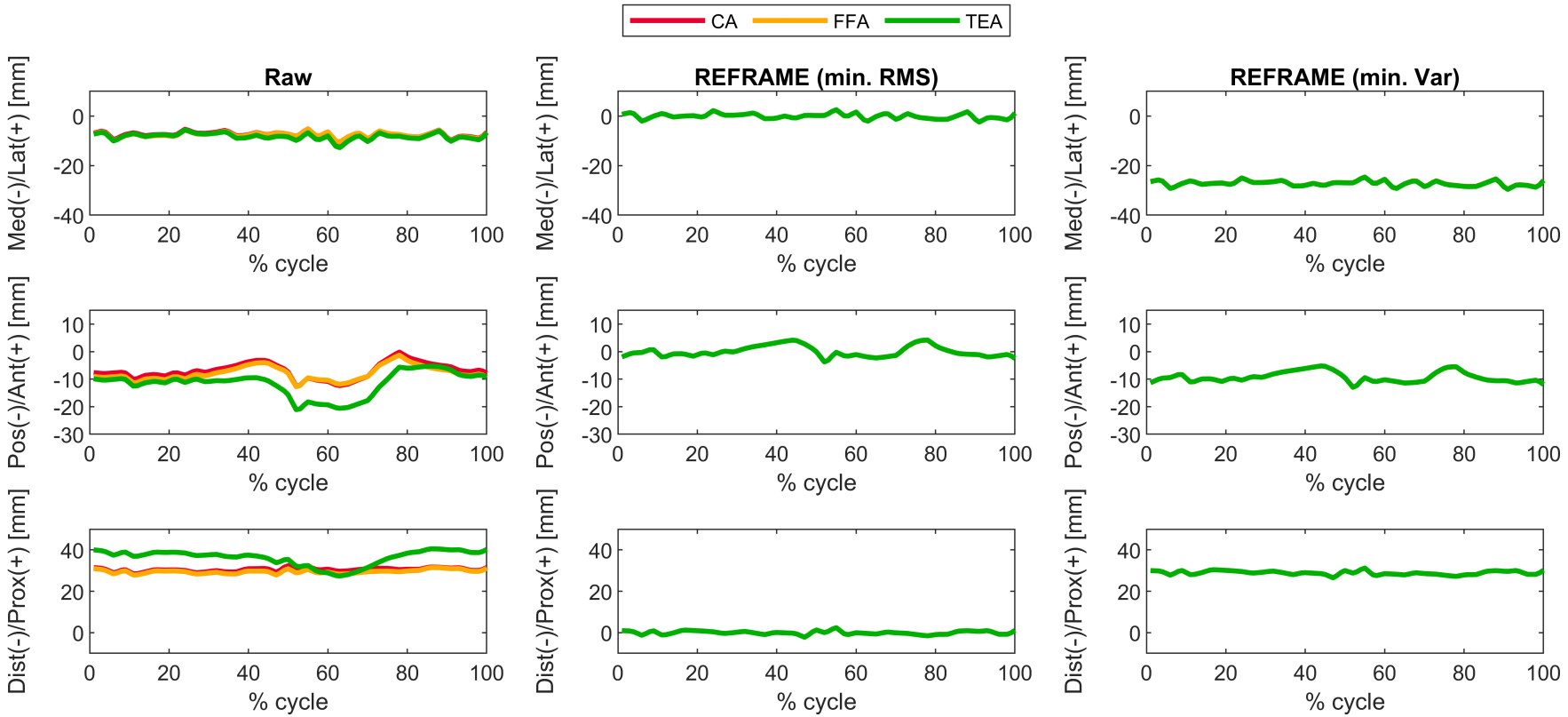

Supplementary Figure S68: Subject 7; Trial 2 – Translational kinematics: Joint translations (in mm) of the femoral relative to the tibial origin for one cycle of stair descent, before (raw, first column) and after application of the REFRAME optimisation (second column: based on the minimisation of translational root-mean-square; third column: based on the minimisation of translational variances), for all three axis approaches (CA: cylindrical axis; FFA: functional flexion axis; TEA: transepicondylar axis). CA, FFA and TEA signals are shown in **all** subplots, but due to curve overlap in the second and third columns, CA and FFA are covered by TEA.

3.7.3 Trial 3

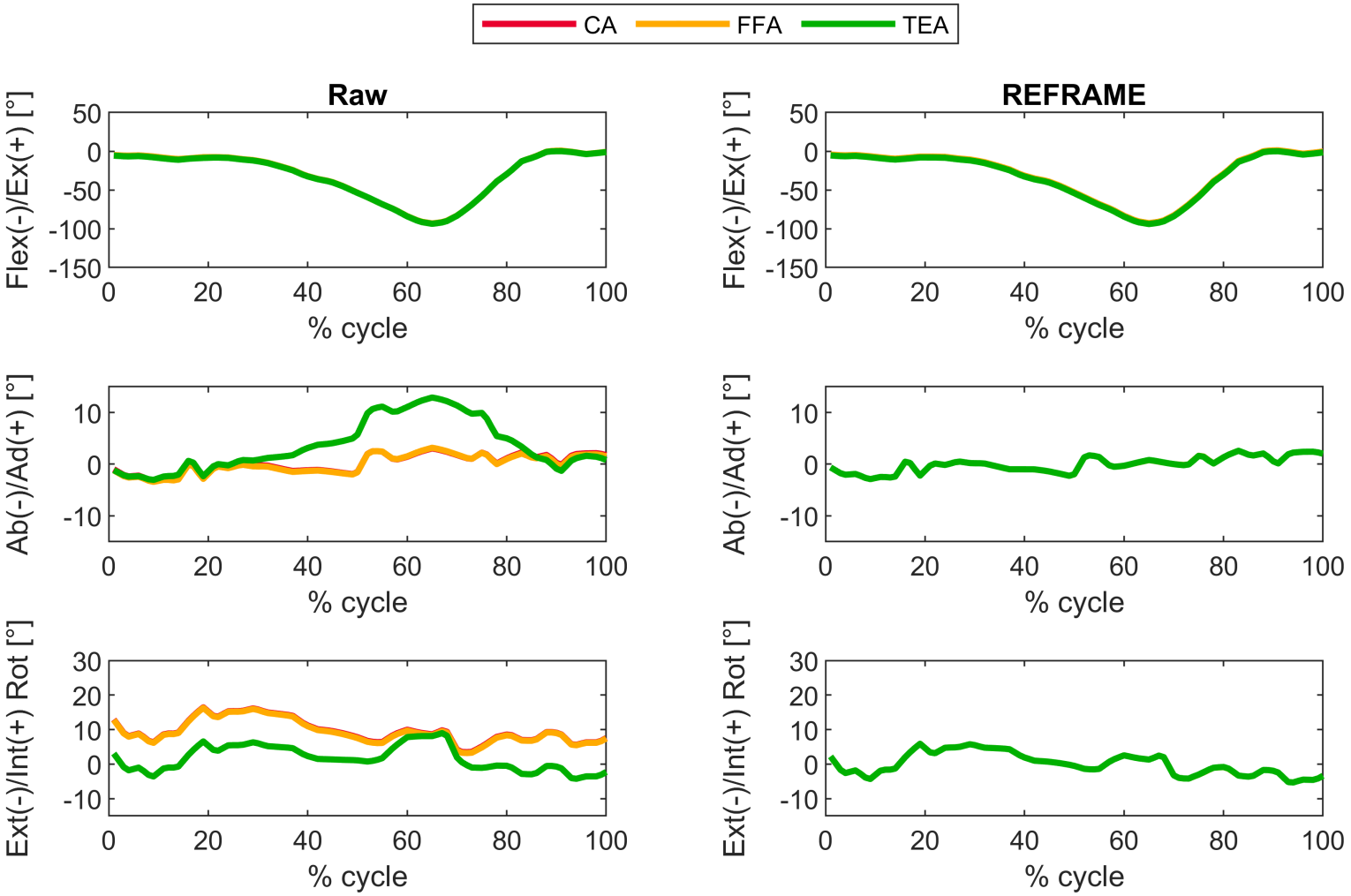

Supplementary Figure S69: Subject 7; Trial 3 – Rotational kinematics: Joint rotations (in degrees) of the tibial relative to the femoral segment frame for one cycle of stair descent, before (raw) and after REFRAME optimisation, for all three axis approaches (CA: cylindrical axis; FFA: functional flexion axis; TEA: transepicondylar axis). CA, FFA and TEA signals are shown in **all** subplots, but due to curve overlap in right-hand side plots, CA and FFA are covered by TEA. Note to readers from a clinical background: knee extension is illustrated here as **positive** because following the right-hand rule it corresponds with a positive rotation around the laterally pointing mediolateral axis for a right knee.

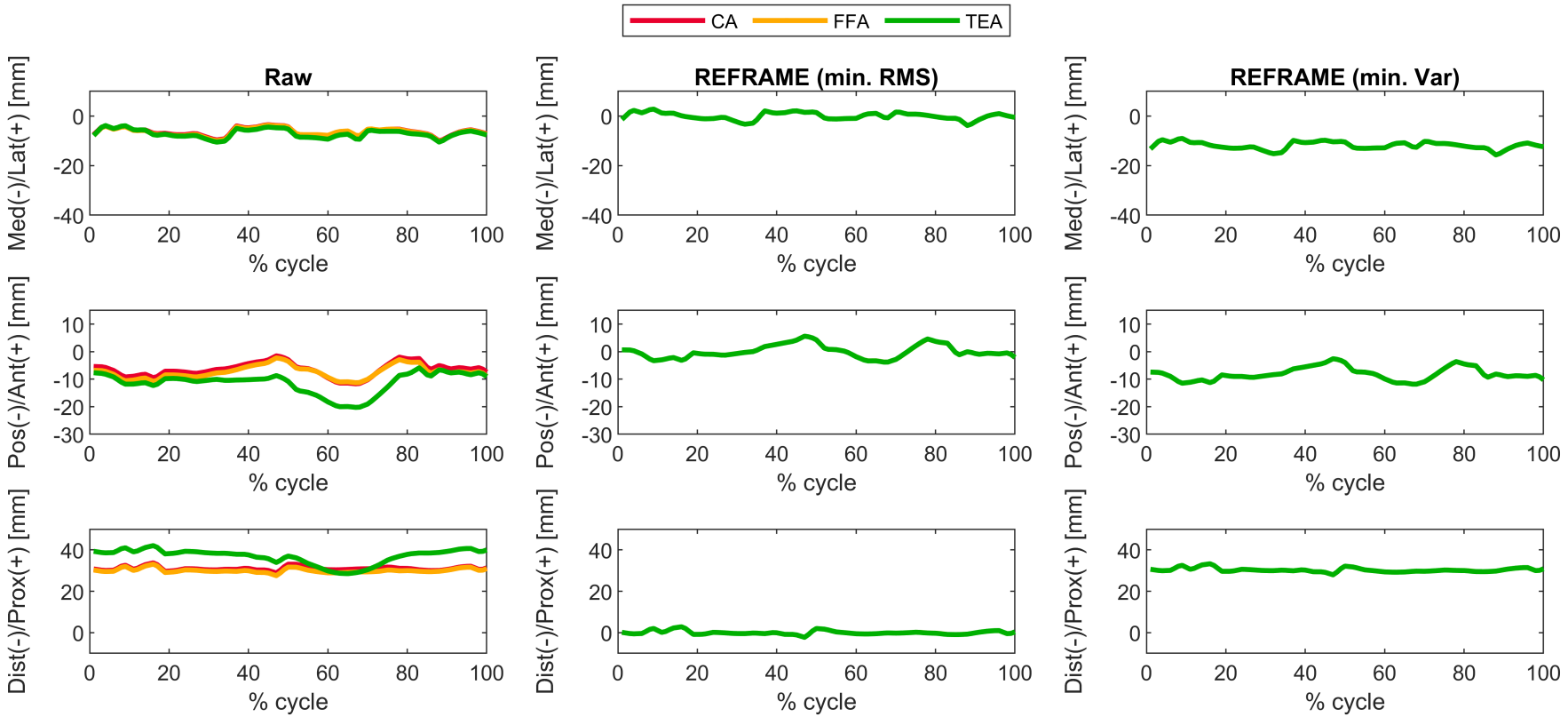

Supplementary Figure S70: Subject 7; Trial 3 – Translational kinematics: Joint translations (in mm) of the femoral relative to the tibial origin for one cycle of stair descent, before (raw, first column) and after application of the REFRAME optimisation (second column: based on the minimisation of translational root-mean-square; third column: based on the minimisation of translational variances), for all three axis approaches (CA: cylindrical axis; FFA: functional flexion axis; TEA: transepicondylar axis). CA, FFA and TEA signals are shown in **all** subplots, but due to curve overlap in the second and third columns, CA and FFA are covered by TEA.

3.7.4 Trial 4

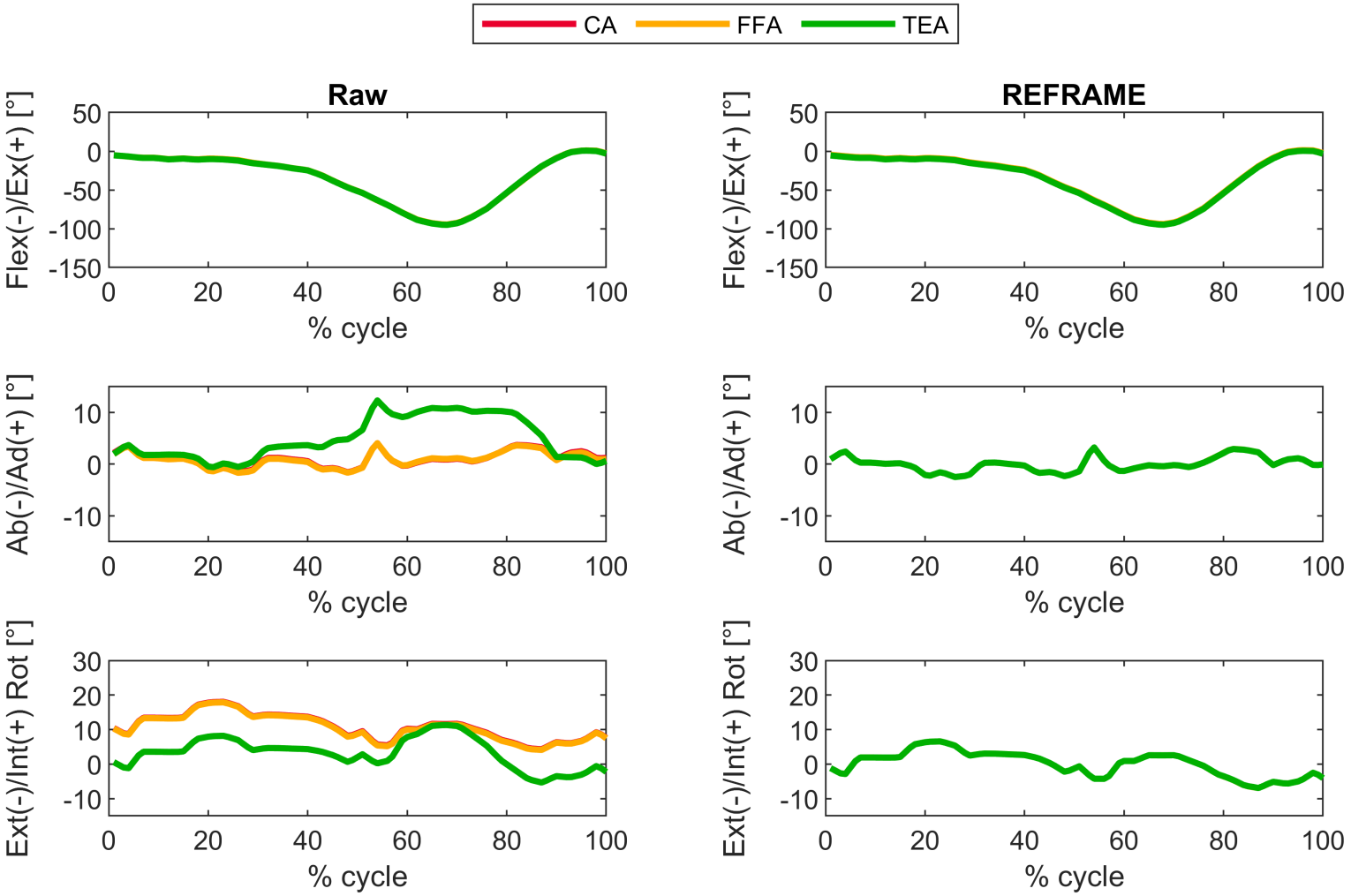

Supplementary Figure S71: Subject 7; Trial 4 – Rotational kinematics: Joint rotations (in degrees) of the tibial relative to the femoral segment frame for one cycle of stair descent, before (raw) and after REFRAME optimisation, for all three axis approaches (CA: cylindrical axis; FFA: functional flexion axis; TEA: transepicondylar axis). CA, FFA and TEA signals are shown in **all** subplots, but due to curve overlap in right-hand side plots, CA and FFA are covered by TEA. Note to readers from a clinical background: knee extension is illustrated here as **positive** because following the right-hand rule it corresponds with a positive rotation around the laterally pointing mediolateral axis for a right knee.

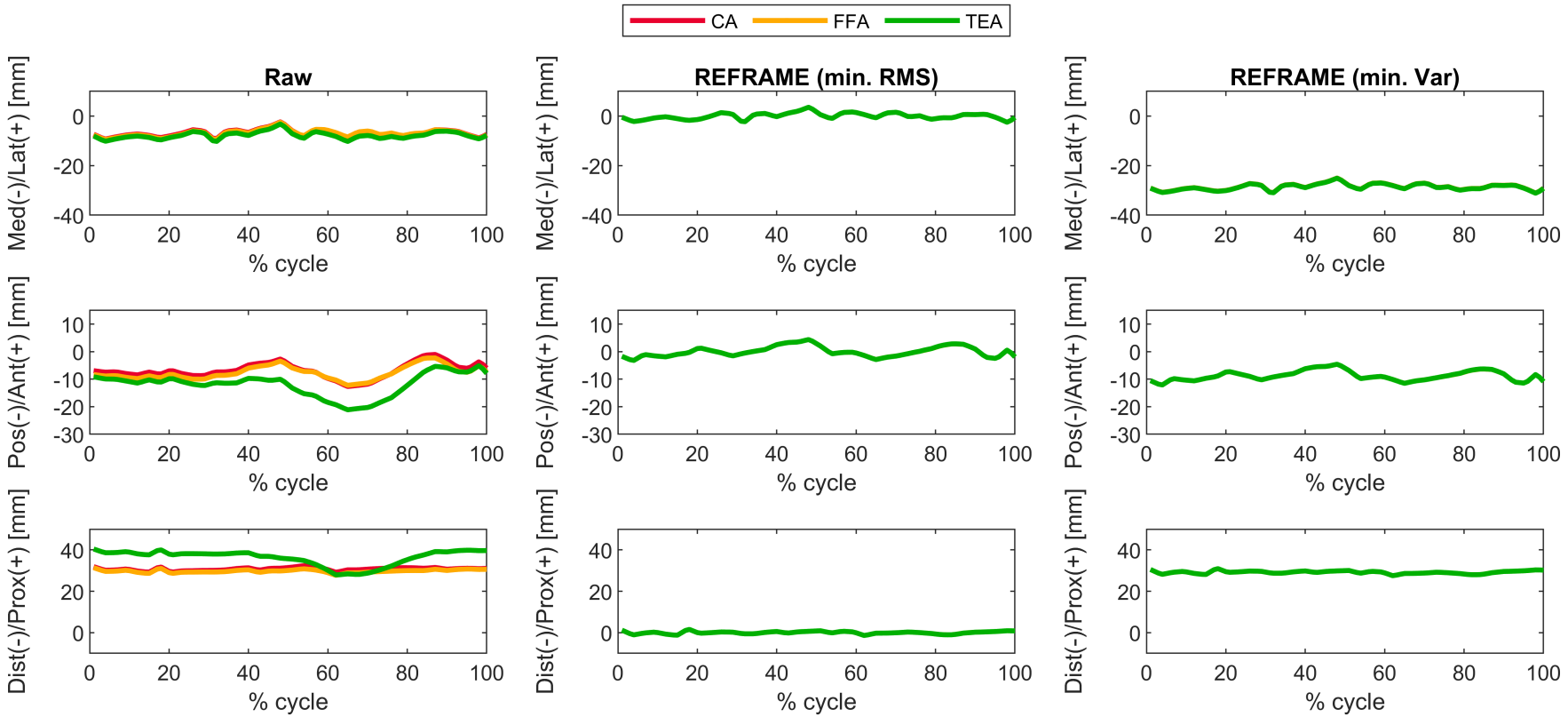

Supplementary Figure S72: Subject 7; Trial 4 – Translational kinematics: Joint translations (in mm) of the femoral relative to the tibial origin for one cycle of stair descent, before (raw, first column) and after application of the REFRAME optimisation (second column: based on the minimisation of translational root-mean-square; third column: based on the minimisation of translational variances), for all three axis approaches (CA: cylindrical axis; FFA: functional flexion axis; TEA: transepicondylar axis). CA, FFA and TEA signals are shown in **all** subplots, but due to curve overlap in the second and third columns, CA and FFA are covered by TEA.

3.7.5 Trial 5

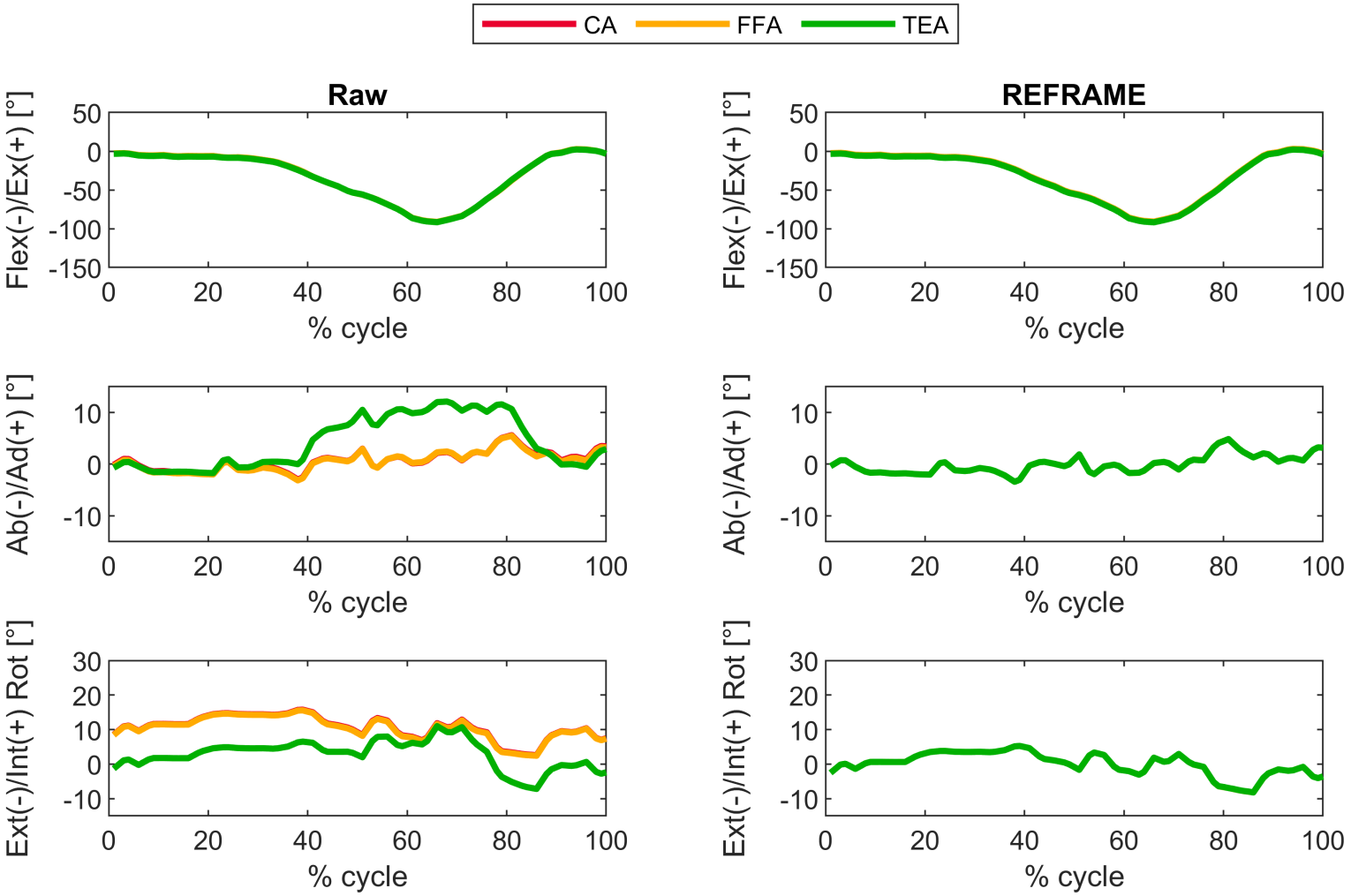

Supplementary Figure S73: Subject 7; Trial 5 – Rotational kinematics: Joint rotations (in degrees) of the tibial relative to the femoral segment frame for one cycle of stair descent, before (raw) and after REFRAME optimisation, for all three axis approaches (CA: cylindrical axis; FFA: functional flexion axis; TEA: transepicondylar axis). CA, FFA and TEA signals are shown in **all** subplots, but due to curve overlap in right-hand side plots, CA and FFA are covered by TEA. Note to readers from a clinical background: knee extension is illustrated here as **positive** because following the right-hand rule it corresponds with a positive rotation around the laterally pointing mediolateral axis for a right knee.

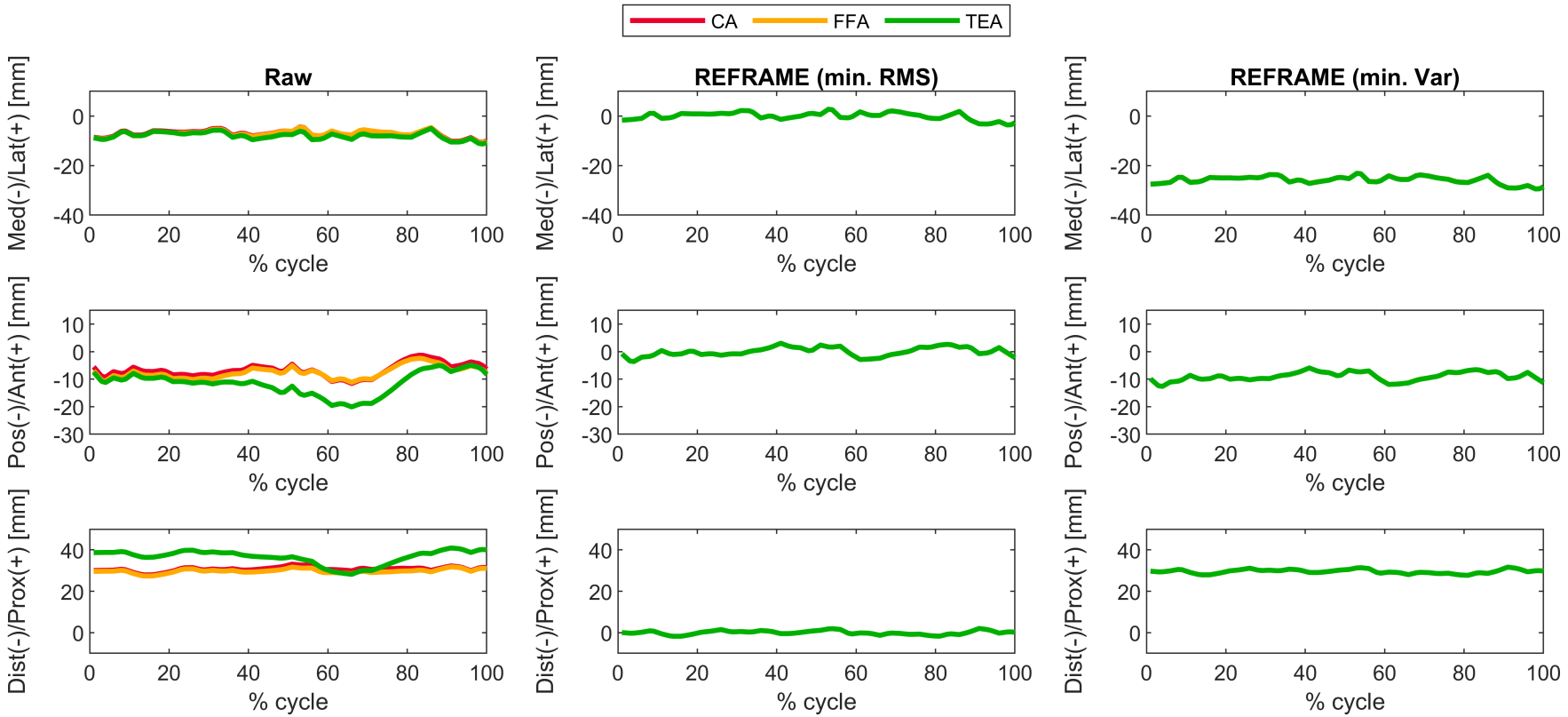

Supplementary Figure S74: Subject 7; Trial 5 – Translational kinematics: Joint translations (in mm) of the femoral relative to the tibial origin for one cycle of stair descent, before (raw, first column) and after application of the REFRAME optimisation (second column: based on the minimisation of translational root-mean-square; third column: based on the minimisation of translational variances), for all three axis approaches (CA: cylindrical axis; FFA: functional flexion axis; TEA: transepicondylar axis). CA, FFA and TEA signals are shown in **all** subplots, but due to curve overlap in the second and third columns, CA and FFA are covered by TEA.

3.8 Subject 8

3.8.1 Trial 1

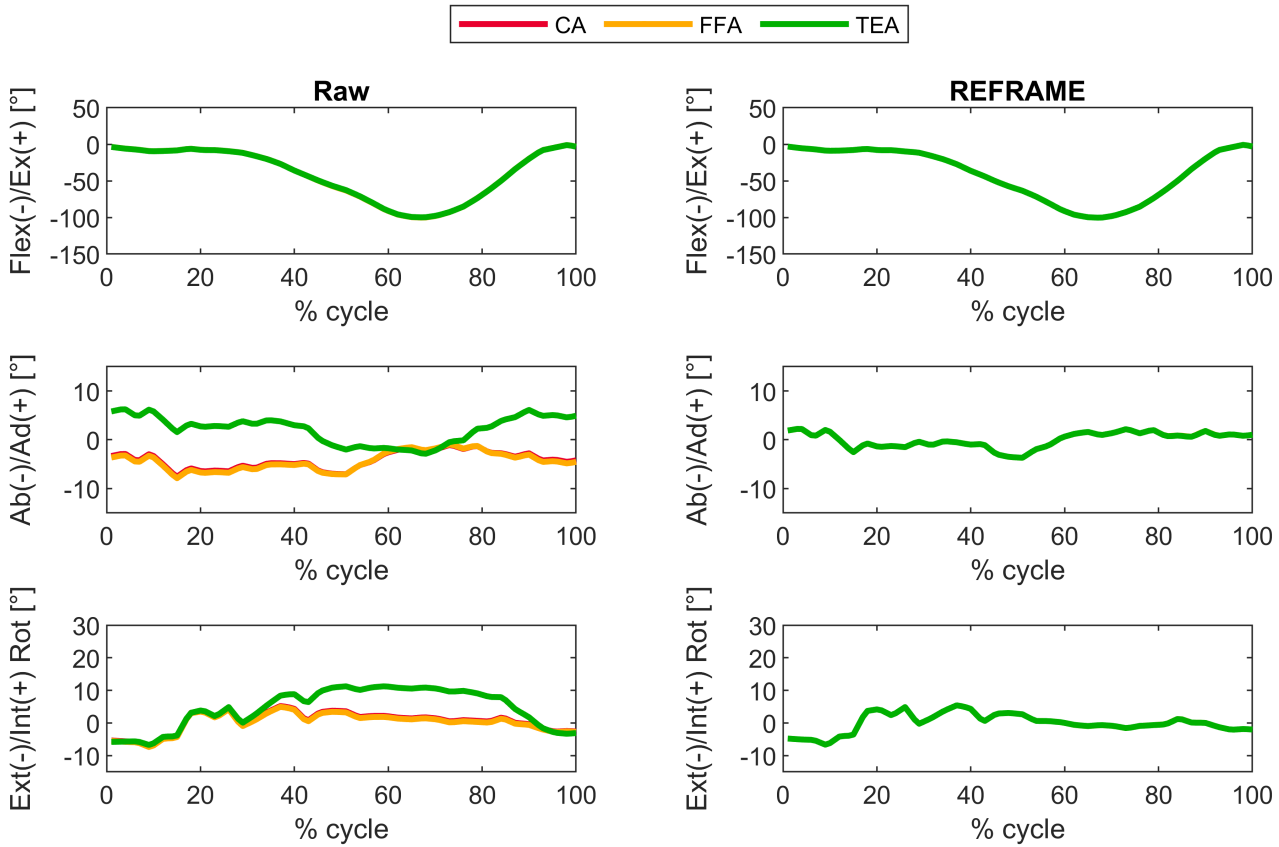

Supplementary Figure S75: Subject 8; Trial 1 – Rotational kinematics: Joint rotations (in degrees) of the tibial relative to the femoral segment frame for one cycle of stair descent, before (raw) and after REFRAME optimisation, for all three axis approaches (CA: cylindrical axis; FFA: functional flexion axis; TEA: transepicondylar axis). CA, FFA and TEA signals are shown in **all** subplots, but due to curve overlap in right-hand side plots, CA and FFA are covered by TEA. Note to readers from a clinical background: knee extension is illustrated here as **positive** because following the right-hand rule it corresponds with a positive rotation around the laterally pointing mediolateral axis for a right knee.

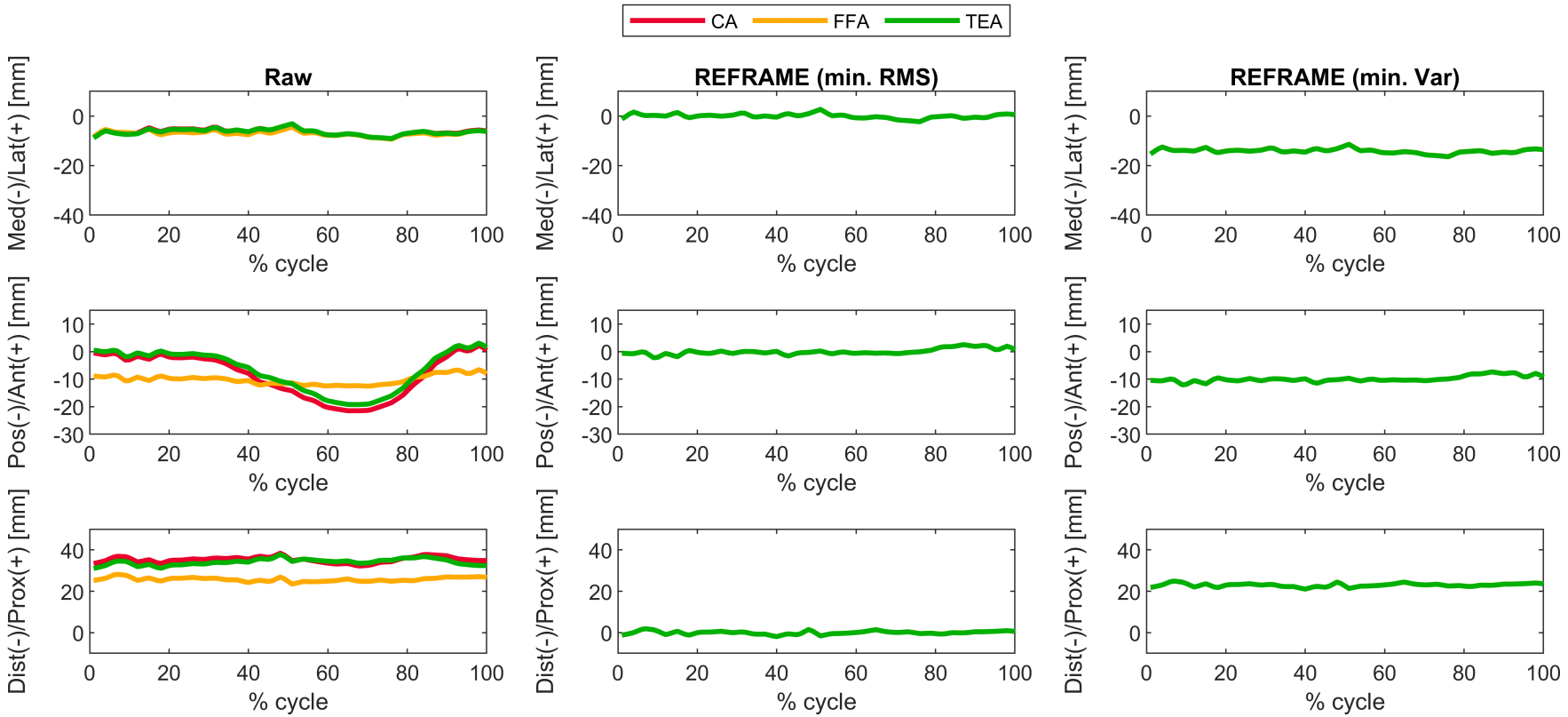

Supplementary Figure S76: Subject 8; Trial 1 – Translational kinematics: Joint translations (in mm) of the femoral relative to the tibial origin for one cycle of stair descent, before (raw, first column) and after application of the REFRAME optimisation (second column: based on the minimisation of translational root-mean-square; third column: based on the minimisation of translational variances), for all three axis approaches (CA: cylindrical axis; FFA: functional flexion axis; TEA: transepicondylar axis). CA, FFA and TEA signals are shown in **all** subplots, but due to curve overlap in the second and third columns, CA and FFA are covered by TEA.

3.8.2 Trial 2

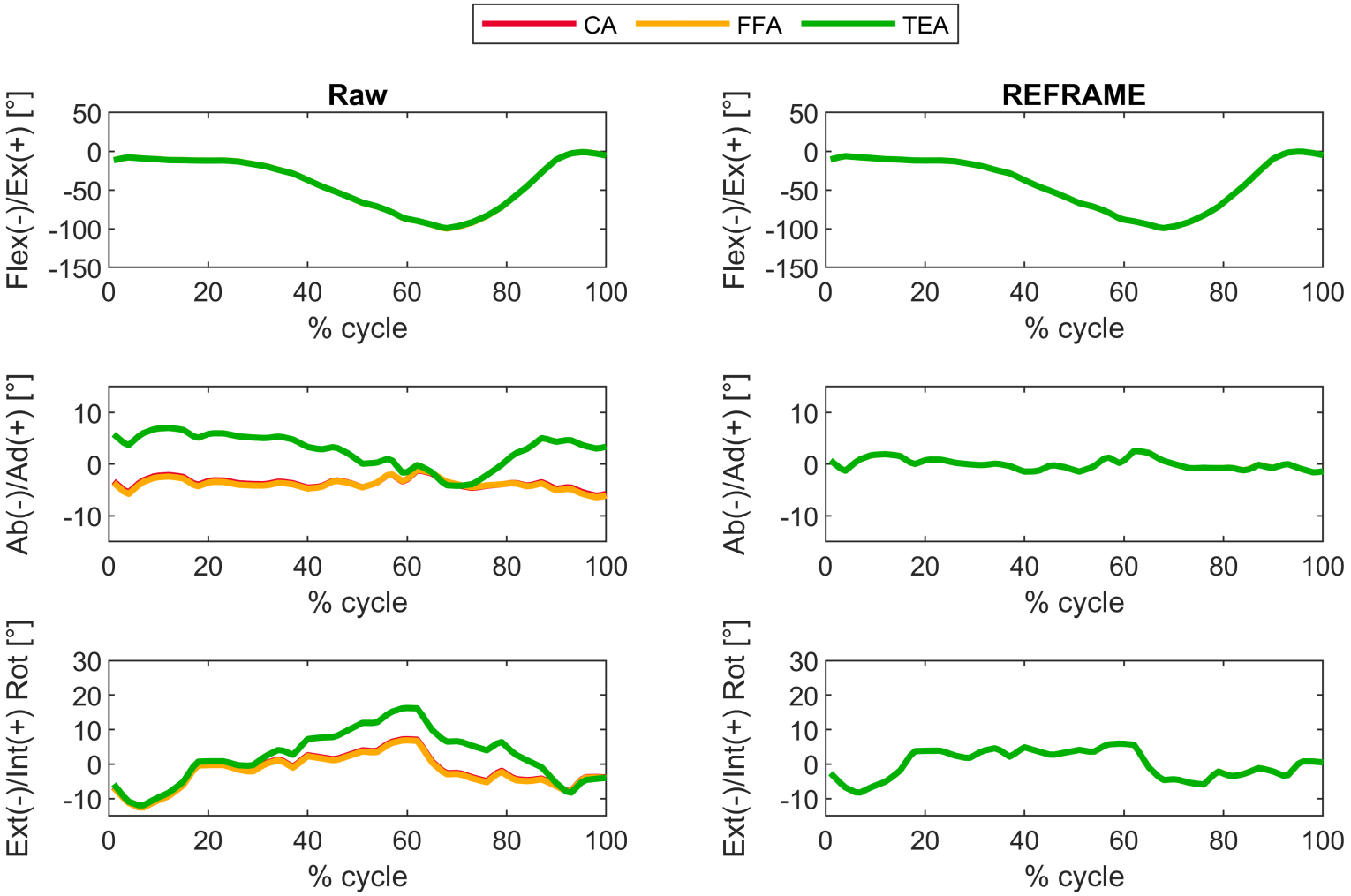

Supplementary Figure S77: Subject 8; Trial 2 – Rotational kinematics: Joint rotations (in degrees) of the tibial relative to the femoral segment frame for one cycle of stair descent, before (raw) and after REFRAME optimisation, for all three axis approaches (CA: cylindrical axis; FFA: functional flexion axis; TEA: transepicondylar axis). CA, FFA and TEA signals are shown in **all** subplots, but due to curve overlap in right-hand side plots, CA and FFA are covered by TEA. Note to readers from a clinical background: knee extension is illustrated here as **positive** because following the right-hand rule it corresponds with a positive rotation around the laterally pointing mediolateral axis for a right knee.

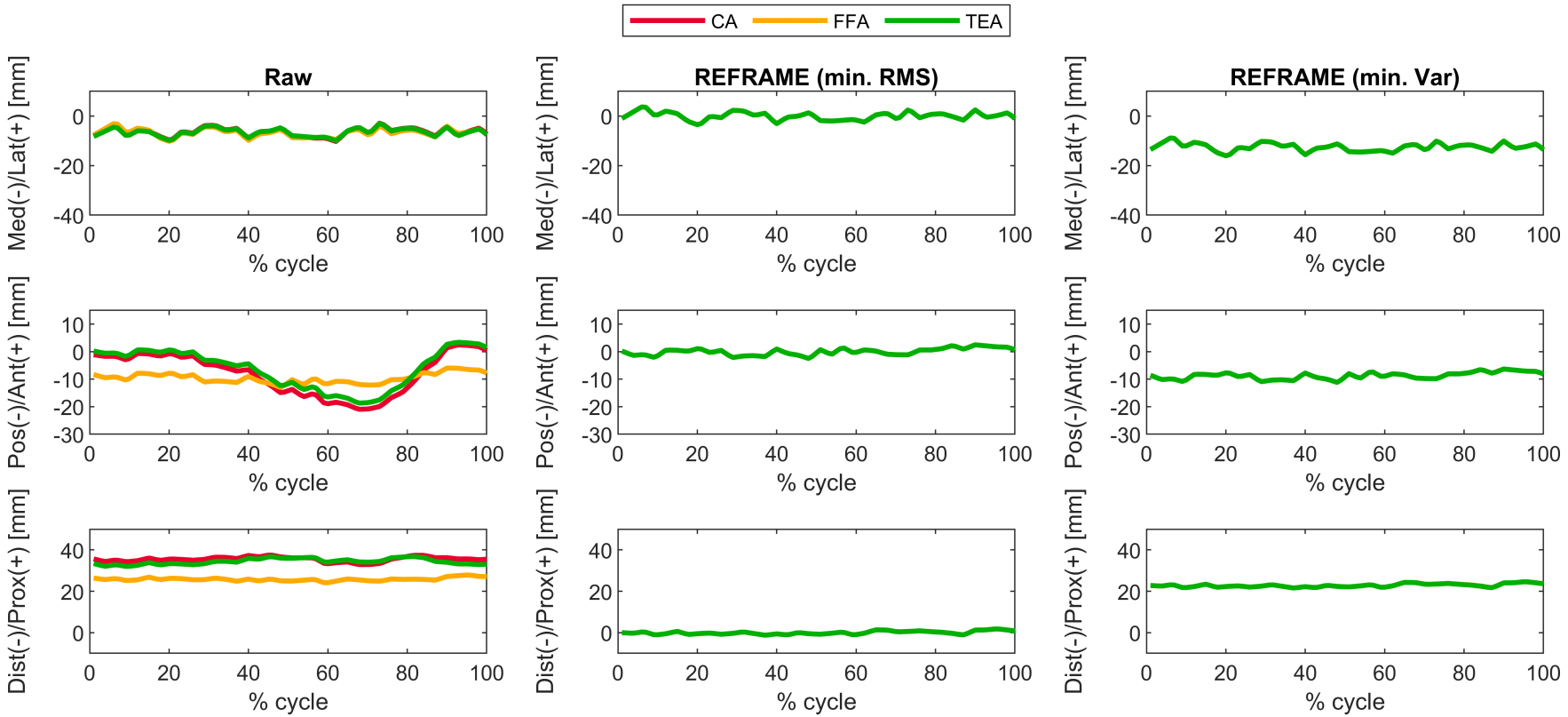

Supplementary Figure S78: Subject 8; Trial 2 – Translational kinematics: Joint translations (in mm) of the femoral relative to the tibial origin for one cycle of stair descent, before (raw, first column) and after application of the REFRAME optimisation (second column: based on the minimisation of translational root-mean-square; third column: based on the minimisation of translational variances), for all three axis approaches (CA: cylindrical axis; FFA: functional flexion axis; TEA: transepicondylar axis). CA, FFA and TEA signals are shown in **all** subplots, but due to curve overlap in the second and third columns, CA and FFA are covered by TEA.

3.8.3 Trial 3

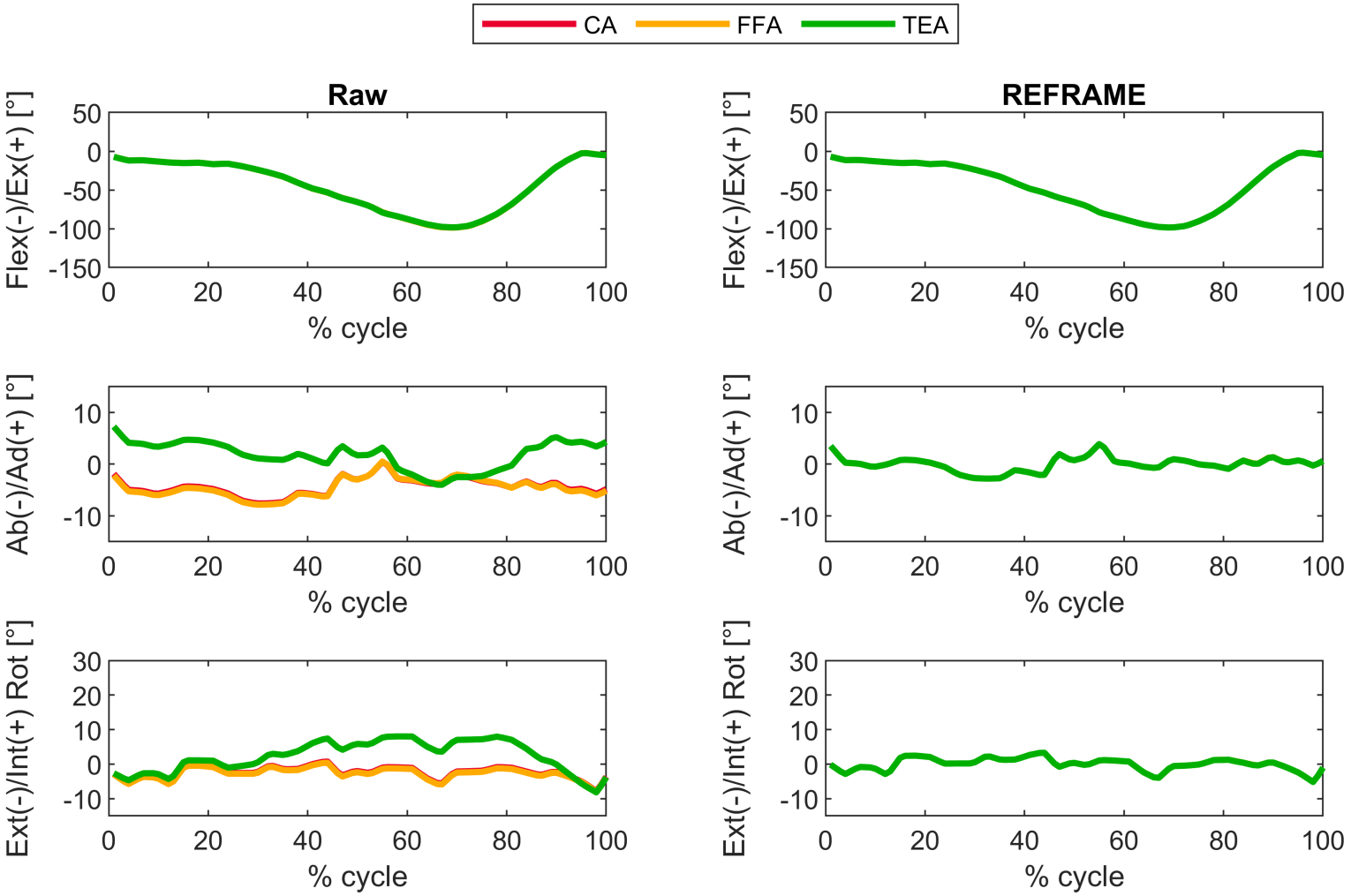

Supplementary Figure S79: Subject 8; Trial 3 – Rotational kinematics: Joint rotations (in degrees) of the tibial relative to the femoral segment frame for one cycle of stair descent, before (raw) and after REFRAME optimisation, for all three axis approaches (CA: cylindrical axis; FFA: functional flexion axis; TEA: transepicondylar axis). CA, FFA and TEA signals are shown in **all** subplots, but due to curve overlap in right-hand side plots, CA and FFA are covered by TEA. Note to readers from a clinical background: knee extension is illustrated here as **positive** because following the right-hand rule it corresponds with a positive rotation around the laterally pointing mediolateral axis for a right knee.

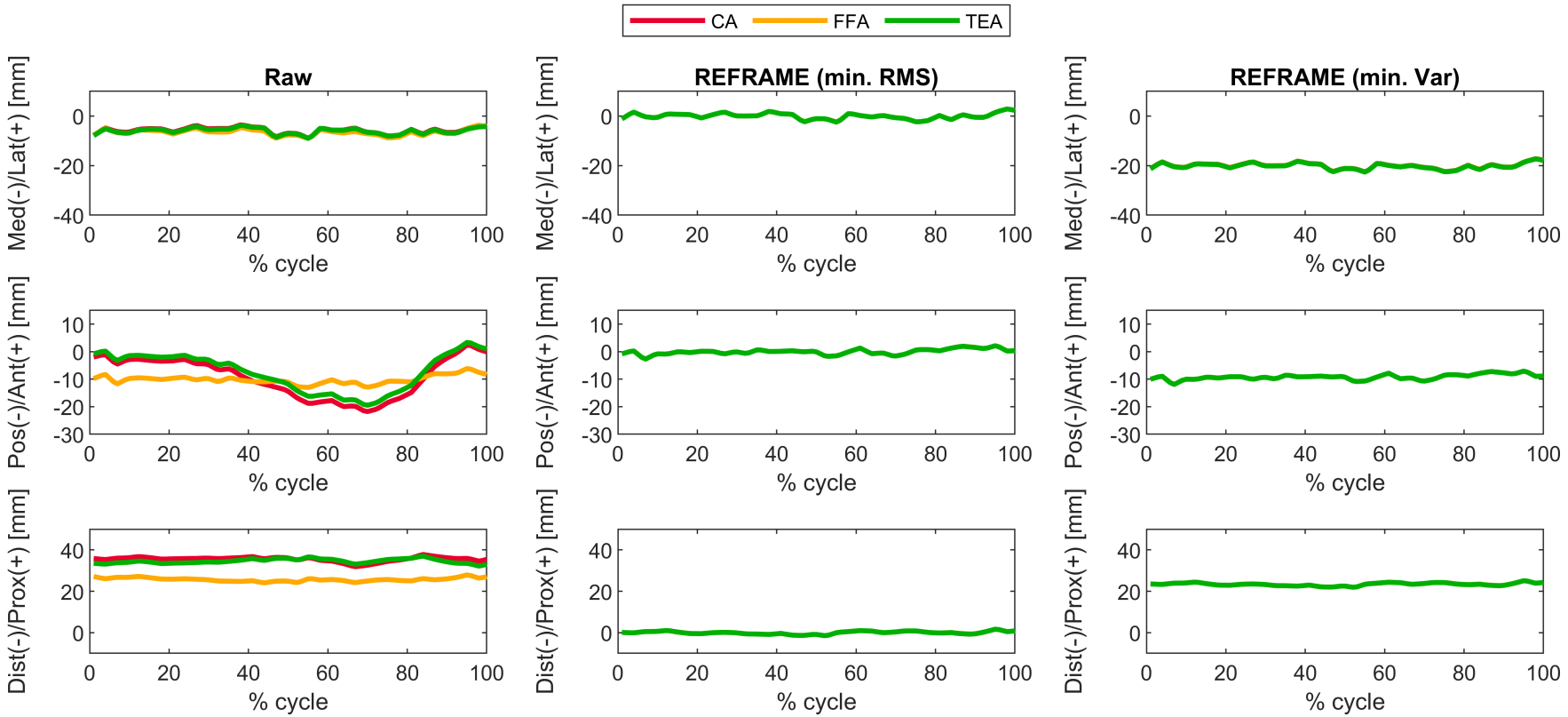

Supplementary Figure S80: Subject 8; Trial 3 – Translational kinematics: Joint translations (in mm) of the femoral relative to the tibial origin for one cycle of stair descent, before (raw, first column) and after application of the REFRAME optimisation (second column: based on the minimisation of translational root-mean-square; third column: based on the minimisation of translational variances), for all three axis approaches (CA: cylindrical axis; FFA: functional flexion axis; TEA: transepicondylar axis). CA, FFA and TEA signals are shown in **all** subplots, but due to curve overlap in the second and third columns, CA and FFA are covered by TEA.

3.8.4 Trial 4

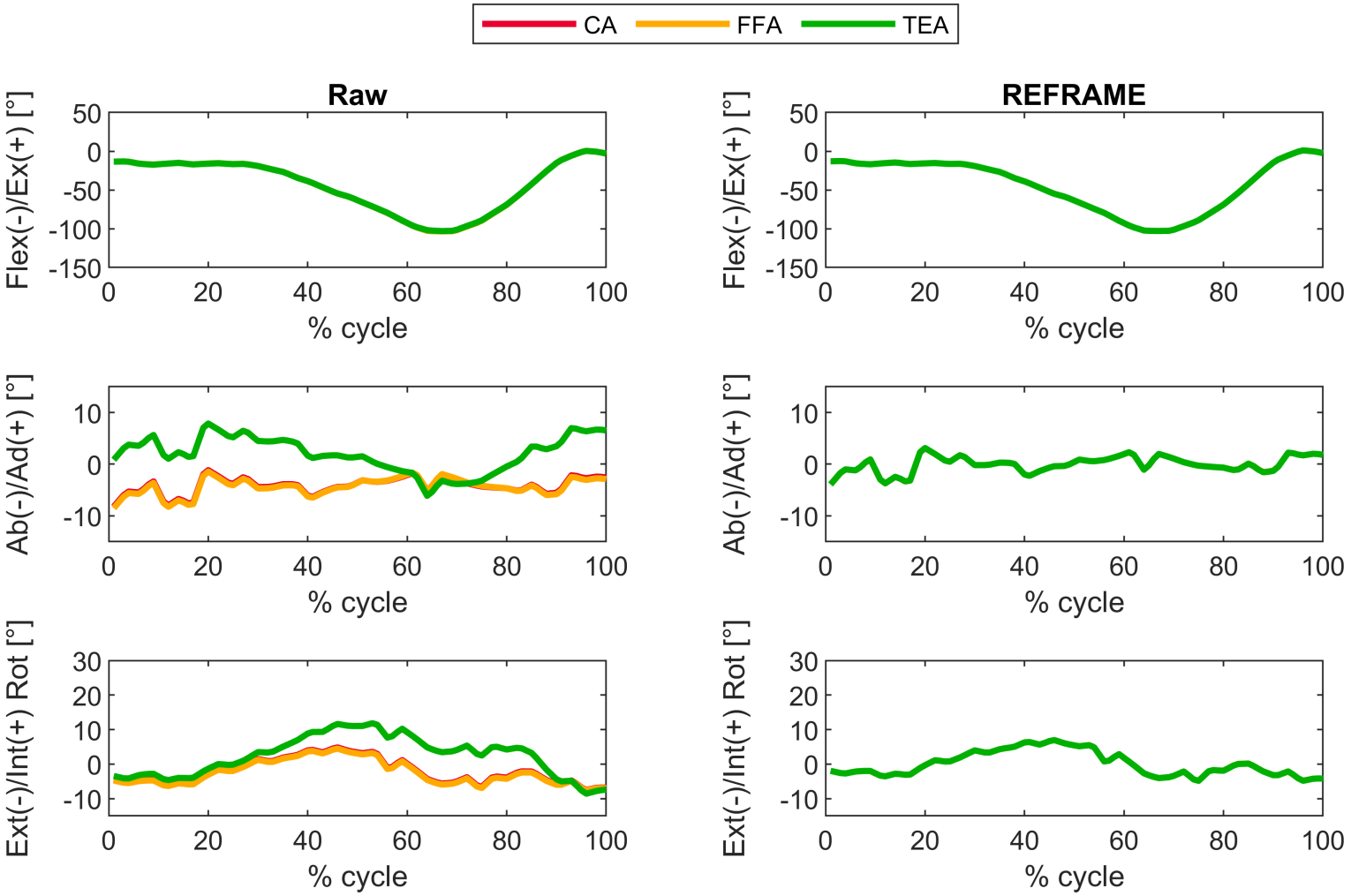

Supplementary Figure S81: Subject 8; Trial 4 – Rotational kinematics: Joint rotations (in degrees) of the tibial relative to the femoral segment frame for one cycle of stair descent, before (raw) and after REFRAME optimisation, for all three axis approaches (CA: cylindrical axis; FFA: functional flexion axis; TEA: transepicondylar axis). CA, FFA and TEA signals are shown in **all** subplots, but due to curve overlap in right-hand side plots, CA and FFA are covered by TEA. Note to readers from a clinical background: knee extension is illustrated here as **positive** because following the right-hand rule it corresponds with a positive rotation around the laterally pointing mediolateral axis for a right knee.

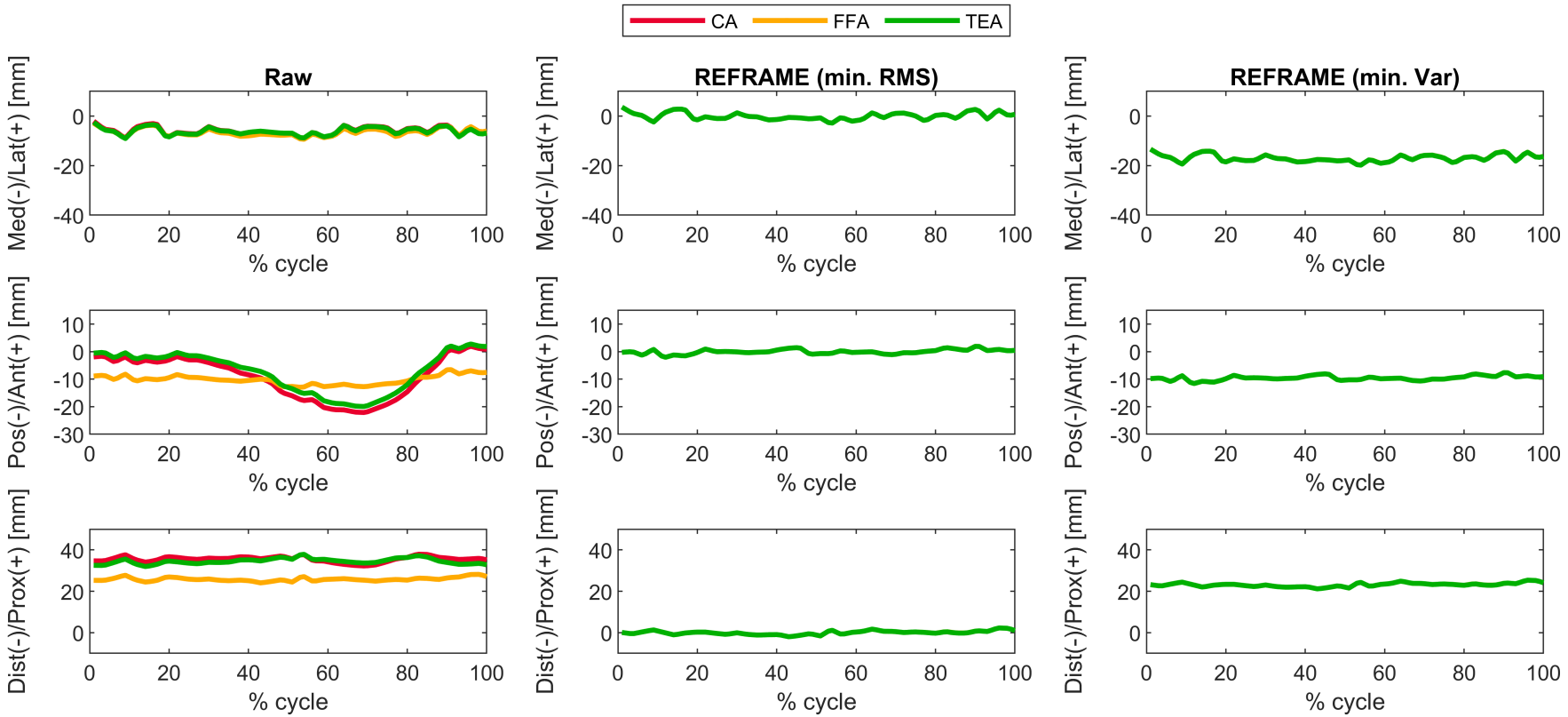

Supplementary Figure S82: Subject 8; Trial 4 – Translational kinematics: Joint translations (in mm) of the femoral relative to the tibial origin for one cycle of stair descent, before (raw, first column) and after application of the REFRAME optimisation (second column: based on the minimisation of translational root-mean-square; third column: based on the minimisation of translational variances), for all three axis approaches (CA: cylindrical axis; FFA: functional flexion axis; TEA: transepicondylar axis). CA, FFA and TEA signals are shown in **all** subplots, but due to curve overlap in the second and third columns, CA and FFA are covered by TEA.

3.8.5 Trial 5

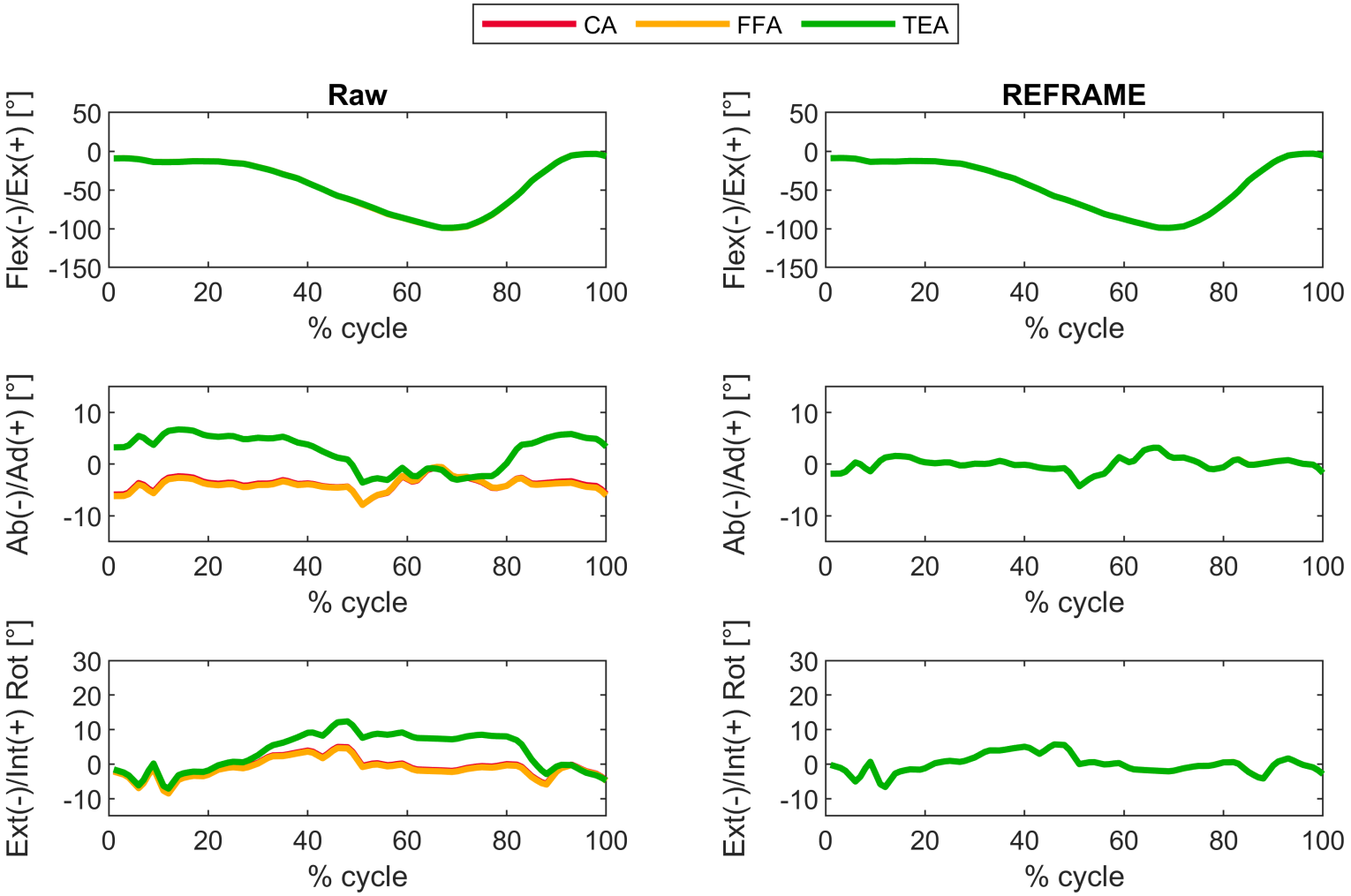

Supplementary Figure S83: Subject 8; Trial 5 – Rotational kinematics: Joint rotations (in degrees) of the tibial relative to the femoral segment frame for one cycle of stair descent, before (raw) and after REFRAME optimisation, for all three axis approaches (CA: cylindrical axis; FFA: functional flexion axis; TEA: transepicondylar axis). CA, FFA and TEA signals are shown in **all** subplots, but due to curve overlap in right-hand side plots, CA and FFA are covered by TEA. Note to readers from a clinical background: knee extension is illustrated here as **positive** because following the right-hand rule it corresponds with a positive rotation around the laterally pointing mediolateral axis for a right knee.

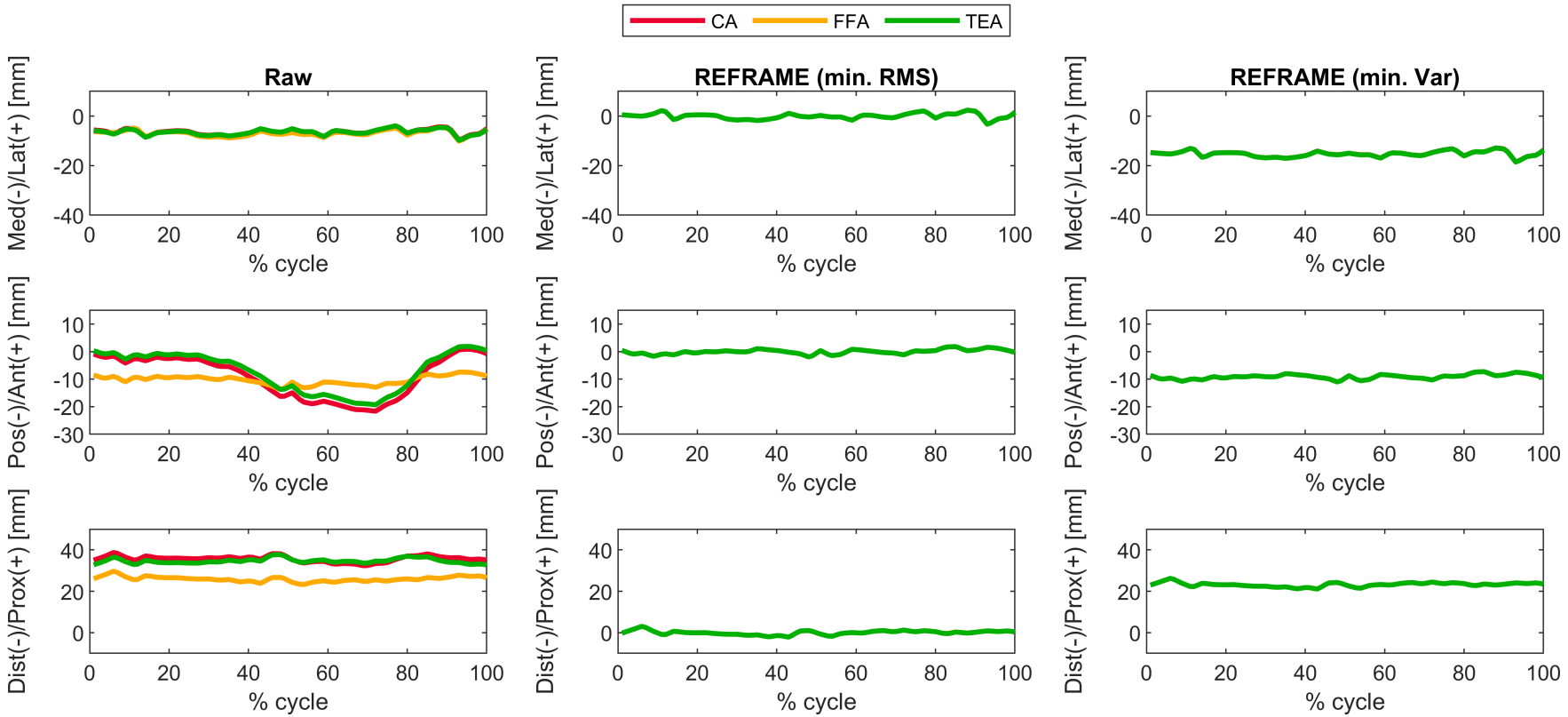

Supplementary Figure S84: Subject 8; Trial 5 – Translational kinematics: Joint translations (in mm) of the femoral relative to the tibial origin for one cycle of stair descent, before (raw, first column) and after application of the REFRAME optimisation (second column: based on the minimisation of translational root-mean-square; third column: based on the minimisation of translational variances), for all three axis approaches (CA: cylindrical axis; FFA: functional flexion axis; TEA: transepicondylar axis). CA, FFA and TEA signals are shown in **all** subplots, but due to curve overlap in the second and third columns, CA and FFA are covered by TEA.

3.9 Subject 9

3.9.1 Trial 1

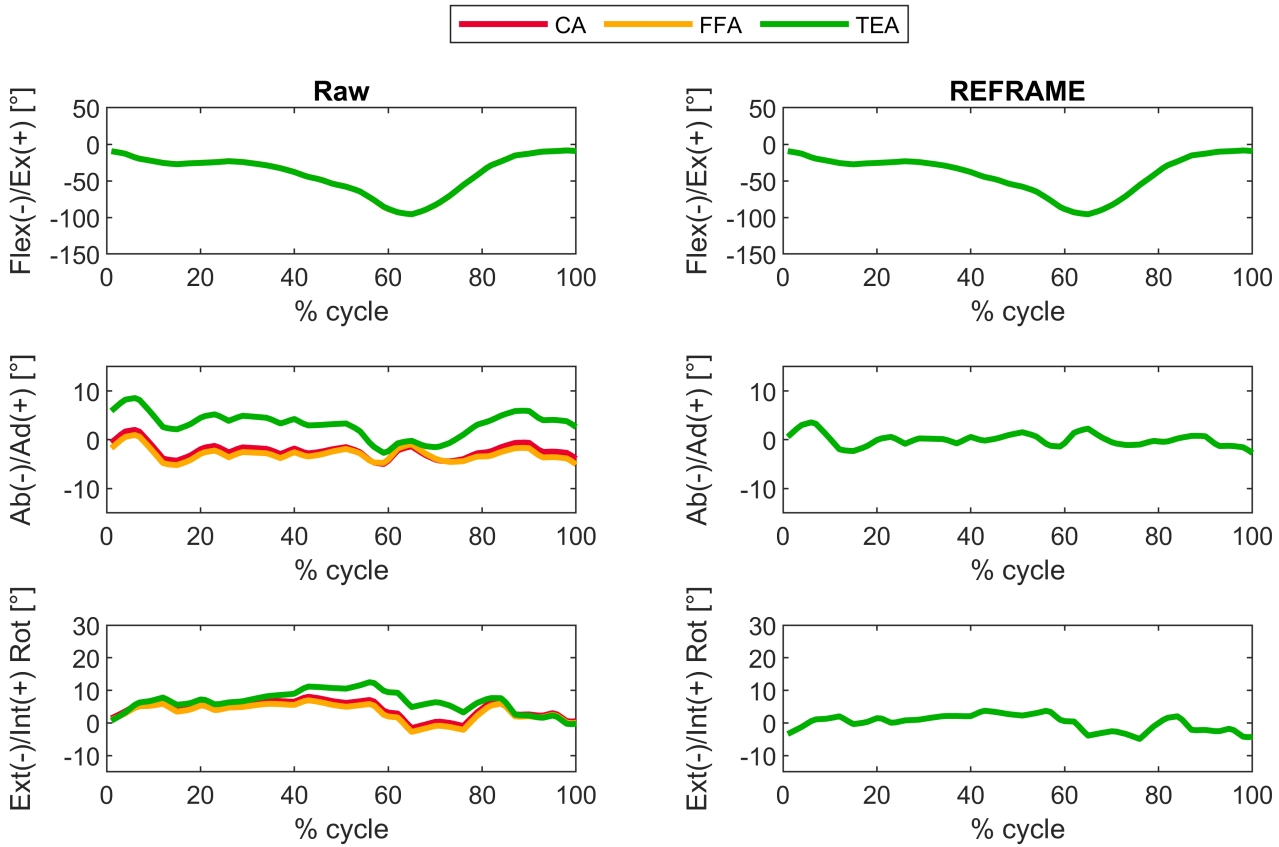

Supplementary Figure S85: Subject 9; Trial 1 – Rotational kinematics: Joint rotations (in degrees) of the tibial relative to the femoral segment frame for one cycle of stair descent, before (raw) and after REFRAME optimisation, for all three axis approaches (CA: cylindrical axis; FFA: functional flexion axis; TEA: transepicondylar axis). CA, FFA and TEA signals are shown in **all** subplots, but due to curve overlap in right-hand side plots, CA and FFA are covered by TEA. Note to readers from a clinical background: knee extension is illustrated here as **positive** because following the right-hand rule it corresponds with a positive rotation around the laterally pointing mediolateral axis for a right knee.

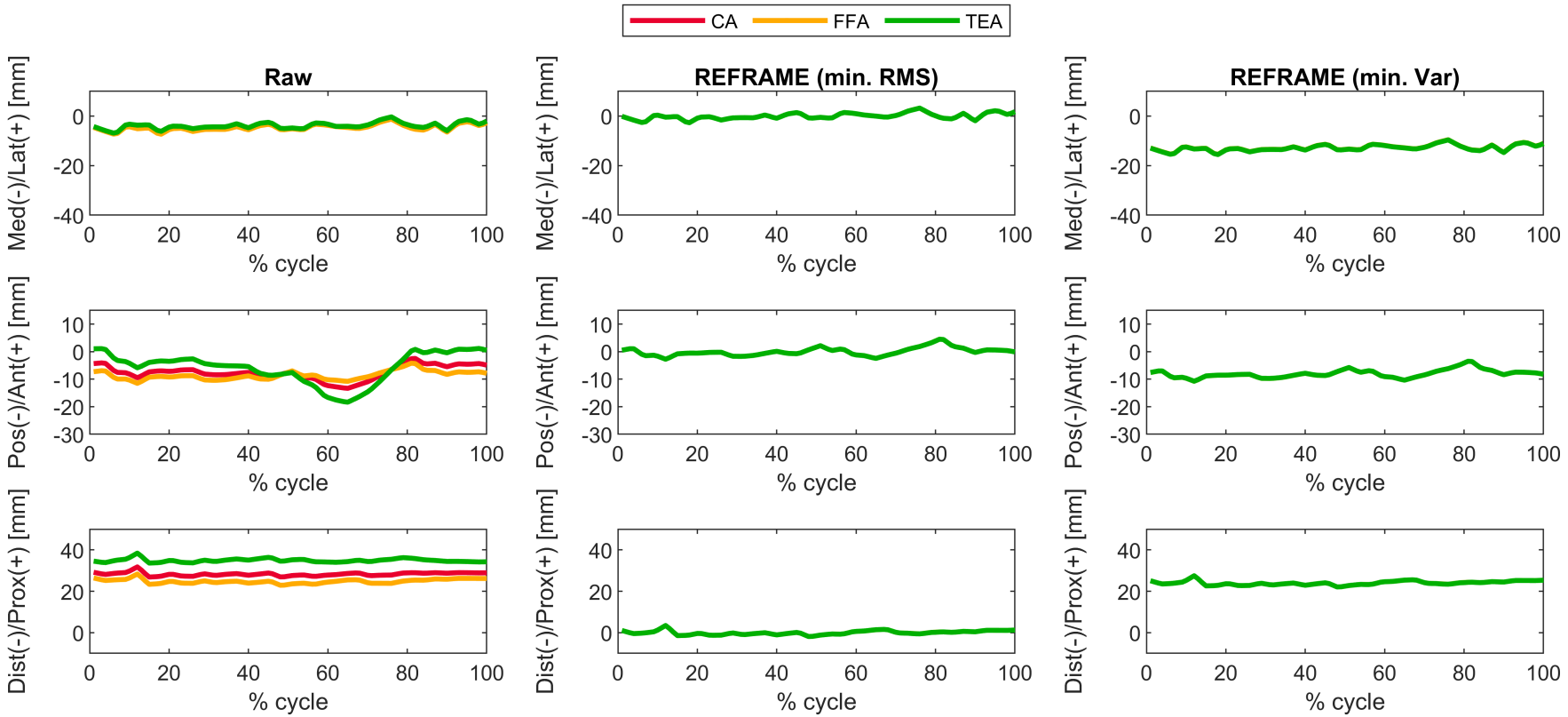

Supplementary Figure S86: Subject 9; Trial 1 – Translational kinematics: Joint translations (in mm) of the femoral relative to the tibial origin for one cycle of stair descent, before (raw, first column) and after application of the REFRAME optimisation (second column: based on the minimisation of translational root-mean-square; third column: based on the minimisation of translational variances), for all three axis approaches (CA: cylindrical axis; FFA: functional flexion axis; TEA: transepicondylar axis). CA, FFA and TEA signals are shown in **all** subplots, but due to curve overlap in the second and third columns, CA and FFA are covered by TEA.

3.9.2 Trial 2

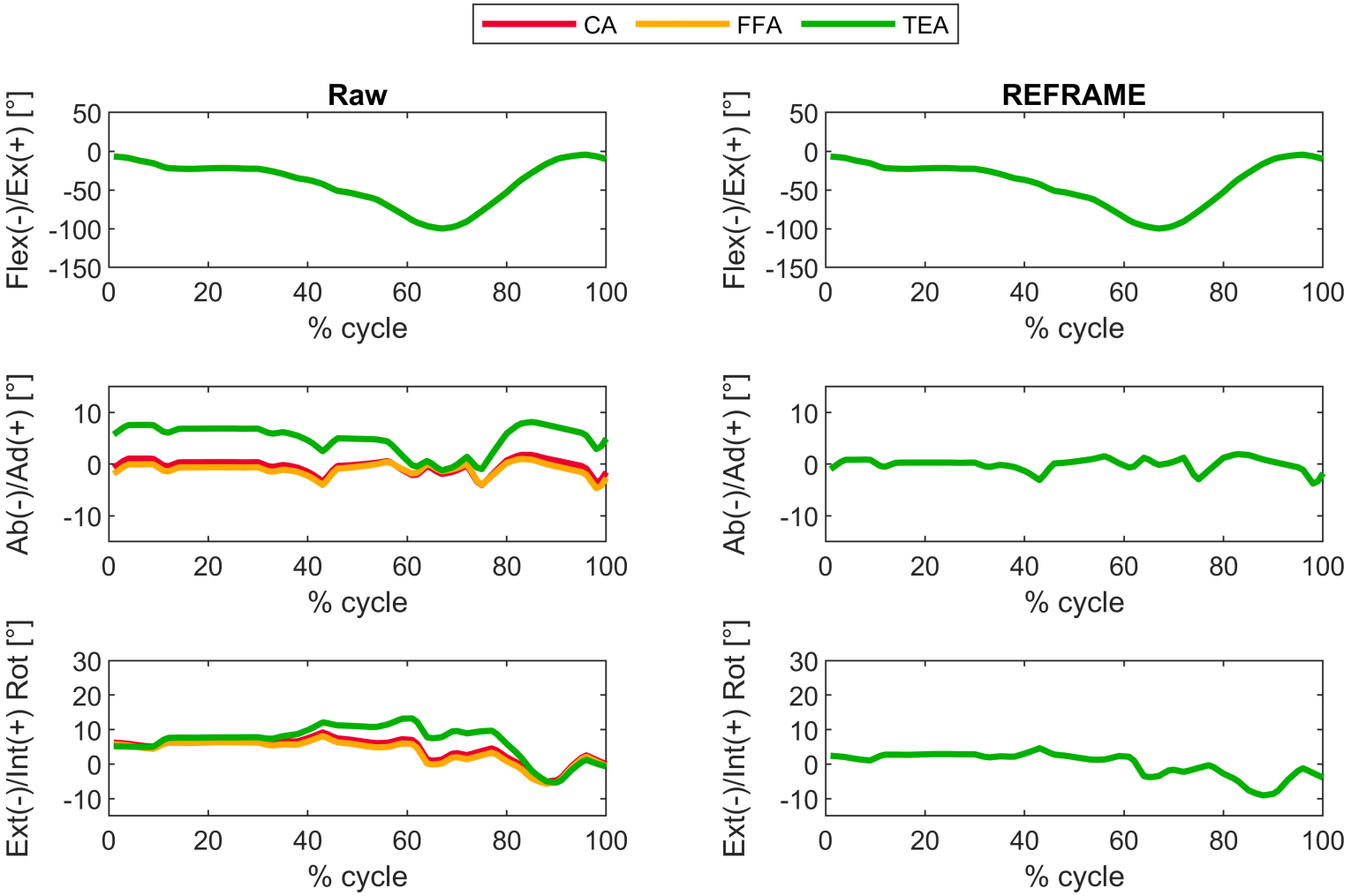

Supplementary Figure S87: Subject 9; Trial 2 – Rotational kinematics: Joint rotations (in degrees) of the tibial relative to the femoral segment frame for one cycle of stair descent, before (raw) and after REFRAME optimisation, for all three axis approaches (CA: cylindrical axis; FFA: functional flexion axis; TEA: transepicondylar axis). CA, FFA and TEA signals are shown in **all** subplots, but due to curve overlap in right-hand side plots, CA and FFA are covered by TEA. Note to readers from a clinical background: knee extension is illustrated here as **positive** because following the right-hand rule it corresponds with a positive rotation around the laterally pointing mediolateral axis for a right knee.

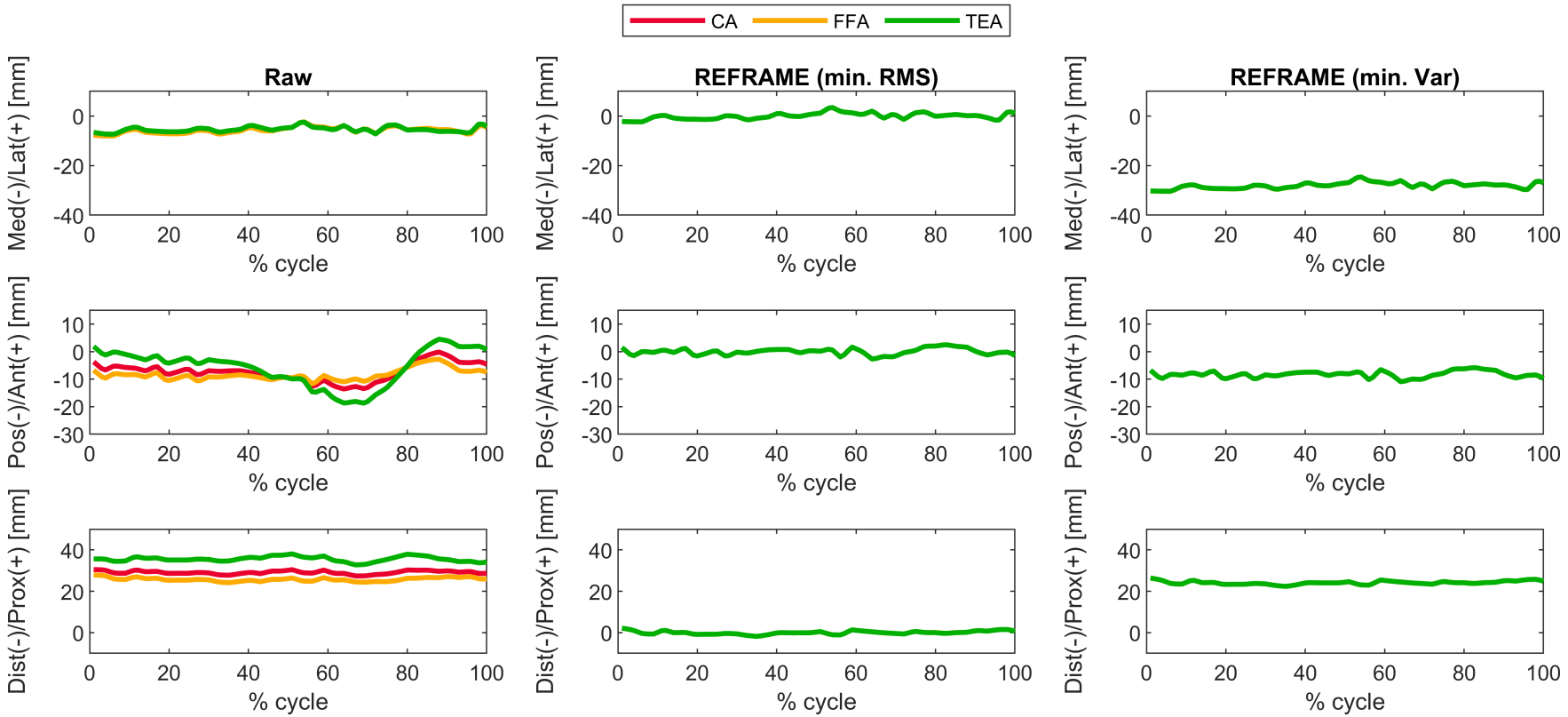

Supplementary Figure S88: Subject 9; Trial 2 – Translational kinematics: Joint translations (in mm) of the femoral relative to the tibial origin for one cycle of stair descent, before (raw, first column) and after application of the REFRAME optimisation (second column: based on the minimisation of translational root-mean-square; third column: based on the minimisation of translational variances), for all three axis approaches (CA: cylindrical axis; FFA: functional flexion axis; TEA: transepicondylar axis). CA, FFA and TEA signals are shown in **all** subplots, but due to curve overlap in the second and third columns, CA and FFA are covered by TEA.

3.9.3 Trial 3

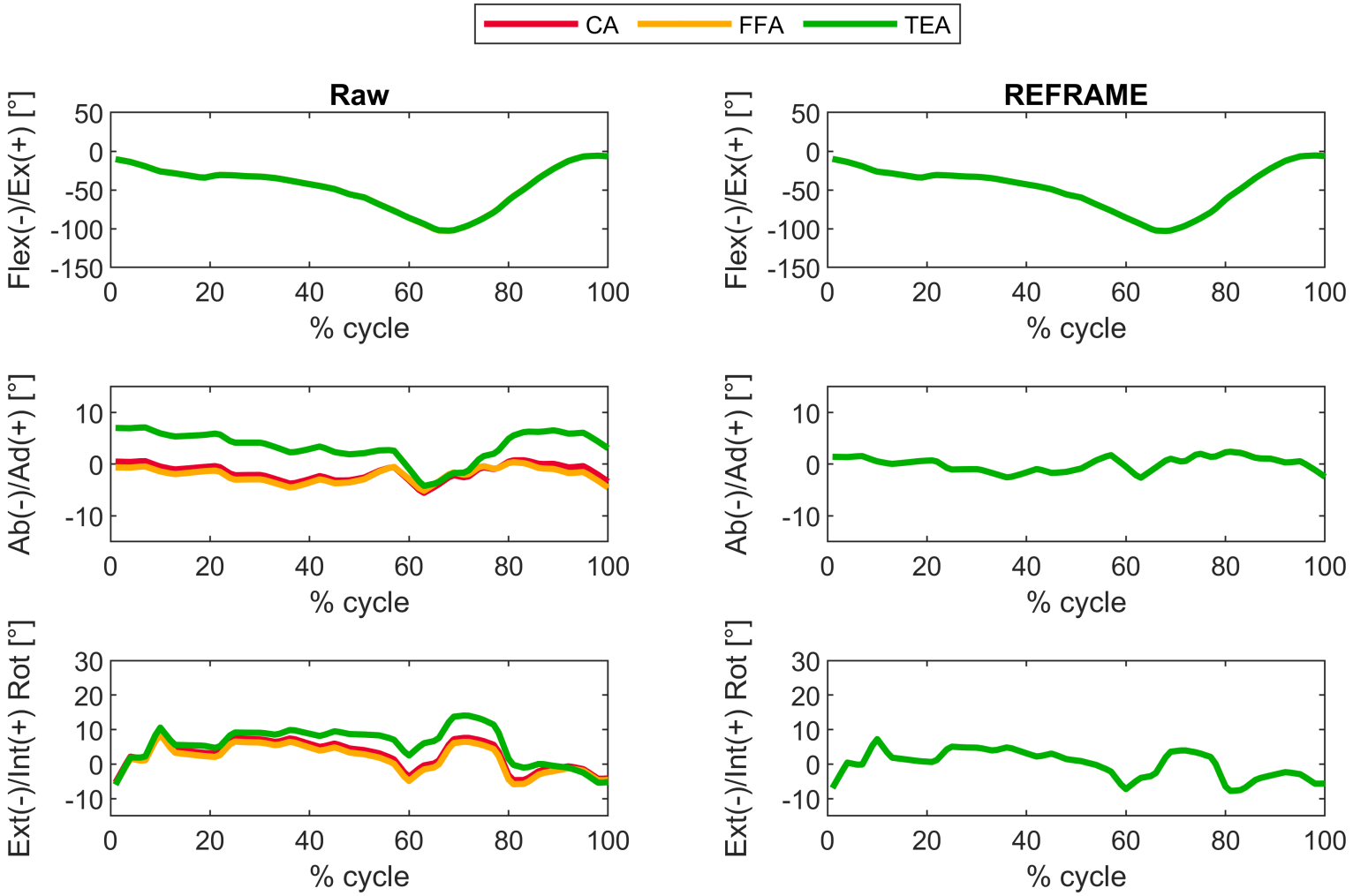

Supplementary Figure S89: Subject 9; Trial 3 – Rotational kinematics: Joint rotations (in degrees) of the tibial relative to the femoral segment frame for one cycle of stair descent, before (raw) and after REFRAME optimisation, for all three axis approaches (CA: cylindrical axis; FFA: functional flexion axis; TEA: transepicondylar axis). CA, FFA and TEA signals are shown in **all** subplots, but due to curve overlap in right-hand side plots, CA and FFA are covered by TEA. Note to readers from a clinical background: knee extension is illustrated here as **positive** because following the right-hand rule it corresponds with a positive rotation around the laterally pointing mediolateral axis for a right knee.

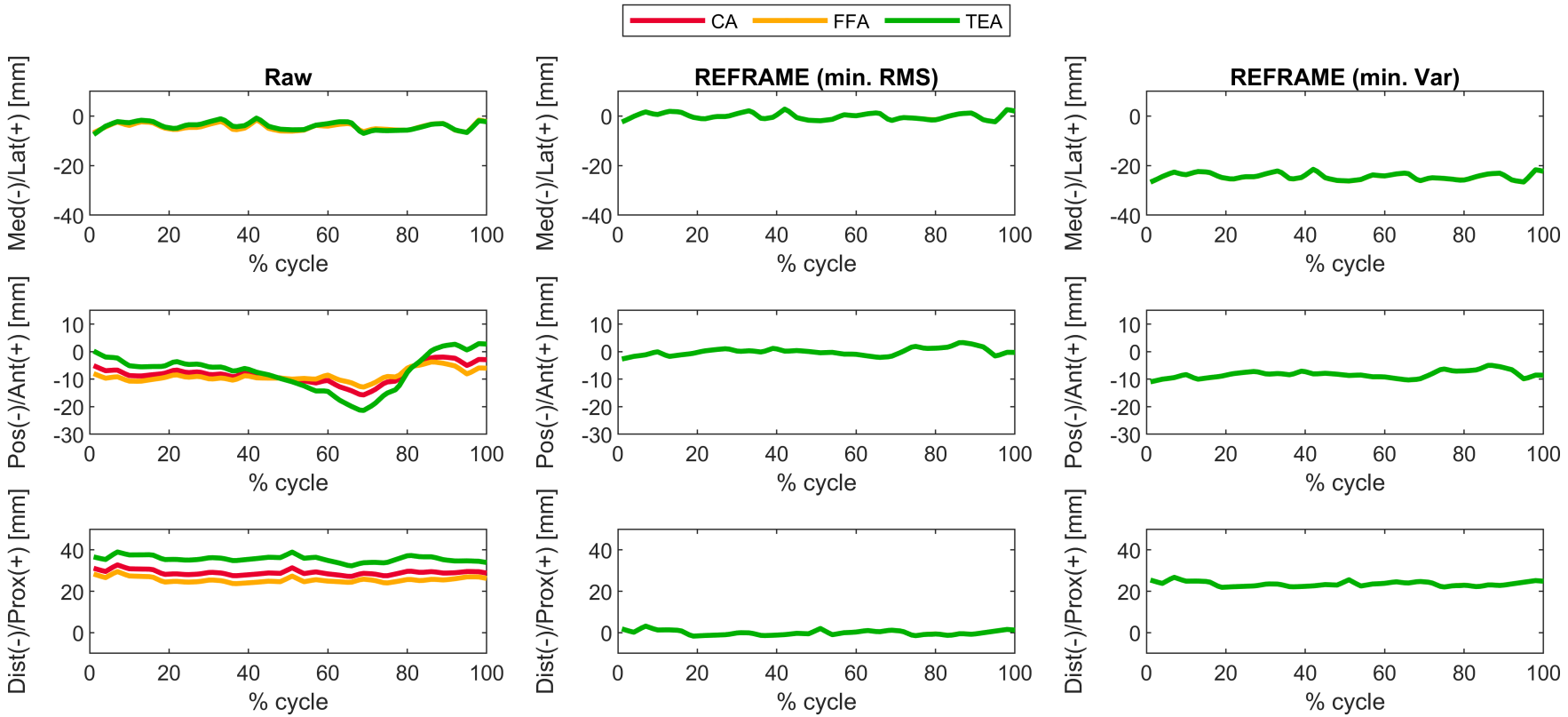

Supplementary Figure S90: Subject 9; Trial 3 – Translational kinematics: Joint translations (in mm) of the femoral relative to the tibial origin for one cycle of stair descent, before (raw, first column) and after application of the REFRAME optimisation (second column: based on the minimisation of translational root-mean-square; third column: based on the minimisation of translational variances), for all three axis approaches (CA: cylindrical axis; FFA: functional flexion axis; TEA: transepicondylar axis). CA, FFA and TEA signals are shown in **all** subplots, but due to curve overlap in the second and third columns, CA and FFA are covered by TEA.

3.9.4 Trial 4

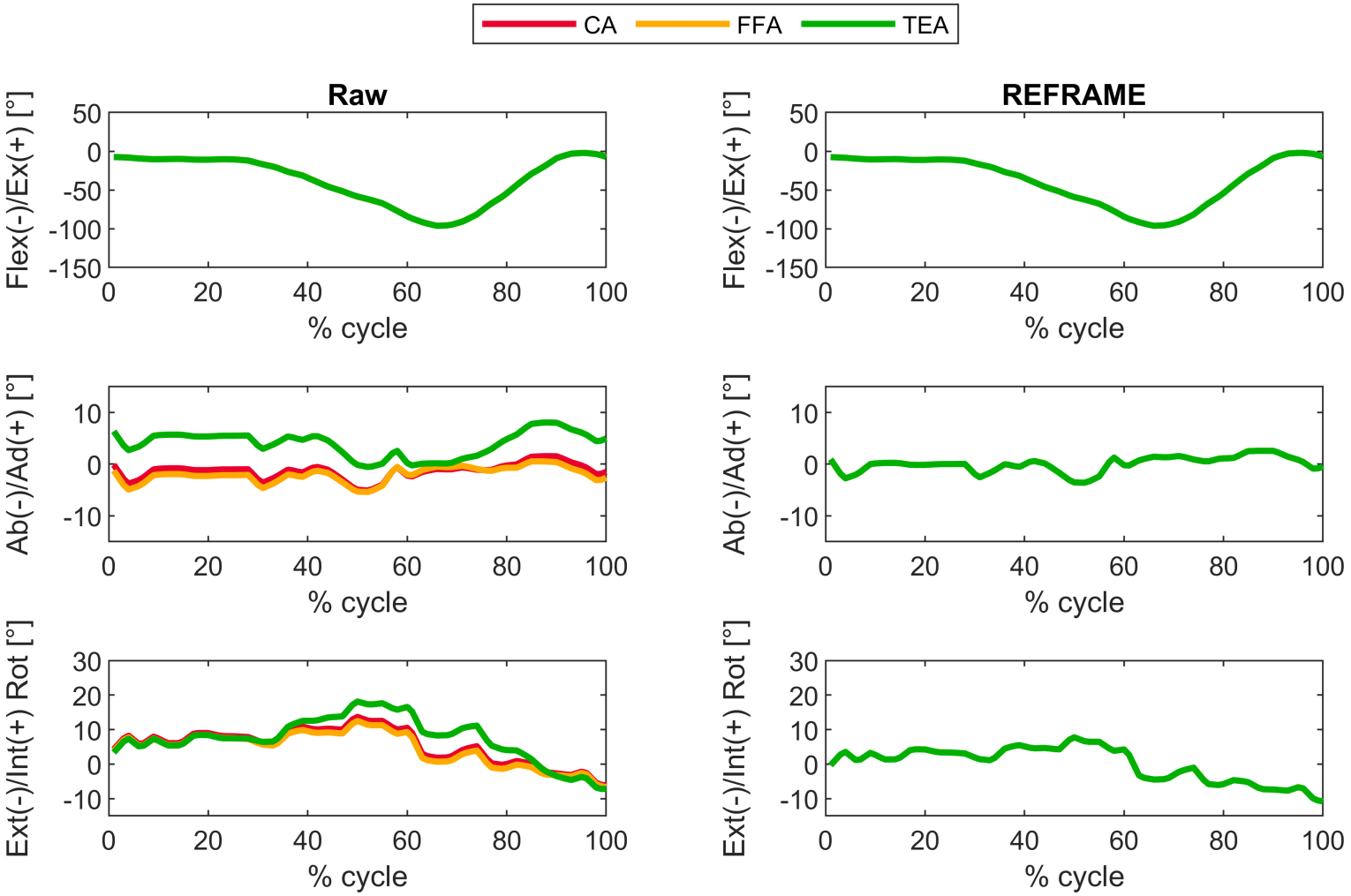

Supplementary Figure S91: Subject 9; Trial 4 – Rotational kinematics: Joint rotations (in degrees) of the tibial relative to the femoral segment frame for one cycle of stair descent, before (raw) and after REFRAME optimisation, for all three axis approaches (CA: cylindrical axis; FFA: functional flexion axis; TEA: transepicondylar axis). CA, FFA and TEA signals are shown in **all** subplots, but due to curve overlap in right-hand side plots, CA and FFA are covered by TEA. Note to readers from a clinical background: knee extension is illustrated here as **positive** because following the right-hand rule it corresponds with a positive rotation around the laterally pointing mediolateral axis for a right knee.

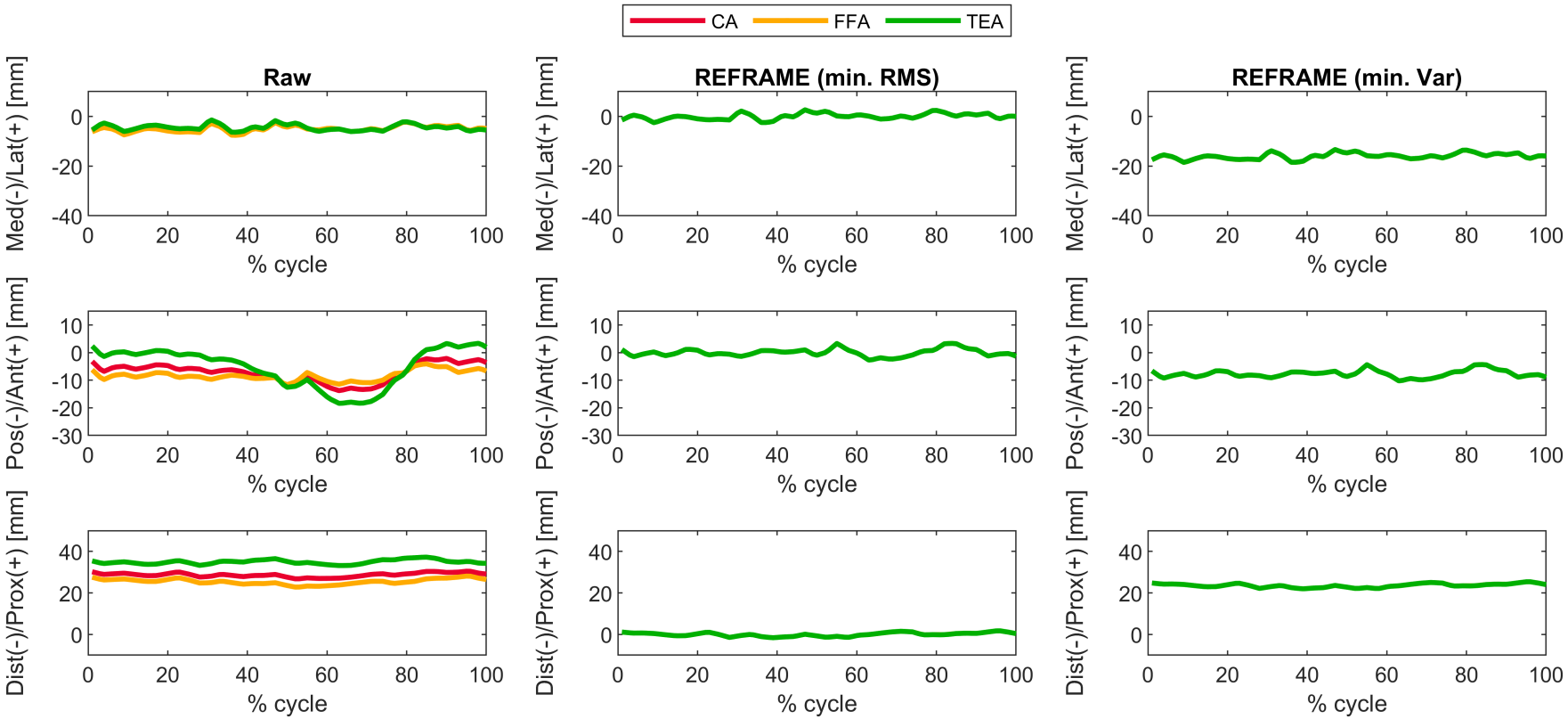

Supplementary Figure S92: Subject 9; Trial 4 – Translational kinematics: Joint translations (in mm) of the femoral relative to the tibial origin for one cycle of stair descent, before (raw, first column) and after application of the REFRAME optimisation (second column: based on the minimisation of translational root-mean-square; third column: based on the minimisation of translational variances), for all three axis approaches (CA: cylindrical axis; FFA: functional flexion axis; TEA: transepicondylar axis). CA, FFA and TEA signals are shown in **all** subplots, but due to curve overlap in the second and third columns, CA and FFA are covered by TEA.

3.9.5 Trial 5

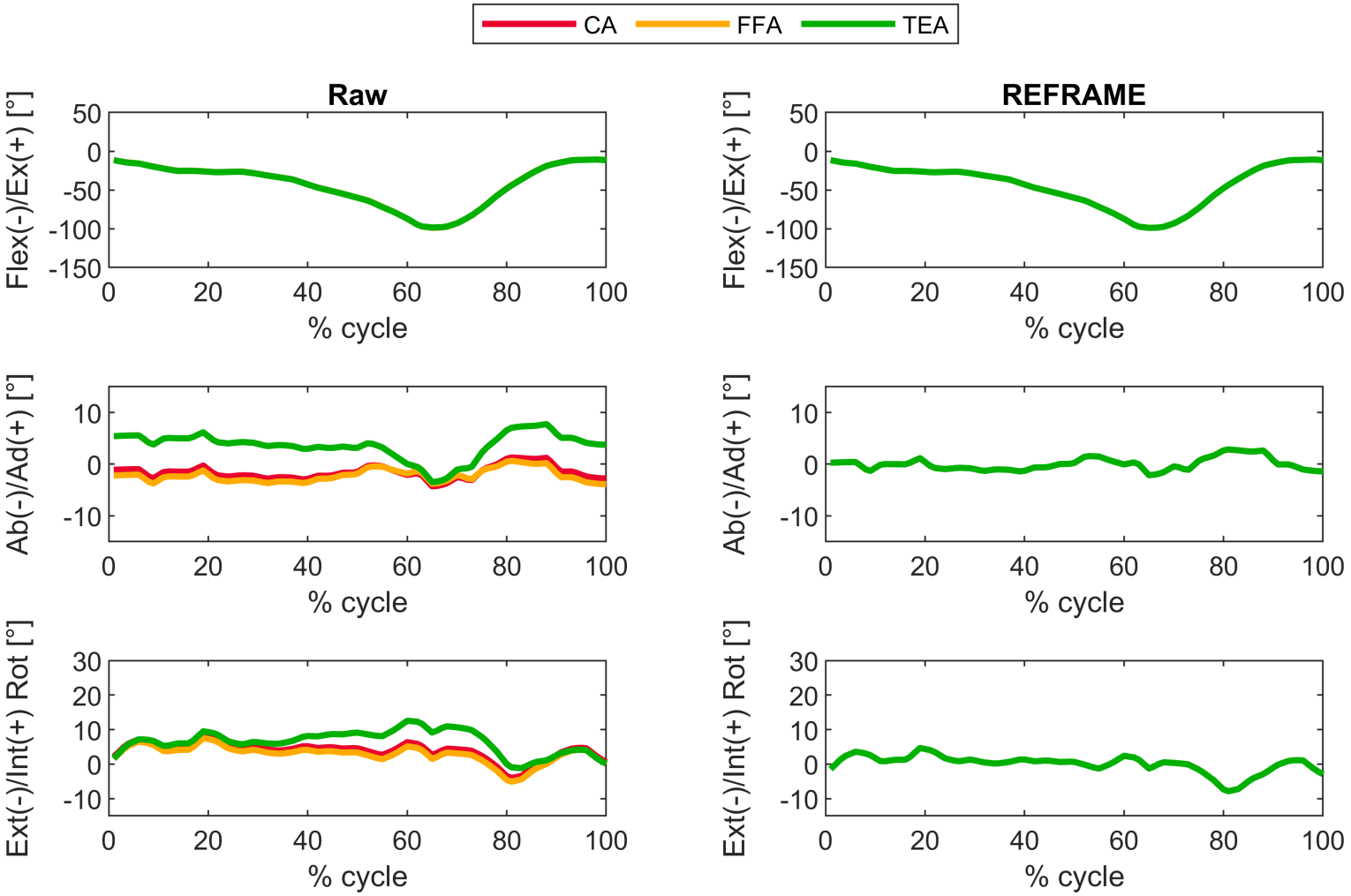

Supplementary Figure S93: Subject 9; Trial 5 – Rotational kinematics: Joint rotations (in degrees) of the tibial relative to the femoral segment frame for one cycle of stair descent, before (raw) and after REFRAME optimisation, for all three axis approaches (CA: cylindrical axis; FFA: functional flexion axis; TEA: transepicondylar axis). CA, FFA and TEA signals are shown in **all** subplots, but due to curve overlap in right-hand side plots, CA and FFA are covered by TEA. Note to readers from a clinical background: knee extension is illustrated here as **positive** because following the right-hand rule it corresponds with a positive rotation around the laterally pointing mediolateral axis for a right knee.

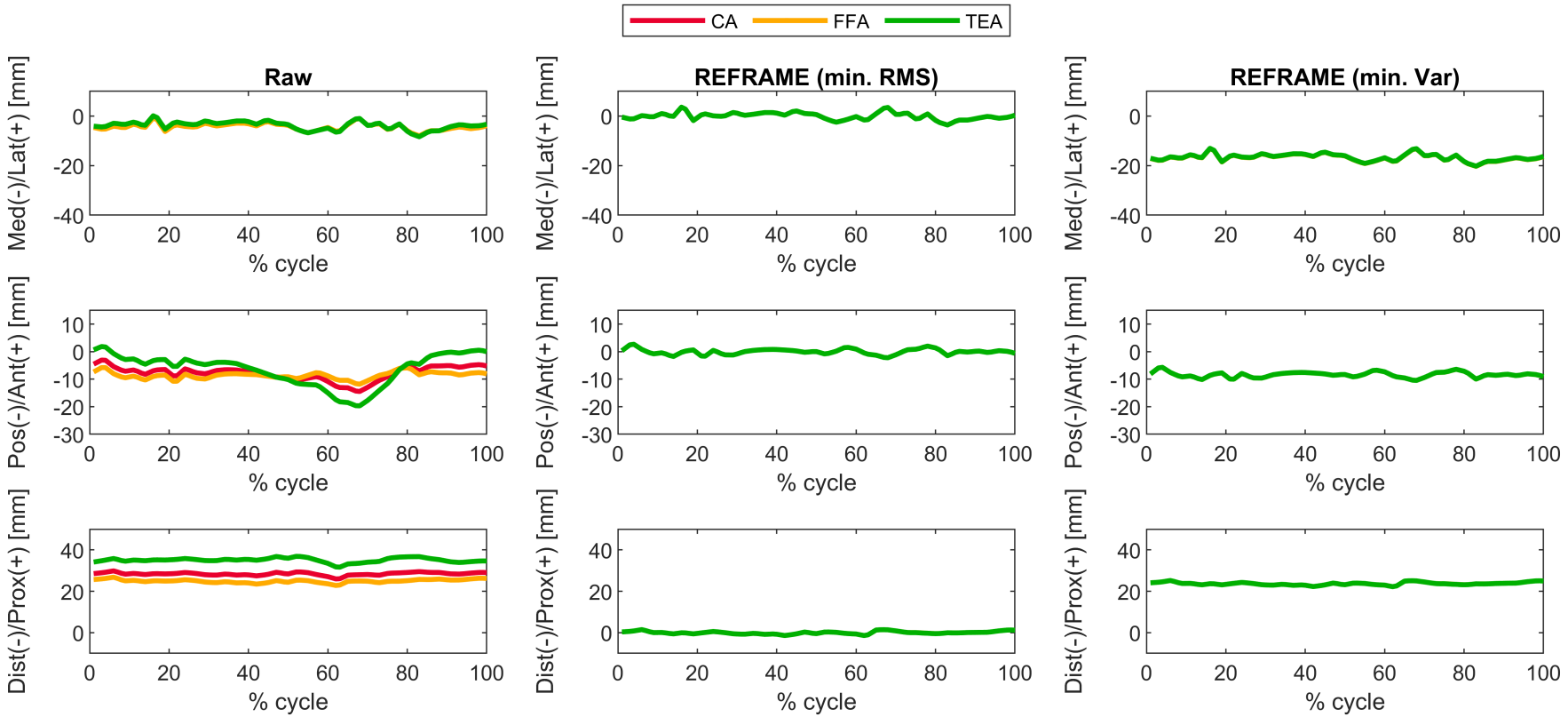

Supplementary Figure S94: Subject 9; Trial 5 – Translational kinematics: Joint translations (in mm) of the femoral relative to the tibial origin for one cycle of stair descent, before (raw, first column) and after application of the REFRAME optimisation (second column: based on the minimisation of translational root-mean-square; third column: based on the minimisation of translational variances), for all three axis approaches (CA: cylindrical axis; FFA: functional flexion axis; TEA: transepicondylar axis). CA, FFA and TEA signals are shown in **all** subplots, but due to curve overlap in the second and third columns, CA and FFA are covered by TEA.

3.10 Subject 10

3.10.1 Trial 1

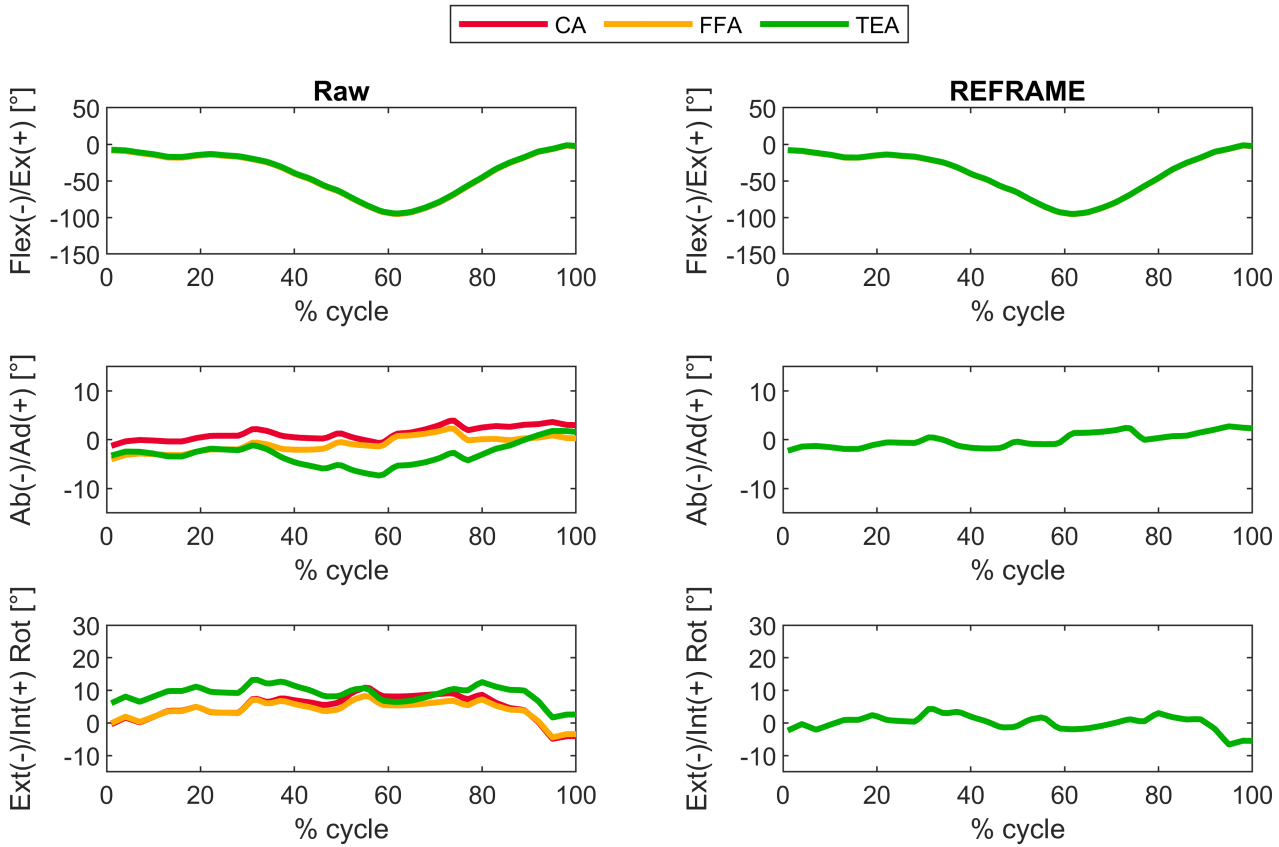

Supplementary Figure S95: Subject 10; Trial 1 – Rotational kinematics: Joint rotations (in degrees) of the tibial relative to the femoral segment frame for one cycle of stair descent, before (raw) and after REFRAME optimisation, for all three axis approaches (CA: cylindrical axis; FFA: functional flexion axis; TEA: transepicondylar axis). CA, FFA and TEA signals are shown in **all** subplots, but due to curve overlap in right-hand side plots, CA and FFA are covered by TEA. Note to readers from a clinical background: knee extension is illustrated here as **positive** because following the right-hand rule it corresponds with a positive rotation around the laterally pointing mediolateral axis for a right knee.

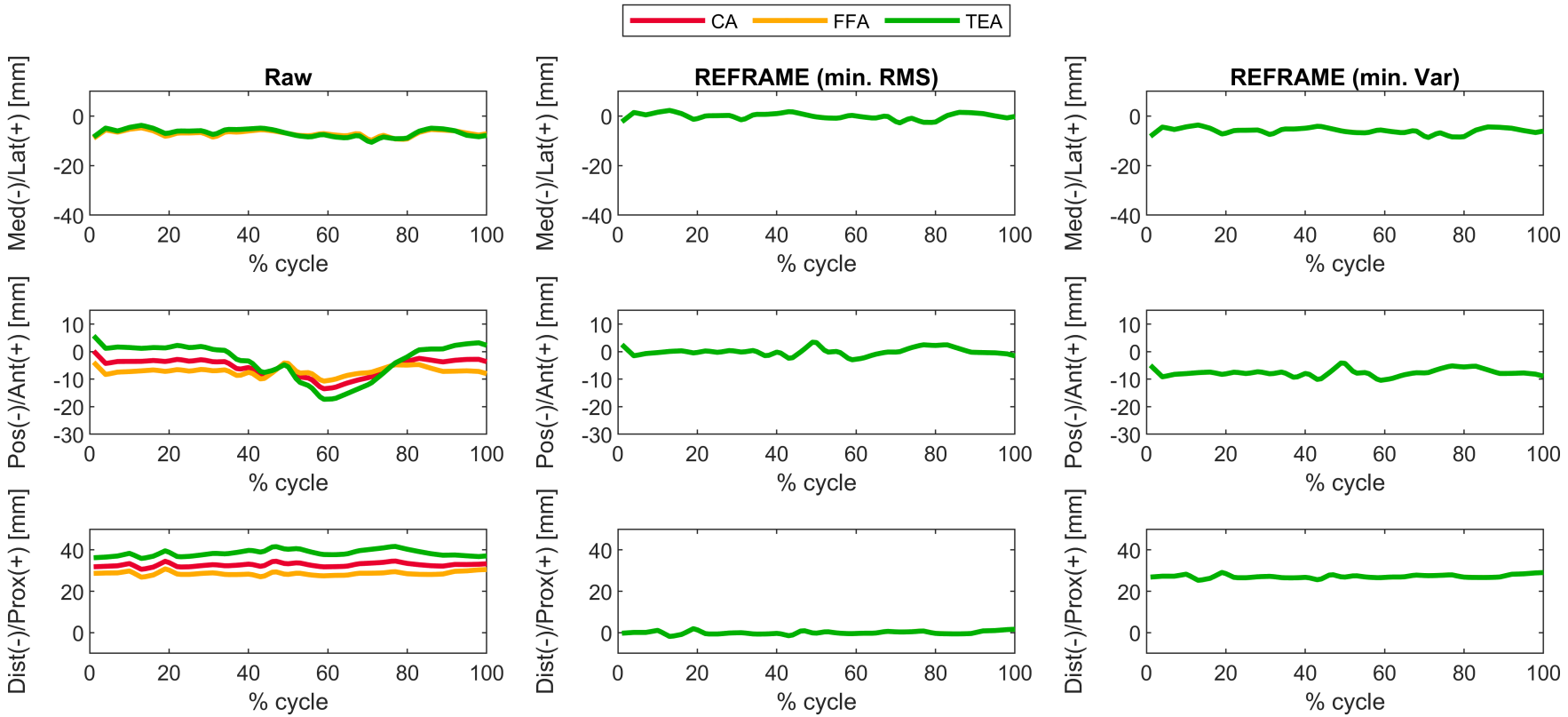

Supplementary Figure S96: Subject 10; Trial 1 – Translational kinematics: Joint translations (in mm) of the femoral relative to the tibial origin for one cycle of stair descent, before (raw, first column) and after application of the REFRAME optimisation (second column: based on the minimisation of translational root-mean-square; third column: based on the minimisation of translational variances), for all three axis approaches (CA: cylindrical axis; FFA: functional flexion axis; TEA: transepicondylar axis). CA, FFA and TEA signals are shown in **all** subplots, but due to curve overlap in the second and third columns, CA and FFA are covered by TEA.

3.10.2 Trial 2

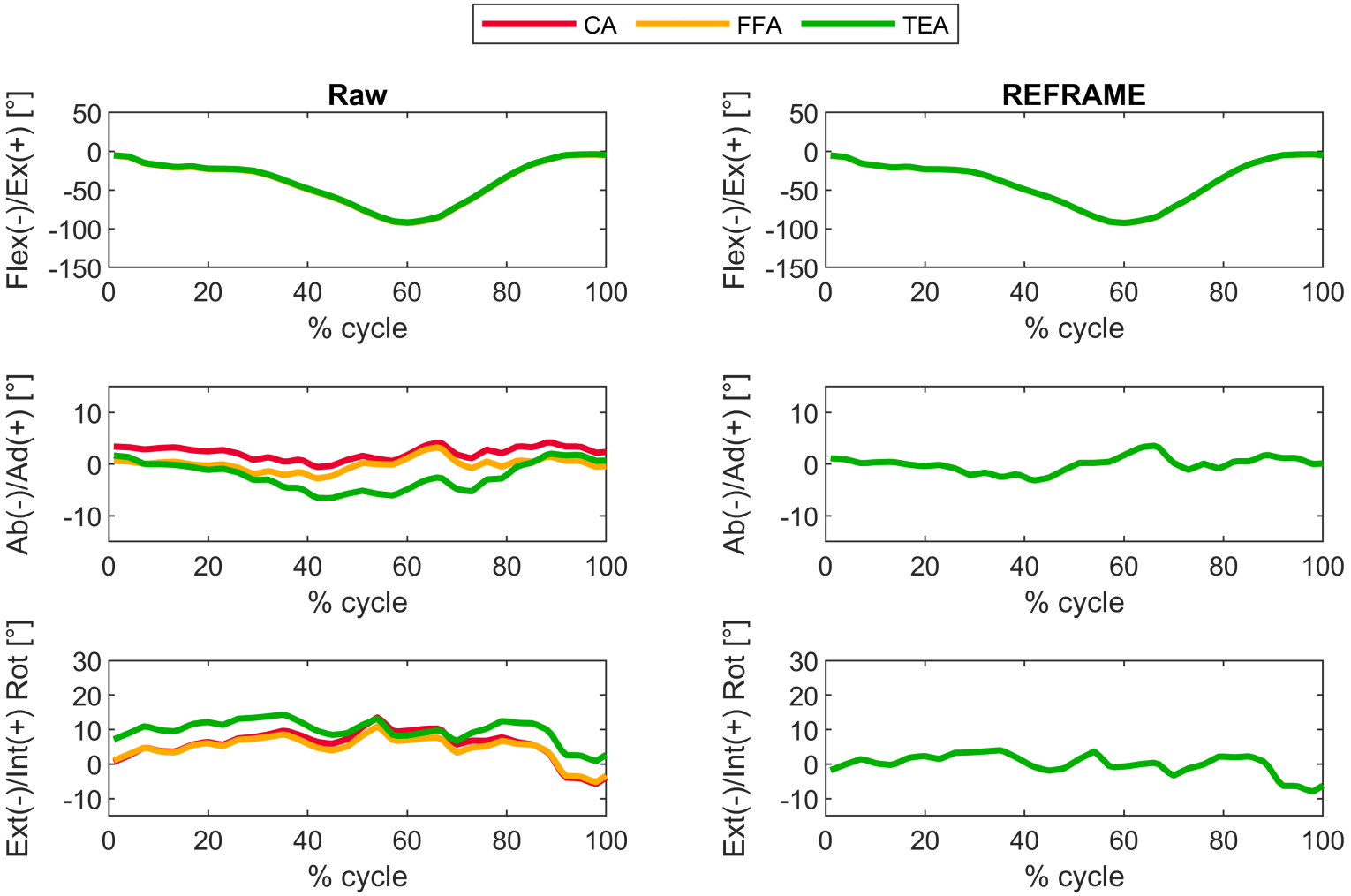

Supplementary Figure S97: Subject 10; Trial 2 – Rotational kinematics: Joint rotations (in degrees) of the tibial relative to the femoral segment frame for one cycle of stair descent, before (raw) and after REFRAME optimisation, for all three axis approaches (CA: cylindrical axis; FFA: functional flexion axis; TEA: transepicondylar axis). CA, FFA and TEA signals are shown in **all** subplots, but due to curve overlap in right-hand side plots, CA and FFA are covered by TEA. Note to readers from a clinical background: knee extension is illustrated here as **positive** because following the right-hand rule it corresponds with a positive rotation around the laterally pointing mediolateral axis for a right knee.

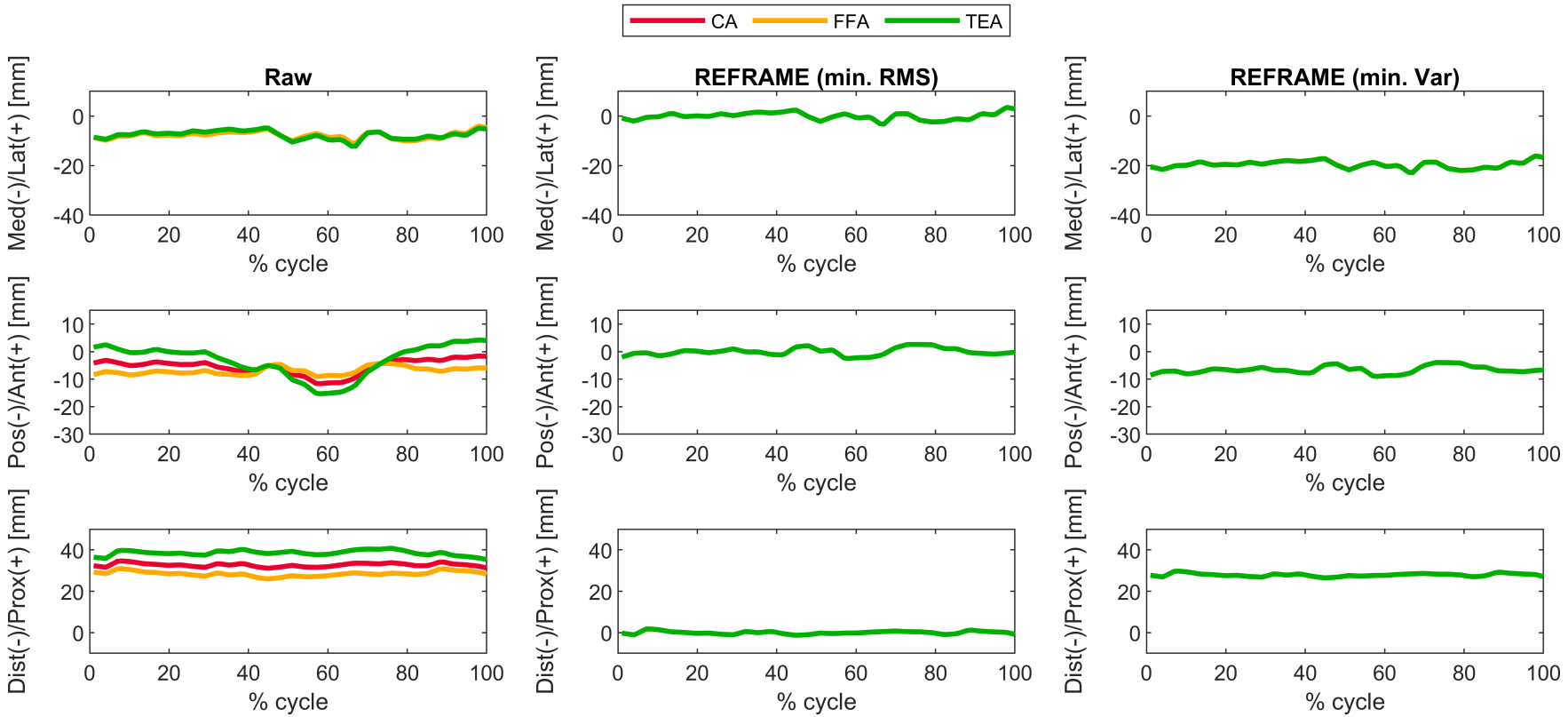

Supplementary Figure S98: Subject 10; Trial 2 – Translational kinematics: Joint translations (in mm) of the femoral relative to the tibial origin for one cycle of stair descent, before (raw, first column) and after application of the REFRAME optimisation (second column: based on the minimisation of translational root-mean-square; third column: based on the minimisation of translational variances), for all three axis approaches (CA: cylindrical axis; FFA: functional flexion axis; TEA: transepicondylar axis). CA, FFA and TEA signals are shown in **all** subplots, but due to curve overlap in the second and third columns, CA and FFA are covered by TEA.

3.10.3 Trial 3

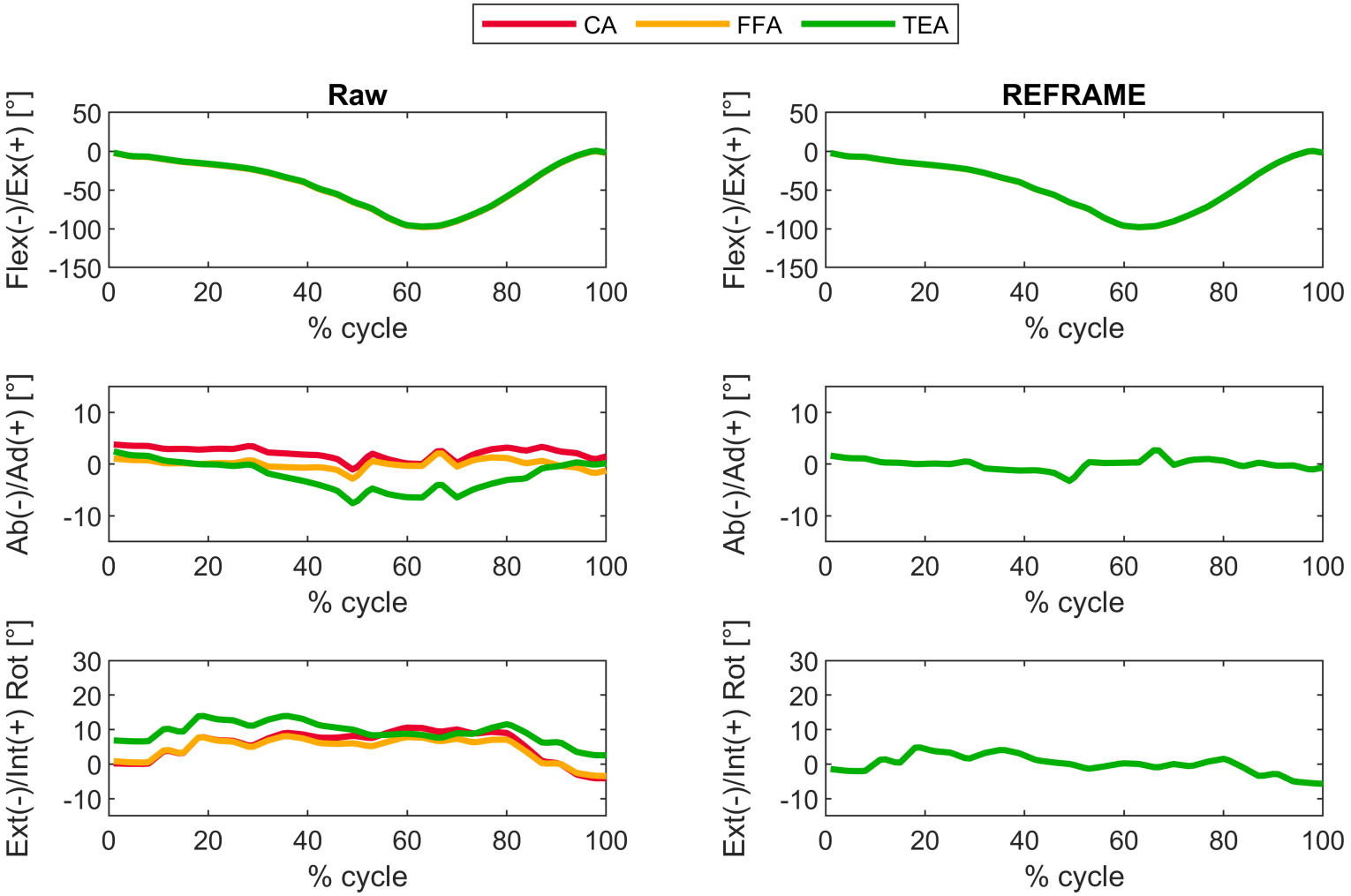

Supplementary Figure S99: Subject 10; Trial 3 – Rotational kinematics: Joint rotations (in degrees) of the tibial relative to the femoral segment frame for one cycle of stair descent, before (raw) and after REFRAME optimisation, for all three axis approaches (CA: cylindrical axis; FFA: functional flexion axis; TEA: transepicondylar axis). CA, FFA and TEA signals are shown in **all** subplots, but due to curve overlap in right-hand side plots, CA and FFA are covered by TEA. Note to readers from a clinical background: knee extension is illustrated here as **positive** because following the right-hand rule it corresponds with a positive rotation around the laterally pointing mediolateral axis for a right knee.

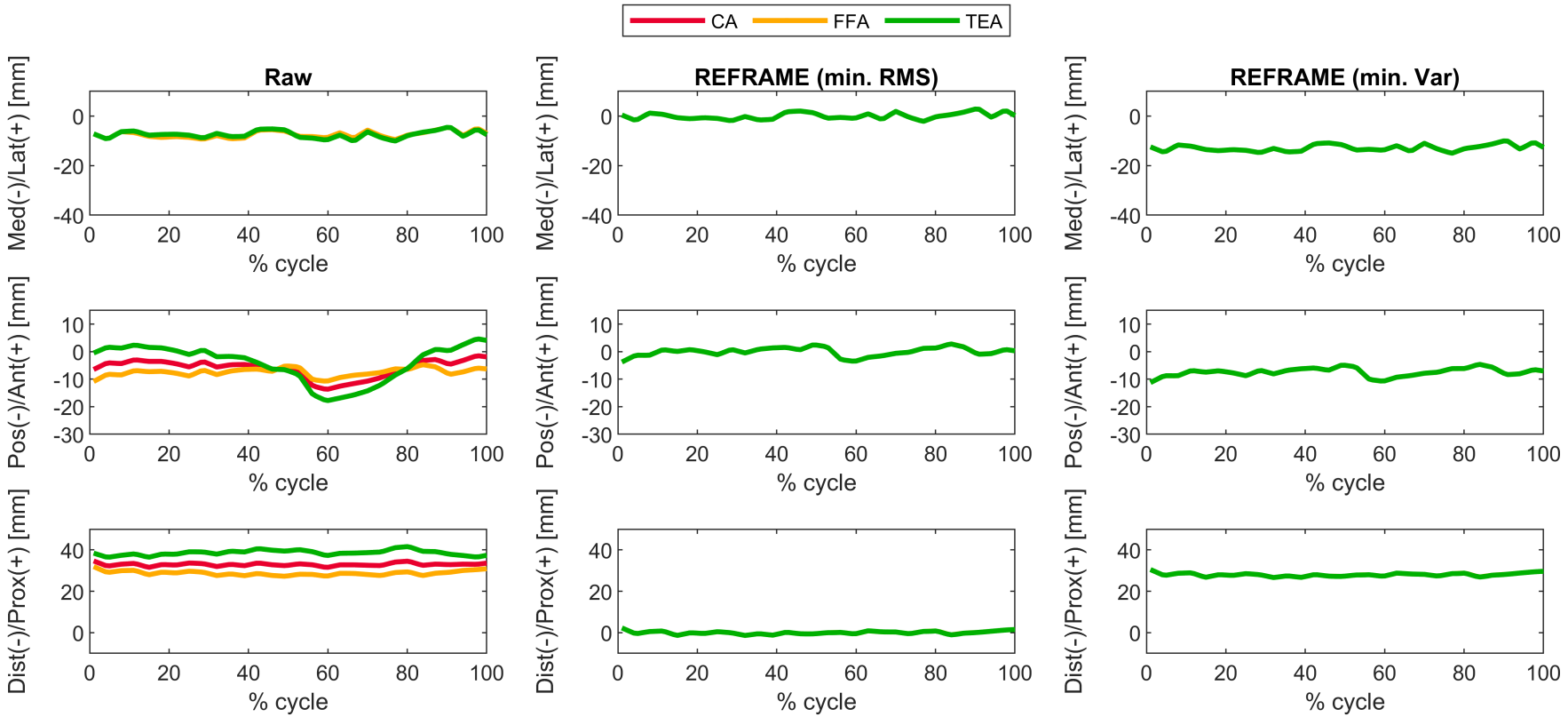

Supplementary Figure S100: Subject 10; Trial 3 – Translational kinematics: Joint translations (in mm) of the femoral relative to the tibial origin for one cycle of stair descent, before (raw, first column) and after application of the REFRAME optimisation (second column: based on the minimisation of translational root-mean-square; third column: based on the minimisation of translational variances), for all three axis approaches (CA: cylindrical axis; FFA: functional flexion axis; TEA: transepicondylar axis). CA, FFA and TEA signals are shown in **all** subplots, but due to curve overlap in the second and third columns, CA and FFA are covered by TEA.

3.10.4 Trial 4

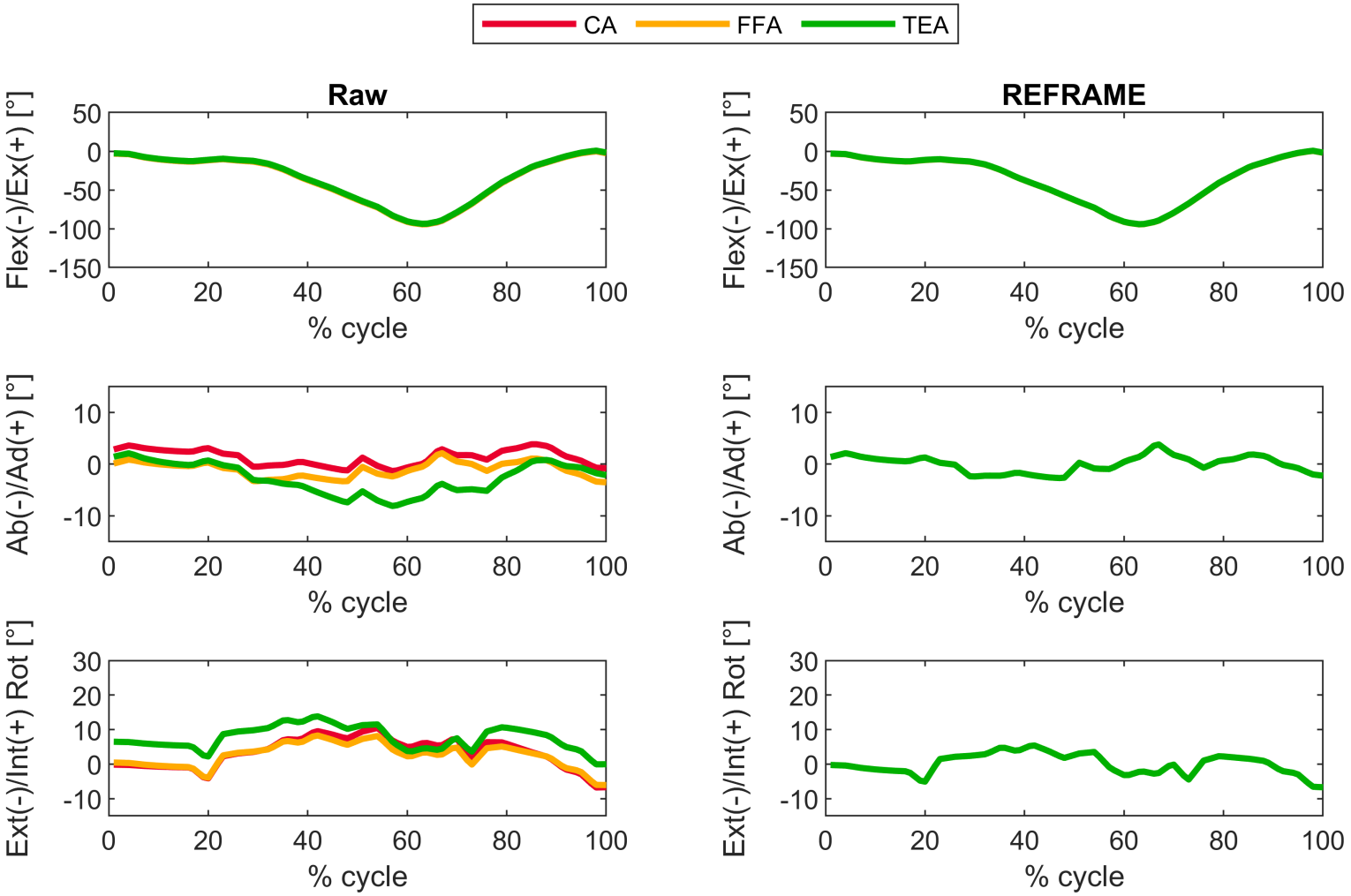

Supplementary Figure S101: Subject 10; Trial 4 – Rotational kinematics: Joint rotations (in degrees) of the tibial relative to the femoral segment frame for one cycle of stair descent, before (raw) and after REFRAME optimisation, for all three axis approaches (CA: cylindrical axis; FFA: functional flexion axis; TEA: transepicondylar axis). CA, FFA and TEA signals are shown in **all** subplots, but due to curve overlap in right-hand side plots, CA and FFA are covered by TEA. Note to readers from a clinical background: knee extension is illustrated here as **positive** because following the right-hand rule it corresponds with a positive rotation around the laterally pointing mediolateral axis for a right knee.

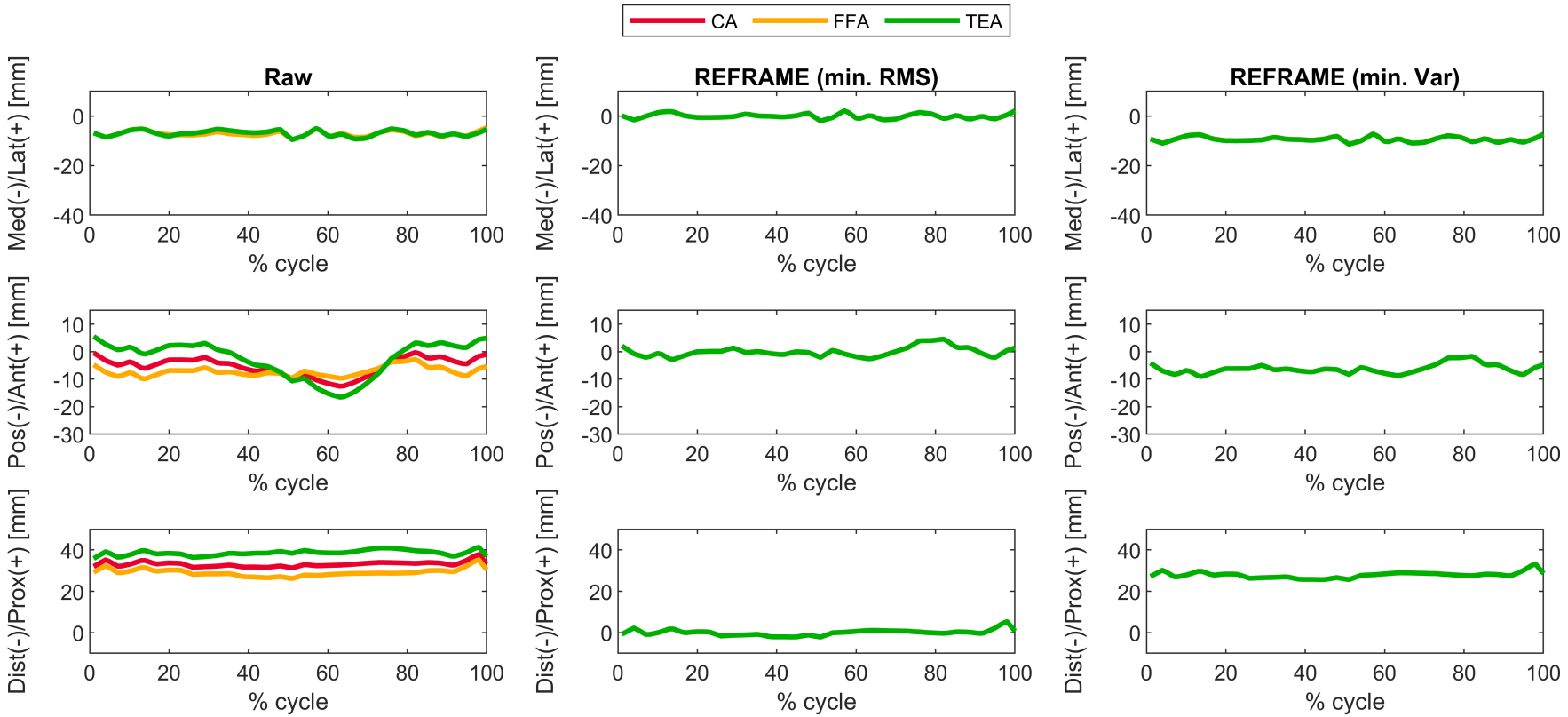

Supplementary Figure S102: Subject 10; Trial 4 – Translational kinematics: Joint translations (in mm) of the femoral relative to the tibial origin for one cycle of stair descent, before (raw, first column) and after application of the REFRAME optimisation (second column: based on the minimisation of translational root-mean-square; third column: based on the minimisation of translational variances), for all three axis approaches (CA: cylindrical axis; FFA: functional flexion axis; TEA: transepicondylar axis). CA, FFA and TEA signals are shown in **all** subplots, but due to curve overlap in the second and third columns, CA and FFA are covered by TEA.

3.10.5 Trial 5

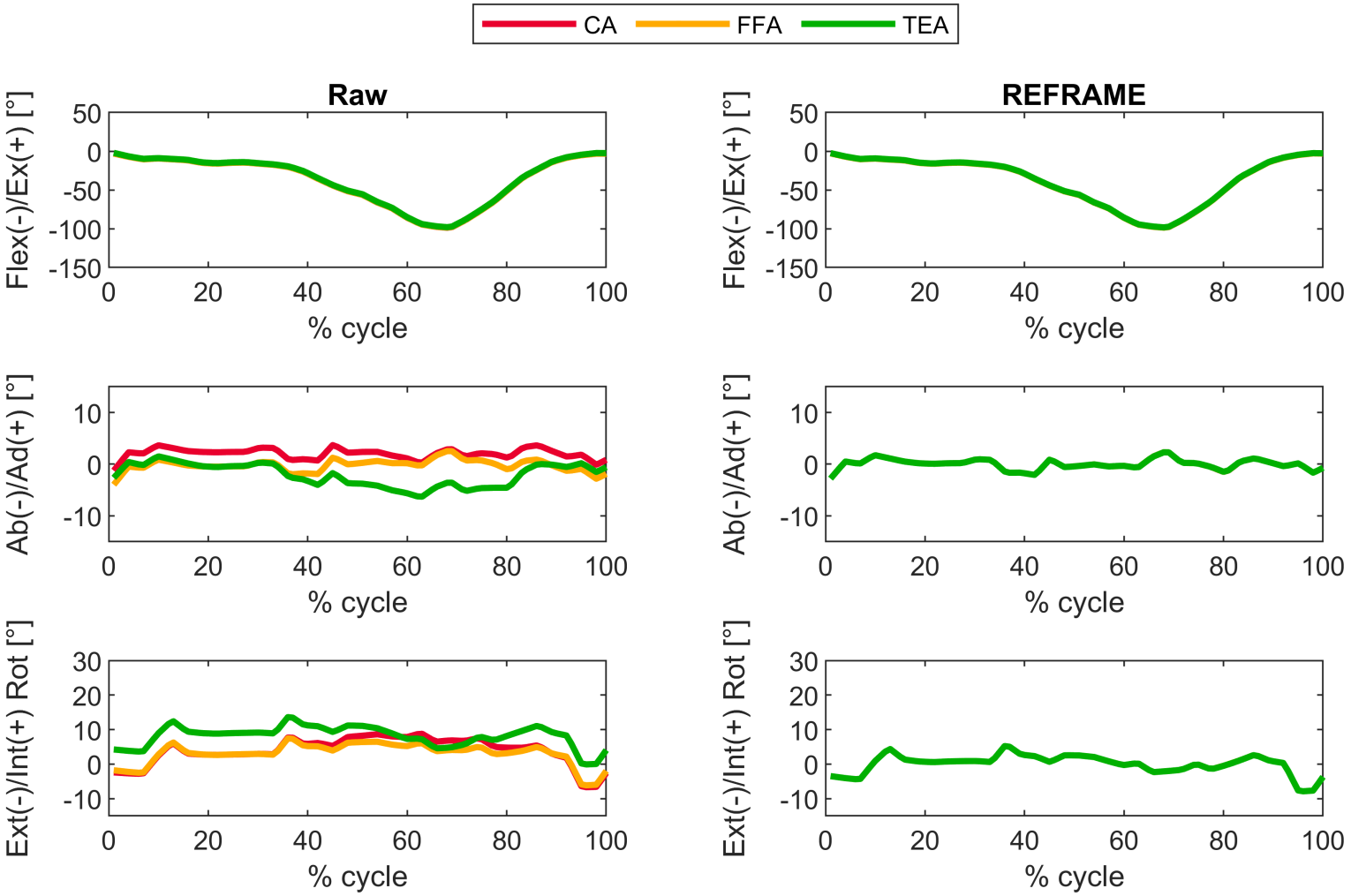

Supplementary Figure S103: Subject 10; Trial 5 – Rotational kinematics: Joint rotations (in degrees) of the tibial relative to the femoral segment frame for one cycle of stair descent, before (raw) and after REFRAME optimisation, for all three axis approaches (CA: cylindrical axis; FFA: functional flexion axis; TEA: transepicondylar axis). CA, FFA and TEA signals are shown in **all** subplots, but due to curve overlap in right-hand side plots, CA and FFA are covered by TEA. Note to readers from a clinical background: knee extension is illustrated here as **positive** because following the right-hand rule it corresponds with a positive rotation around the laterally pointing mediolateral axis for a right knee.

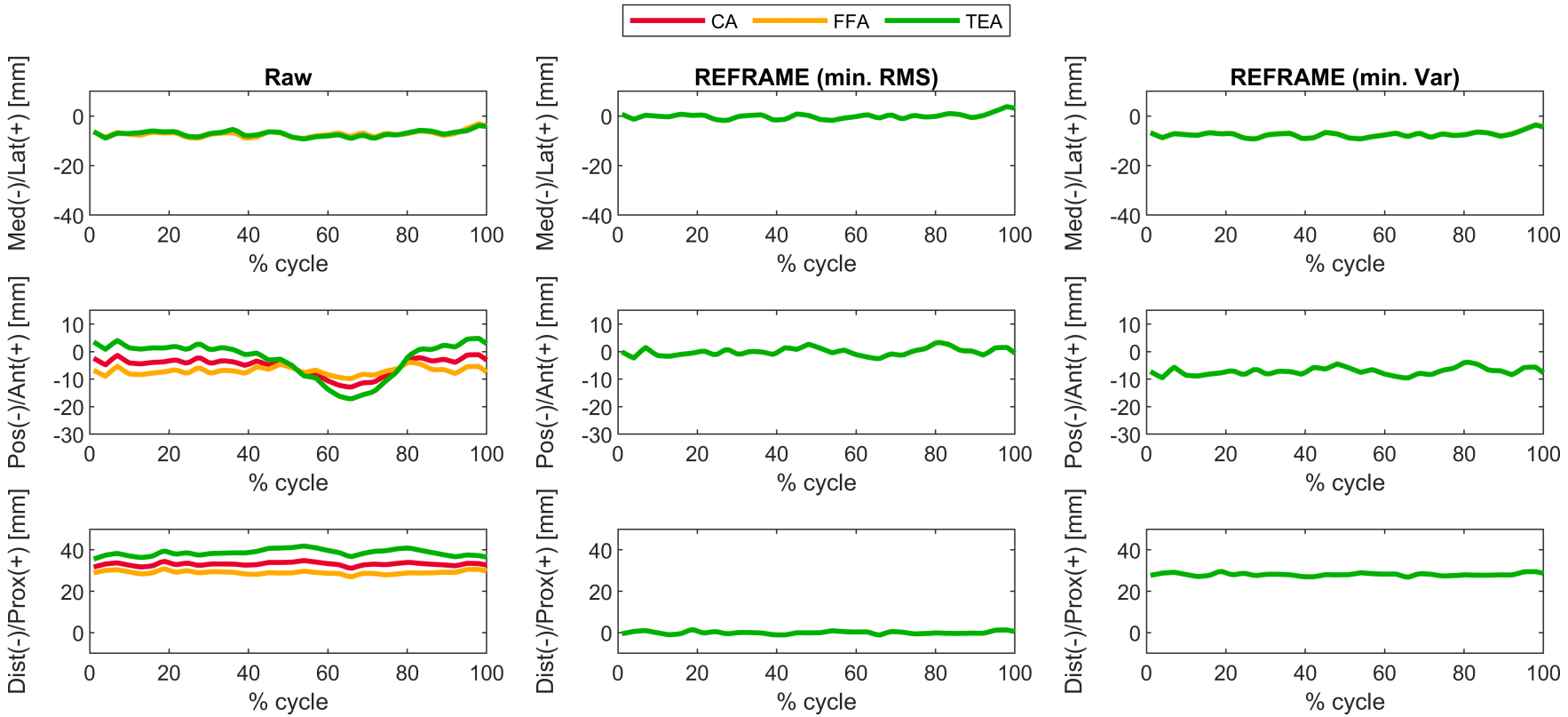

Supplementary Figure S104: Subject 10; Trial 5 – Translational kinematics: Joint translations (in mm) of the femoral relative to the tibial origin for one cycle of stair descent, before (raw, first column) and after application of the REFRAME optimisation (second column: based on the minimisation of translational root-mean-square; third column: based on the minimisation of translational variances), for all three axis approaches (CA: cylindrical axis; FFA: functional flexion axis; TEA: transepicondylar axis). CA, FFA and TEA signals are shown in **all** subplots, but due to curve overlap in the second and third columns, CA and FFA are covered by TEA.